

Reports

9-1-1994

A PC-Based Tidal Prism Water Quality Model for Small Coastal Basins and Tidal Creeks

Albert Y. Kuo
Virginia Institute of Marine Science

Kyeong Park
Virginia Institute of Marine Science

Follow this and additional works at: <https://scholarworks.wm.edu/reports>



Part of the [Marine Biology Commons](#)

Recommended Citation

Kuo, A. Y., & Park, K. (1994) A PC-Based Tidal Prism Water Quality Model for Small Coastal Basins and Tidal Creeks. Special Reports in Applied Marine Science and Ocean Engineering (SRAMSOE) No. 324. Virginia Institute of Marine Science, College of William and Mary. <https://doi.org/10.21220/V5VQ9S>

This Report is brought to you for free and open access by W&M ScholarWorks. It has been accepted for inclusion in Reports by an authorized administrator of W&M ScholarWorks. For more information, please contact scholarworks@wm.edu.

A PC-BASED TIDAL PRISM WATER QUALITY MODEL
FOR SMALL COASTAL BASINS AND TIDAL CREEKS

by

Albert Y. Kuo and Kyeong Park

A Report to the

Virginia Coastal Resources Management Program
Virginia Department of Environmental Quality

Special Report No. 324
in Applied Marine Science and
Ocean Engineering

School of Marine Science/Virginia Institute of Marine Science
The College of William and Mary in Virginia
Gloucester Point, VA 23062

September 1994



A PC-BASED TIDAL PRISM WATER QUALITY MODEL
FOR SMALL COASTAL BASINS AND TIDAL CREEKS

by

Albert Y. Kuo and Kyeong Park

A Report to the

Virginia Coastal Resources Management Program
Virginia Department of Environmental Quality

Special Report No. 324
in Applied Marine Science and
Ocean Engineering

School of Marine Science/Virginia Institute of Marine Science
The College of William and Mary in Virginia
Gloucester Point, VA 23062

September 1994

This study was funded, in part, by the Department of Environmental Quality's Coastal Resources Management Program through Grant #NA37OZ0360-01 of the National Oceanic and Atmospheric Administration, Office of Ocean and Coastal Resource Management, under the Coastal Zone Management Act of 1972, as amended. The views expressed herein are those of the authors and do not necessarily reflect the views of NOAA or any of its subagencies.

Table of Contents

	<u>Page</u>
List of Tables	iii
List of Figures	iv
Acknowledgements	v
I. Introduction	1
II. Formulation of Physical Transport Processes	4
II-1. Segmentation of a Water Body	5
II-2. Determination of Segment Lengths	6
II-3. Formulation for a Conservative Substance	7
II-4. Method of Solution for Nonconservative Water Quality State Variables	16
III. Kinetic Formulation for Water Quality State Variables	24
III-1. Algae	24
III-2. Organic Carbon	30
III-3. Phosphorus	35
III-4. Nitrogen	41
III-5. Silica	46
III-6. Chemical Oxygen Demand	48
III-7. Dissolved Oxygen	49
III-8. Total Suspended Solid	51
III-9. Total Active Metal	52
III-10. Fecal Coliform Bacteria	54
III-11. Temperature	54
III-12. Method of Solution for Kinetic Equations	55
III-13. Parameter Evaluation	66
IV. Sediment Process Model	74
IV-1. Depositional Flux	75
IV-2. Diagenesis Flux	77
IV-3. Sediment Flux	78
IV-4. Silica	90
IV-5. Sediment temperature	92
IV-6. Method of Solution	92
IV-7. Parameter Evaluation	97
V. Model Operation (Execution)	113
References	115
Appendix A. Program Organization for Input and Output Files	A-1
Appendix B. Graphic Interface	B-1

List of Tables

<u>Table</u>		<u>Page</u>
3-1.	Parameters related to algae in water column	67
3-2.	Parameters related to organic carbon in water column	68
3-3.	Parameters related to phosphorus in water column	69
3-4.	Parameters related to nitrogen in water column	70
3-5.	Parameters related to silica in water column	71
3-6.	Parameters related to chemical oxygen demand and dissolved oxygen in water column	71
3-7.	Parameters related to total suspended solid, total active metal, fecal coliform bacteria and temperature in water column	72
4-1.	Assignment of water column particulate organic matter (POM) to sediment G classes used in Cerco & Cole (1994)	109
4-2.	Sediment burial rates (W) used in Cerco & Cole (1994)	109
A-1.	Data file organization for water column model	A-32
A-2.	Data file organization for sediment process model	A-34

List of Figures

<u>Figure</u>	<u>Page</u>
2-1. Segmentation of a water body	18
2-2. Graphical method of segmentation of a water body	19
2-3. Flows across transects at flood and ebb tides	20
2-4. Mass transport across transects for the Type-2 segment i with branch k . . .	21
2-5. Mass transport across transects for the Type-3 segment (k,n) with storage area	22
2-6. Solution method for a nonconservative substance with "n" times of BGC update for a half tidal cycle	23
3-1. A schematic diagram for water column water quality model	73
4-1. Sediment layers and processes included in sediment process model	110
4-2. A schematic diagram for sediment process model	111
4-3. Benthic stress (a) and its effect on particle mixing (b) as a function of overlying dissolved oxygen concentration	112

Acknowledgements

We would like to express our appreciation for helpful discussions to Carl F. Cerco of US Army Corps of Engineers on water column kinetics, and James E. Bauer and Robert J. Diaz of Virginia Institute of Marine Science and Dominic M. DiToro of the Manhattan College on sediment processes. We also thank Robert J. Byrne and Bruce J. Neilson of Virginia Institute of Marine Science for their guidance and suggestions.

This study was funded, in part, by the Department of Environmental Quality's Coastal Resources Management Program through Grant #NA37OZ0360-01 of the National Oceanic and Atmospheric Administration, Office of Ocean and Coastal Resource Management, under the Coastal Zone Management Act of 1972, as amended.

The views expressed herein are those of the authors and do not necessarily reflect the views of NOAA or any of its subagencies.

Chapter I. Introduction

To simulate the eutrophication process and its impact on the anoxic/hypoxic conditions in Chesapeake Bay, the EPA Chesapeake Bay program has sponsored the development of a three-dimensional model. The model consists of hydrodynamic model (Johnson et al. 1991), water quality model (Cerco & Cole 1994) and benthic process model (DiToro & Fitzpatrick 1993). Results from the model application to the Bay mainstem and major tributaries indicated that nutrient loads from Virginia tributaries do not contribute significantly to the degraded water quality conditions of the Bay mainstem (Thomann et al. 1994). The Bay conditions, however, can impact water quality characteristics of the estuarine portion of the lower Bay tributaries (Kuo & Park 1992).

The upper Bay tributaries have a firm 40% nutrient reduction allocation target. The lower Bay Virginia tributaries have only interim 40% reduction targets, although continued nutrient reductions in these tributaries and coastal basins will benefit the water quality and resources within the tributaries themselves. Therefore, the strategies for Virginia tributaries will emphasize continuing current nutrient reduction efforts while final reduction targets are developed.

The 1992 Amendment of the Chesapeake Bay Agreement recognizes that model refinement and enhancements are required in modeling the major tributaries. As well, and of great significance, is the linkage of the modeling efforts to consequences for living marine resources. To this end, the Bay Program just started to sponsor modeling refinements in Virginia's three major tributaries: the James, York and Rappahannock rivers. The Bay Program efforts, however, do not include the minor coastal basins and tidal creeks fringing the Bay mainstem and major tributaries. The coastal basins, connecting the land masses to the shallow waters of the Bay mainstem and major tributaries, constitute the pathway of nutrients and sediments that either support or repress the fringing marine resources. The application of a three-dimensional model to small coastal basins is impractical due to their limited size and relatively shallow depths, and the model furthermore is too complicated for local jurisdictions to use. Adoption of a tidal prism model would be a cost-effective approach to fill the gap. This report documents development of a tidal prism model including water column water quality

model and sediment process model for small coastal basins.

To provide a tool for water quality management of small coastal basins, the Virginia Institute of Marine Science has developed a tidal prism model in the late 1970s (Kuo & Neilson 1988). The tidal prism model simulates the physical transport processes in terms of the concept of tidal flushing (Ketchum 1951). The implementation of the concept in numerical computation is simple and straightforward, and thus ideal for small coastal basins including those with a high degree of branching. The model was applied to several small coastal basins in Virginia (Ho et al. 1977; Cerco & Kuo 1981), and has been employed by Virginia Water Control Board for point source wasteload allocations and by local planning district commissions to address impacts of nonpoint source management. The Corps of Engineers also has used the model to assess the water quality impact of canal construction in the Lynnhaven Bay system (Kuo & Hyer 1979).

The tidal prism model described in Kuo & Neilson (1988) simulates the conditions in the main channel and its primary branches (those connected to the main channel) only. The model is modified to include shallow embayments connected to the primary branches, which allows the model to simulate the conditions in the secondary branches (those connected to the primary branches). The modified model treats the secondary branches as storage areas, which exchange the water masses with the primary branches as tide rises and falls. A new solution scheme, in which decoupling of the kinetic processes from the physical transport and external sources results in a simple and efficient computational procedure, is developed and used for the present model. The formulation of physical transport processes and the new solution scheme are described in Chapter II. The kinetic portion of the tidal prism model in Kuo & Neilson (1988) is expanded to more completely describe eutrophication processes and to be comparable with the modeling efforts in the Bay mainstem and major tributaries. First, the kinetic formulations used in the Chesapeake Bay three-dimensional water quality model (Cerco & Cole 1994) are modified and used in the present model. The kinetic formulations for water quality state variables, with the parameter values evaluated in Cerco & Cole (1994), are described in Chapter III. Second, the sediment process model that was used for modeling of the Chesapeake Bay mainstem and major tributaries (DiToro & Fitzpatrick 1993) is slightly modified and incorporated into the present model to enhance

the predictive capability of the model. Chapter IV describes the sediment process model along with the parameter values evaluated in DiToro & Fitzpatrick (1993). Chapter V describes the general execution of the model. Input data file organization is described in Appendix A. The graphic interface, which facilitates the model use, is described in Appendix B.

Chapter II. Formulation of Physical Transport Processes

The tidal prism model predicts the longitudinal distribution of conservative and nonconservative substances at slack-before-ebb (high slackwater), therefore it is more applicable to an elongated coastal embayments or tidal creeks. The rise and fall of the tide at the mouth of an embayment or tidal creek cause an exchange of water masses through the entrance. This results in the temporary storage of large amounts of sea and fresh water in the creek during flood tide and the drainage of these waters during ebb tide. The volume of these waters is known as the tidal prism. Since water brought into the creek on flood tide mixes with the creek water, a portion of the pollutant mass in the creek is flushed out on ebb tide. This flushing mechanism due to the rise and fall of the tide is called tidal flushing. The model of transport by tidal flushing is based on the division of the prototype water body into segments, each of which is considered to be completely mixed at high tide. The length of each segment is defined by the tidal excursion, the average distance travelled by a water particle on the flood tide, because this is the maximum length over which complete mixing can be assumed.

Kuo & Neilson (1988) modified and expanded the tidal prism theory of Ketchum (1951) to make the model applicable to cases where the creek is branched and/or freshwater discharge is negligibly small. Their model retained some of the assumptions used by Ketchum. One intrinsic assumption is that the tide rises and falls simultaneously throughout the water body, which is most applicable to small coastal embayments. The tidal creek also is assumed to be in hydrodynamic equilibrium. That is, the net seaward transport of freshwater over a tidal cycle is equal to the volume of freshwater during the same period.

The tidal prism model in Kuo & Neilson (1988) calculates the physical transport processes in the main channel and its primary branches (those connected to the main channel) only. The model is modified to include shallow embayments connected to the primary branches, which allows the model to calculate the physical transport processes in the secondary branches (those connected to the primary branches). The modified model treats the secondary branches as storage areas, which exchange the water masses with the primary branches as tide rises and falls. The formulation of physical transport processes

including this modification is described in this chapter.

II-1. Segmentation of a Water Body

Segmentation starts at the mouth of the creek (Kuo & Neilson 1988). The water body outside of the mouth is denoted as the 1st segment (Fig. 2-1). The adjacent segment within the creek is indexed as the 2nd segment. The 1st transect is across the mouth and the 2nd transect is chosen such that a water particle will move from the 1st to the 2nd transect over flood tide. Therefore, the tidal prism, or intertidal volume, upriver of the 2nd transect must be large enough to accommodate the low tide volume in the 2nd segment plus the volume of freshwater inflow upriver of the 2nd transect over flood tide, i.e.,

$$P_2 = V_2 + R_2 \quad \text{or} \quad V_2 = P_2 - R_2 \quad (2-1)$$

P_2 = tidal prism, or intertidal volume, upriver of the 2nd transect including those in branches

V_2 = low tide volume of the 2nd segment

R_2 = volume of freshwater entering the creek upriver of the 2nd transect during a half tidal cycle. If R_2 varies in time, the median value of R_2 should be used.

In general, a water particle at the (i-1)th transect at the beginning of flood tide should move to the ith transect at the end of flood tide. Thus:

$$P_i = V_i + R_i \quad (2-2)$$

$$V_i = P_i - R_i = (P_{i+1} + p_{i+1}) - (R_{i+1} + r_{i+1}) \quad (2-2-1)$$

$$= V_{i+1} + p_{i+1} - r_{i+1} \quad (2-2-2)$$

$$= VH_{i+1} - r_{i+1} \quad (2-2-3)$$

P_i = tidal prism upriver of the ith transect including those in branches

V_i = low tide volume of the ith segment

R_i = volume of freshwater entering the creek upriver of the ith transect during a half tidal cycle

p_i = local tidal prism of the ith segment

r_i = volume of lateral inflow into the ith segment during a half tidal cycle including point

and nonpoint source discharges

$$VH_i = \text{high tide volume of the } i^{\text{th}} \text{ segment} = V_{i+1} + p_{i+1}.$$

From the definitions:

$$P_i = \sum_{n=i+1}^{I+1} p_n \quad \text{and} \quad R_i = \sum_{n=i+1}^{I+1} r_n \quad (2-2-4)$$

Equation 2-2-3 states that the low tide volume of a segment is equal to the high tide volume of its immediate upriver segment less the lateral freshwater inflow into that segment.

It may be seen from Eq. 2-2-1 that V_i approaches zero as P_i decreases toward the head of tide. Therefore, an infinite number of segments will result unless a cut-off criterion is defined. One guideline is to continue segmentation until a segment length becomes smaller than its width. As this condition is reached, the remainder of the tidal creek is combined into one single segment, the I^{th} segment (Fig. 2-1). The prism upriver of the I^{th} transect is equal to the freshwater discharge upriver of the I^{th} transect, i.e., $P_I = R_I$. The length of the I^{th} segment will be larger than the local tidal excursion and complete mixing cannot be achieved within this segment. The model simulated concentration at this segment still represents the average value of the segment, however. Landward of the I^{th} transect, the creek behaves more like a fluvial stream than a tidal creek and flushing is due solely to the freshwater discharge. Segmentation in the freshwater section is arbitrary and governed only by the spatial resolution desired and the segment length-to-width ratio.

For branches, segmentation also starts at the branch-main channel junction. As the 1st segment in the main channel is outside of the creek mouth, the 1st segment in the k^{th} branch entering the i^{th} main channel segment, denoted as the $(k,1)^{\text{th}}$ segment, is located in the main channel. That is, the $(k,1)^{\text{th}}$ segment shares the same segment as the i^{th} segment. Segmentation in branches proceeds upriver in the same manner as the main channel.

II-2. Determination of Segment Lengths

Figure 2-2 shows, for a hypothetical tidal creek, the accumulated low tide volume,

$VA(x)$, and the difference between the tidal prism and the river inflow upriver of a point, $[P(x) - R(x)]$, plotted as a function of x , the distance from the mouth. $VA(x)$ is defined as the accumulated low tide volume of the main channel from the mouth to any distance x . $P(x)$ is defined as the intertidal volume upriver of a transect located at x . $R(x)$ is defined as the freshwater input, summed over a half tidal cycle, which enters the creek upriver of a transect located at x .

The volume, $P(0) = P_1$, is the intertidal volume of the entire creek. $R(0) = R_1$ is the total freshwater input to the creek including river flow, and point and nonpoint source discharges. The volume V_1 is a dummy volume located outside the creek mouth and the first volume within the creek is defined as V_2 (Section II-1). To satisfy the assumption of complete mixing within each segment, segment lengths must be less than or equal to the local tidal excursions. Therefore, the low tide volume of the first segment within the creek (V_2) should equal the intertidal volume (P_2) minus the river flow (R_2) upriver of its upriver boundary transect (Eq. 2-1). This point, where $V_2 = P_2 - R_2$, can be determined graphically or by interpolation of a table of values of $VA(x)$ and $[P(x) - R(x)]$. Segmentation continues upriver in this manner until the cut-off guideline is approached (see Section II-1).

In a segment where branch comes in (e.g., 4th segment in Fig. 2-2), the intertidal volume of the branch, PT , should be included in determining the segment volume. $P(x)$ is defined to include the tidal prism of the branch and $R(x)$ is defined to include the freshwater input from the branch. The value $VA(x)$ remains as the accumulated low tide volume along the main channel. For segments with branches, therefore, the curve $[P(x) - R(x)]$ needs to be extrapolated from the branch junction to the upriver transect of the segment. Each branch may be segmented in the same way as that of the main channel.

II-3. Formulation for a Conservative Substance

The present tidal prism model calculates the segment-average concentrations at high tide (slack-before-ebb). For a conservative substance, the rate of change of mass is determined by physical transport and external sources. Then, the change of mass, Δm , over one tidal cycle may be expressed as:

$$\Delta m = [sources] + [mass in] - [mass out] \quad (2-3)$$

where [sources] include point and nonpoint source input and exchange with storage area over one tidal cycle.

On the flood tide, as the tide propagates upriver, a volume of water

$$PRF_{i-1} = P_{i-1} - R_{i-1} \quad (2-4)$$

moves upriver across the $(i-1)^{\text{th}}$ transect and mixes with the water volume V_i present in the i^{th} segment at low tide (Fig. 2-3). Of this mixed water, the portion $(P_i - R_i)$ moves upriver across the i^{th} transect and mixes with the water in the $(i+1)^{\text{th}}$ segment, V_{i+1} , and so forth. On the ebb tide, a volume of water

$$PRE_i = P_i + R_i \quad (2-5)$$

moves downriver across the i^{th} transect, pushing a volume $(P_{i-1} + R_{i-1})$ across the $(i-1)^{\text{th}}$ transect, and so forth, thus completing tidal flushing (Fig. 2-3).

II-3-1. Transport during ebb tide

For transects downriver of the I^{th} transect (i.e., $i \leq I-1$), the water volume moving across the i^{th} transect during ebb tide, PRE_i , may be separated into two parts. The first part is the water in the $(i+1)^{\text{th}}$ segment at high tide, VH_{i+1} . This volume of water has a concentration C_{i+1} , the high tide concentration in the $(i+1)^{\text{th}}$ segment at the beginning of a tidal cycle. The remainder of the water moving across the i^{th} transect has a volume:

$$Res1 = PRE_i - VH_{i+1} \quad (2-6)$$

This volume of water may be further divided into two parts. One part is from the direct input, including point and nonpoint source discharges, to the $(i+1)^{\text{th}}$ segment, r_{i+1} . The remainder comes through the $(i+1)^{\text{th}}$ transect from the $(i+2)^{\text{th}}$ segment. Thus:

$$Res1 = r_{i+1} + Res2 \quad (2-7)$$

If the volume $Res2$ is still greater than the high tide volume of the $(i+2)^{\text{th}}$ segment, then the volume in excess of VH_{i+2} may be traced further in the same way as $Res1$.

The mass transport into the i^{th} segment during ebb tide may now be expressed as:

$$ETP_i = PRE_i \cdot C_{i+1} \quad \text{if } PRE_i \leq VH_{i+1} \quad \text{or}$$

$$ETP_i = VH_{i+1} \cdot C_{i+1} + \frac{Res1}{r_{i+1}} \frac{WP_{i+1} + WNP_{i+1}}{2} \quad \text{or}$$

if $PRE_i > VH_{i+1}$ *and* $Res1 \leq r_{i+1}$

$$ETP_i = VH_{i+1} \cdot C_{i+1} + \frac{WP_{i+1} + WNP_{i+1}}{2} + Res2 \cdot C_{i+2} \quad (2-8)$$

if $Res1 > r_{i+1}$ *and* $Res2 \leq VH_{i+2}$

ETP_i = ebb tide mass transport across the i^{th} transect into the i^{th} segment

WP_{i+1} = point source mass input into the $(i+1)^{\text{th}}$ segment over a tidal cycle

WNP_{i+1} = nonpoint source mass input into the $(i+1)^{\text{th}}$ segment over a tidal cycle

If $Res2 > VH_{i+3}$, the calculation of ETP_i should include additional terms relating to r_{i+2} , VH_{i+3} and so forth, until the volume PRE_i is totally accounted for. Similarly, the ebb tide transport out of the i^{th} segment may be expressed as:

$$ETP_{i-1} = VH_i \cdot C_i + \frac{WP_i + WNP_i}{2} + Res2 \cdot C_{i+1} \quad (2-9)$$

ETP_{i-1} = ebb tide mass transport across the $(i-1)^{\text{th}}$ transect out of the i^{th} segment.

II-3-2. Transport during flood tide

On the flood tide, a volume PRF_i moves upriver across the i^{th} transect into the $(i+1)^{\text{th}}$ segment (Fig. 2-3). It is possible that some fraction of this water is the water that was transported into the i^{th} segment during the previous ebb tide. This fraction of returning old water, which has the concentration C_{i+1} is defined as a returning ratio, α_i , at the i^{th} transect. The remaining fraction $(1 - \alpha_i)$ is new water from the i^{th} segment, which has the concentration $C2_i$ where $C2_i$ is the high tide concentration at the end of a tidal cycle. Therefore, the volume PRF_i has the concentration $[\alpha_i \cdot C_{i+1} + (1 - \alpha_i) \cdot C2_i]$. Then, the mass transport into and out of the i^{th} segment during flood tide may be expressed as:

$$FTP_{i-1} = PRF_{i-1} \cdot [\alpha_{i-1} \cdot C_i + (1 - \alpha_{i-1}) C2_{i-1}] \quad (2-10)$$

$$FTP_i = PRF_i \cdot [\alpha_i \cdot C_{i+1} + (1 - \alpha_i) C2_i] \quad (2-11)$$

FTP_{i-1} = flood tide mass transport across the (i-1)th transect into the ith segment

FTP_i = flood tide mass transport across the ith transect out of the ith segment.

II-3-3. Segments in main channel

The present model has four types of segments:

Type-1 = main channel segments without branch

Type-2 = main channel segments with branches

Type-3 = segments in the primary branches

Type-4 = segments in the secondary branches with each branch treated as a single storage area connected to a Type-3 segment.

The governing equations for main channel segments, both Type-1 and Type-2, are given in this section, and those for Type-3 and Type-4 segments are presented in Section II-3-4.

A. Type-1 segment: From Eq. 2-3, the change of mass in the ith segment over an entire tidal cycle can be expressed as:

$$(C2_i - C_i) \cdot (V_i + p_i) = [sources] + ETP_i - ETP_{i-1} - FTP_i + FTP_{i-1} \quad (2-12)$$

The term [sources] includes point and nonpoint source input for main channel segments.

Therefore, for the ith main channel segment:

$$[sources] = WP_i + WNP_i \quad (2-12-1)$$

Letting $VH_i = V_i + p_i$ and substituting Equations 2-10, 2-11 and 2-12-1, Eq. 2-12 can then be solved for $C2_i$:

$$C2_i = TT_i \cdot \left[1 + \frac{PRF_i}{VH_i} (1 - \alpha_i) \right]^{-1} \quad (2-13)$$

$$TT_i = C_i + \frac{WP_i + WNP_i}{VH_i} + \frac{ETP_i - ETP_{i-1}}{VH_i} - \frac{PRF_i}{VH_i} \alpha_i \cdot C_{i+1} + \frac{PRF_{i-1}}{VH_i} [\alpha_{i-1} \cdot C_i + (1 - \alpha_{i-1}) \cdot C2_{i-1}] \quad (2-13-1)$$

For segments landward of the Ith transect (i.e., $i \geq I+1$), the creek becomes a fluvial stream and no water is transported upriver during flood tide. The total volume of

water flowing through the i^{th} transect during a tidal cycle is $2 \cdot R_i$. Equations 2-13 and 2-13-1 are applicable to the fluvial stream if letting

$$PRE_i = 2 \cdot R_i \quad \text{and} \quad PRF_i = 0 \quad (2-14)$$

Similar situations can occur at the inner portion of tidal creek during periods of high freshwater inflow. For a transect in the tidal creek (i.e., $i < I$), the ebb tide transport is always in the downriver direction regardless of freshwater inflow and is calculated using Eq. 2-8. However, when the freshwater inflow exceeds volume increase during flood tide (i.e., $P_i - R_i < 0$), the flood tide transport is in the downriver direction and may be expressed as:

$$FTP_i = (P_i - R_i) \cdot C_{i+1} \quad \text{if } P_i - R_i < 0 \quad (2-15)$$

Note the difference between Equations 2-11 and 2-15. In Eq. 2-15, the negative flow ($P_i - R_i < 0$) indicates that the flood tide transport is in the downriver direction. Under these circumstances, Equations 2-13 and 2-13-1 are still applicable if the conditions in Eq. 2-14 are forced.

B. Type-2 segment: For main channel segments with branches, the mass transport across the 1st branch transects should be considered. For the i^{th} segment with K branches coming in (Fig. 2-4), the extra terms that need to be added in the right-hand side of Eq. 2-12 are:

$$+ \sum_{k=1}^K (ETPT_{k,1} - FTPT_{k,1}) \quad (2-16)$$

The ebb tide mass transport across the $(k,1)^{\text{th}}$ transect, $ETPT_{k,1}$, is identical to Eq. 2-8. The flood tide mass transport across the $(k,1)^{\text{th}}$ transect, $FTPT_{k,1}$, can be expressed from Equations 2-4 and 2-11 as:

$$PRFT_{k,1} = PT_{k,1} - RT_{k,1} \quad (2-16-1)$$

$$FTPT_{k,1} = PRFT_{k,1} \cdot [\alpha T_{k,1} \cdot CT_{k,2} + (1 - \alpha T_{k,1}) C2_i] \quad (2-16-2)$$

The variable names ending with 'T' designate those defined for the primary branches. The equation to be solved for a Type-2 segment may be expressed as:

$$C2_i = TT_i \cdot \left[1 + \frac{PRF_i}{VH_i} (1 - \alpha_i) + \frac{1}{VH_i} \sum_{k=1}^K PRFT_{k,1} (1 - \alpha T_{k,1}) \right]^{-1} \quad (2-17)$$

$$TT_i = C_i + \frac{WP_i + WNP_i}{VH_i} + \frac{ETP_i - ETP_{i-1}}{VH_i} - \frac{PRF_i}{VH_i} \alpha_i \cdot C_{i+1} \\ + \frac{PRF_{i-1}}{VH_i} [\alpha_{i-1} \cdot C_i + (1 - \alpha_{i-1}) \cdot C2_{i-1}] + \frac{1}{VH_i} \sum_{k=1}^K (ETPT_{k,1} - PRFT_{k,1} \cdot \alpha T_{k,1} \cdot CT_{k,2}) \quad (2-17-1)$$

II-3-4. Segments in branch

A. Type-3 segment: The present model treats Type-4 segments as storage areas, which exchange the water and mass with Type-3 segments as tide rises and falls. For segments in the primary branches (Type-3), the term [sources] in Eq. 2-12 includes point and nonpoint source input, and exchange with storage area, if any. Therefore, for the (k,n)th segment:

$$[sources] = (WPT_{k,n} + WNPT_{k,n}) + St_{k,n} \quad (2-18)$$

where $St_{k,n}$ represents the mass exchange over a tidal cycle with storage area at the (k,n)th segment.

During ebb tide, the water surface goes down and storage area acts as a source for Type-3 segment. The ebb tide transport into the (k,n)th segment due to volume change in storage area and lateral inflow may be expressed as:

$$StETP_{k,n} = \left[Stp_{k,n} + \frac{StPQ_{k,n} + StNPQ_{k,n}}{2} \right] StC_{k,n} \quad (2-19)$$

$StETP_{k,n}$ = ebb tide mass transport from the (k,n)th storage area into the (k,n)th segment

$Stp_{k,n}$ = local tidal prism (volume change over a half tidal cycle) in the (k,n)th storage area

$StC_{k,n}$ = high tide concentration in the (k,n)th storage area at the beginning of a tidal cycle

$StPQ_{k,n}$ = point source volume discharge into the (k,n)th storage area over a tidal cycle

$StNPQ_{k,n}$ = nonpoint source volume discharge into the (k,n)th storage area over a tidal cycle

cycle.

During flood, if volume change in storage area, $Stp_{k,n}$, is larger than lateral inflow, $(StPQ_{k,n} + StNPQ_{k,n})/2$, storage area acts as a sink for branch segment. The flood tide transport may be expressed as:

$$StFTP_{k,n} = StQ_{k,n} [St\alpha_{k,n} \cdot StC_{k,n} + (1 - St\alpha_{k,n}) \cdot C2T_{k,n}]$$

$$\text{if } StQ_{k,n} = Stp_{k,n} - \frac{StPQ_{k,n} + StNPQ_{k,n}}{2} > 0 \quad (2-20-1)$$

$StFTP_{k,n}$ = flood tide mass transport into the (k,n)th storage area from the (k,n)th segment

$St\alpha_{k,n}$ = returning ratio for the (k,n)th storage area

$StQ_{k,n}$ is the volume of water entering the (k,n)th storage area from the (k,n)th segment.

Returning ratio, $St\alpha_{k,n}$, represents the fraction of $StQ_{k,n}$ originated from the (k,n)th storage area, i.e., the fraction of $StQ_{k,n}$ that leaves the (k,n)th storage area at falling tide and returns from the (k,n)th segment at the following rising tide. However, if lateral inflow exceeds volume increase during flood tide in storage area, the transport is in the opposite direction from storage area into branch segment. Then, the flood tide transport may be expressed as:

$$StFTP_{k,n} = StQ_{k,n} \cdot StC_{k,n} \quad \text{if } StQ_{k,n} = Stp_{k,n} - \frac{StPQ_{k,n} + StNPQ_{k,n}}{2} \leq 0 \quad (2-20-2)$$

In Eq. 2-20-2, the negative transport ($StQ_{k,n} \leq 0$) indicates that the transport is into the (k,n)th segment.

Combining Equations 2-19 and 2-20-1 (or 2-20-2), $St_{k,n}$ in Eq. 2-18, may be expressed as:

$$St_{k,n} = StETP_{k,n} - StFTP_{k,n} \quad (2-21)$$

Then, the mass-balance equation for a Type-3 segment may be expressed as (Fig. 2-5):

$$(C2T_{k,n} - CT_{k,n}) \cdot VHT_{k,n} = (WPT_{k,n} + WNPT_{k,n}) + ETPT_{k,n} - ETPT_{k,n-1}$$

$$- FTPT_{k,n} + FTPT_{k,n-1} + StETP_{k,n} - StFTP_{k,n} \quad (2-22)$$

Substituting equivalent form of Eq. 2-11 or Eq. 2-16-2 for $FTPT_{k,n}$ and Eq. 2-20-1 or Eq. 2-20-2 for $StFTP_{k,n}$, Eq. 2-22 can be solved for $C2T_{k,n}$ for a Type-3 segment:

$$C2T_{k,n} = TTT_{k,n} \cdot \left[1 + \frac{PRFT_{k,n}}{VHT_{k,n}} (1 - \alpha T_{k,n}) + \lambda \cdot \frac{StQ_{k,n}}{VHT_{k,n}} (1 - St\alpha_{k,n}) \right]^{-1} \quad (2-23)$$

$$\begin{aligned} TTT_{k,n} = & CT_{k,n} + \frac{WPT_{k,n} + WNPT_{k,n}}{VHT_{k,n}} + \frac{ETPT_{k,n} - ETPT_{k,n-1}}{VHT_{k,n}} \\ & - \frac{PRFT_{k,n}}{VHT_{k,n}} \alpha T_{k,n} \cdot CT_{k,n+1} + \frac{PRFT_{k,n-1}}{VHT_{k,n}} [\alpha T_{k,n-1} \cdot CT_{k,n} + (1 - \alpha T_{k,n-1}) C2T_{k,n-1}] \\ & + \frac{StETP_{k,n}}{VHT_{k,n}} - \frac{StQ_{k,n}}{VHT_{k,n}} \beta_{k,n} \cdot StC_{k,n} \end{aligned} \quad (2-23-1)$$

$$StQ_{k,n} = Stp_{k,n} - \frac{StPQ_{k,n} + StNPQ_{k,n}}{2} \quad (2-23-2)$$

$$\begin{aligned} \lambda = 1 \quad & \text{and} \quad \beta_{k,n} = St\alpha_{k,n} \quad \text{if } StQ_{k,n} > 0 \\ \lambda = 0 \quad & \text{and} \quad \beta_{k,n} = 1 \quad \text{if } StQ_{k,n} \leq 0 \end{aligned} \quad (2-23-3)$$

For Type-3 segments without storage area, $Stp_{k,n}$, $StPQ_{k,n}$ and $StNPQ_{k,n}$ are set to zero. It results in $StQ_{k,n} = StETP_{k,n} = 0$, making Equations 2-23 and 2-23-1 identical to those for Type-1 segments, main channel segments without branch (Equations 2-13 and 2-13-1).

B. Type-4 segment: Equation 2-23-1 requires evaluation of the concentrations in Type-4 storage area segments, $StC_{k,n}$. During ebb tide, the concentration of a conservative substance in storage area is affected only by external sources including point and nonpoint source loadings, but not by physical transport. Therefore, the mass in the (k,n)th storage area at low tide (slack-before-flood) is:

$$StC_{k,n} \cdot StV_{k,n} + \frac{StWP_{k,n} + StWNP_{k,n}}{2} \quad (2-24-1)$$

$StV_{k,n}$ = low tide volume in the (k,n)th storage area

$StWP_{k,n}$ = point source mass input into the (k,n)th storage area over a tidal cycle

$StWNP_{k,n}$ = nonpoint source mass input into the (k,n)th storage area over a tidal cycle.

During flood tide the mass coming into the storage area is:

$$StFTP_{k,n} + \frac{StWP_{k,n} + StWNP_{k,n}}{2} \quad (2-24-2)$$

These result in the mass in the storage area at high tide:

$$StC2_{k,n} \cdot StVH_{k,n} = StC_{k,n} \cdot StV_{k,n} + StFTP_{k,n} + (StWP_{k,n} + StWNP_{k,n}) \quad (2-24-3)$$

$StC2_{k,n}$ = high tide concentration in the (k,n)th storage area at the end of a tidal cycle

$StVH_{k,n}$ = high tide volume in the (k,n)th storage area = $StV_{k,n} + Stp_{k,n}$.

Then, the concentration in storage area at the end of a tidal cycle modified by physical transport and external sources may be expressed as:

$$StC2_{k,n} = \frac{StC_{k,n} \cdot StV_{k,n} + StFTP_{k,n} + (StWP_{k,n} + StWNP_{k,n})}{StVH_{k,n}} \quad (2-25)$$

If $StQ_{k,n} < 0$, then the negative $StFTP_{k,n}$ in Eq. 2-21 accounts for the mass lost from storage area into Type-3 segment (Eq. 2-20-2).

II-3-5. Method of solution

Suppose that we have a system, in which

- : M = number of main channel segments (Type-1 and Type-2 segments) excluding the fictitious segment outside of the main channel mouth
- : N_k = number of Type-3 segments in the kth primary branch excluding the (k,1)th segments in the main channel
- : k = number of branches (k = 1 ... K).

Then, N (= M + $\sum N_k$) equations will be obtained by writing Eq. 2-13 for Type-1 segments, Eq. 2-17 for Type-2 segments and Eq. 2-23 for Type-3 segments. These equations may be solved for the N unknowns, $C2_i$, if the initial concentrations, C_i and StC_i , and the downstream boundary condition, $C2_1$, are specified. It is assumed that the most upstream segments in both the main channel and the primary branches are chosen such that there is no transport through their landward transects. The upstream boundary conditions, then, are specified using nonpoint source input into the most upstream segments.

The computational sequence is to compute the high tide concentrations in each

segment at the first tidal cycle with a given initial concentration field at the zeroth tidal cycle, and then the concentrations in storage area, if any, are computed using Eq. 2-25. The computed concentration field at the first tidal cycle will then be used as the initial conditions to compute the concentration field at the second tidal cycle, and so forth. Each computation cycle will advance time by the increment of one tidal cycle. Within each computation cycle, the N equations are solved by successive substitution, since $C_{2,i-1}$ is the only unknown upon which $C_{2,i}$ depends.

II-4. Method of Solution for Nonconservative Water Quality State Variables

Equation 2-3 represents the rate of change of mass within a segment due to physical transport and external sources. For nonconservative substances, the rate of change of mass is determined by biogeochemical kinetic processes as well as physical transport and external sources. The change of mass, Δm , over one tidal cycle may be expressed as:

$$\Delta m = [sources] + [mass\ in] - [mass\ out] + [BGC] \quad (2-26)$$

where [BGC] represents the biogeochemical kinetic processes, which may cause an increase or decrease of a particular substance within a segment. The first three terms in the right-hand side of Eq. 2-26 are explained in the previous sections. The last term in Eq. 2-26, [BGC], differs for different substances. The present model has twenty-three nonconservative substances, i.e., water quality state variables, and their kinetic processes included in the model are explained in Chapter III. The solution method of Eq. 2-26 is described in this section.

When solving Eq. 2-26, following the idea in Smolarkiewicz & Margolin (1993), the BGC kinetic term is decoupled from the other three terms in the right-hand side of Eq. 2-26. That is, the calculation of the concentration fields for nonconservative substances is performed in multi-steps. For example, the initial conditions or calculated concentration fields at slack-before-ebb, C_i , which initiates a tidal cycle, are first subject to the BGC kinetic processes for a half tidal cycle to give C_i^* . The concentration fields C_i^* are modified by the physical transport processes and external sources for an entire tidal cycle (using Eq. 2-13, 2-17 or 2-23) to give C_i^{**} . Then, the concentration fields C_i^{**} are again subject to the BGC kinetic processes for the remaining half tidal cycle to give

the concentration fields at the next high tide, C_{2i} .

The above method essentially implies that the time step of calculation for the BGC kinetic term (Δt_{BGC}) is a half tidal cycle. However, the kinetic term may be large enough for some substances in a segment to be consumed completely over a half tidal cycle. One example is the algal uptake of nutrients, which, over a half tidal cycle, may be larger than the nutrients available within a segment. Therefore, the source code is written in such a way that one can divide the calculation of the BGC kinetic term over a half tidal cycle into several shorter time steps to prevent negative concentration. Figure 2-6 illustrates the situation, in which the calculation of the kinetic term is repeated "n" times over a half tidal cycle. The concentration fields C_i are subject to the kinetic processes for "n" times with Δt_{BGC} of (half tidal cycle)/n to give C_i^{*n} . The concentration fields C_i^{*n} are then modified by the physical transport processes and external sources for an entire tidal cycle to give C_i^{**} . The concentration fields C_i^{**} are further subject to the kinetic processes for "n" times with Δt_{BGC} to give C_i^{**n} (= C_{2i}). One will find that $n = 2$ or 3 ($\Delta t_{\text{BGC}} = 3.105$ or 2.07 hours) is often sufficient to prevent negative concentration.

Decoupling the BGC kinetic processes from the physical transport and external sources results in a simple and efficient computational procedure. The update for the physical transport and external sources follows the same solution method explained in Section II-3-5. The update for the BGC kinetic processes, which uses the analytical solution, is explained in Section III-12. The same multi-step calculation is used for the calculation of concentration fields in storage area, if any. The effect of the physical transport and external sources is calculated using Eq. 2-25 (Section II-3-5), and the calculation of the effect of the BGC kinetic processes is explained in Section III-12.

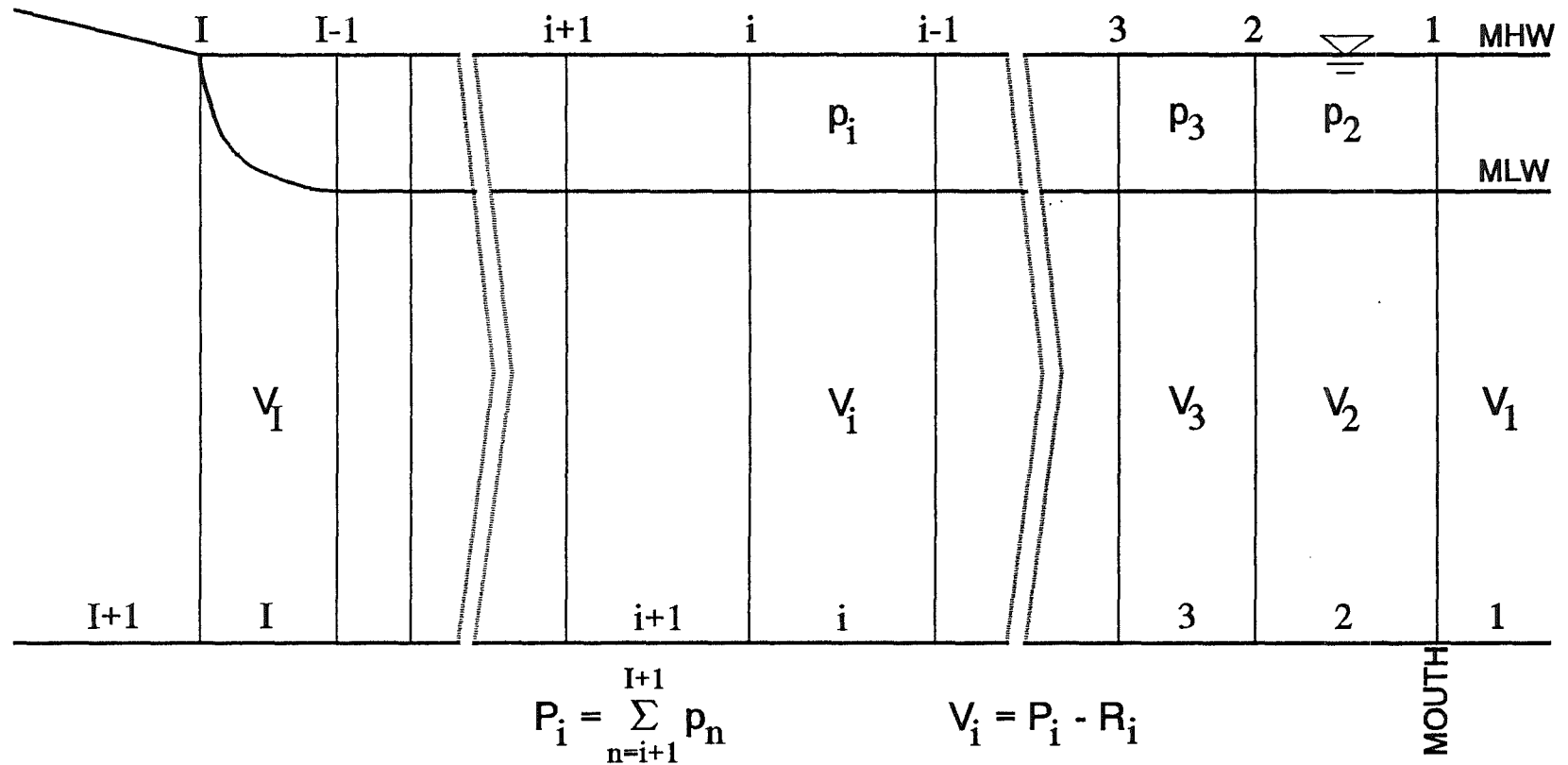


Figure 2-1. Segmentation of a water body.

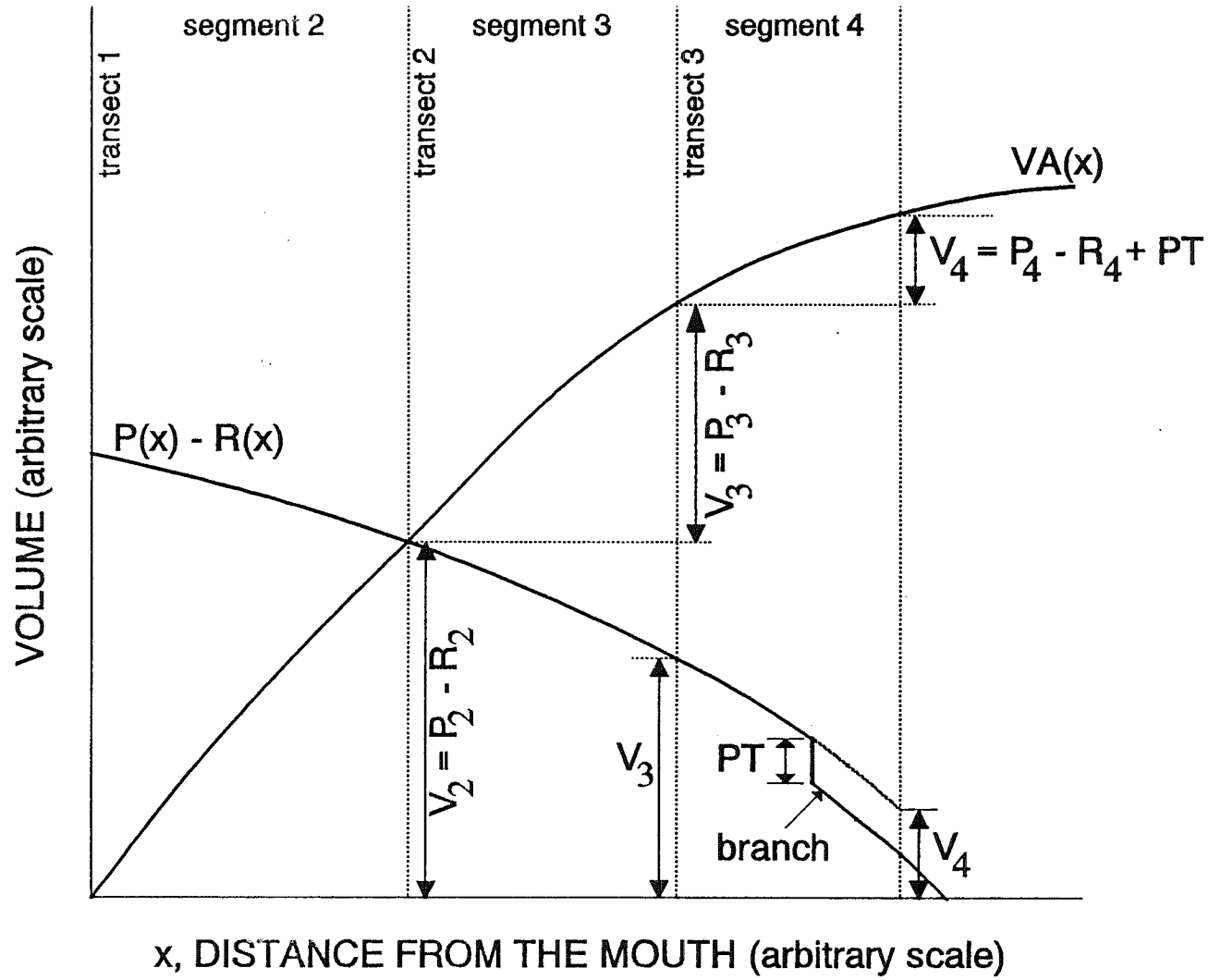


Figure 2-2. Graphical method of segmentation of a water body.

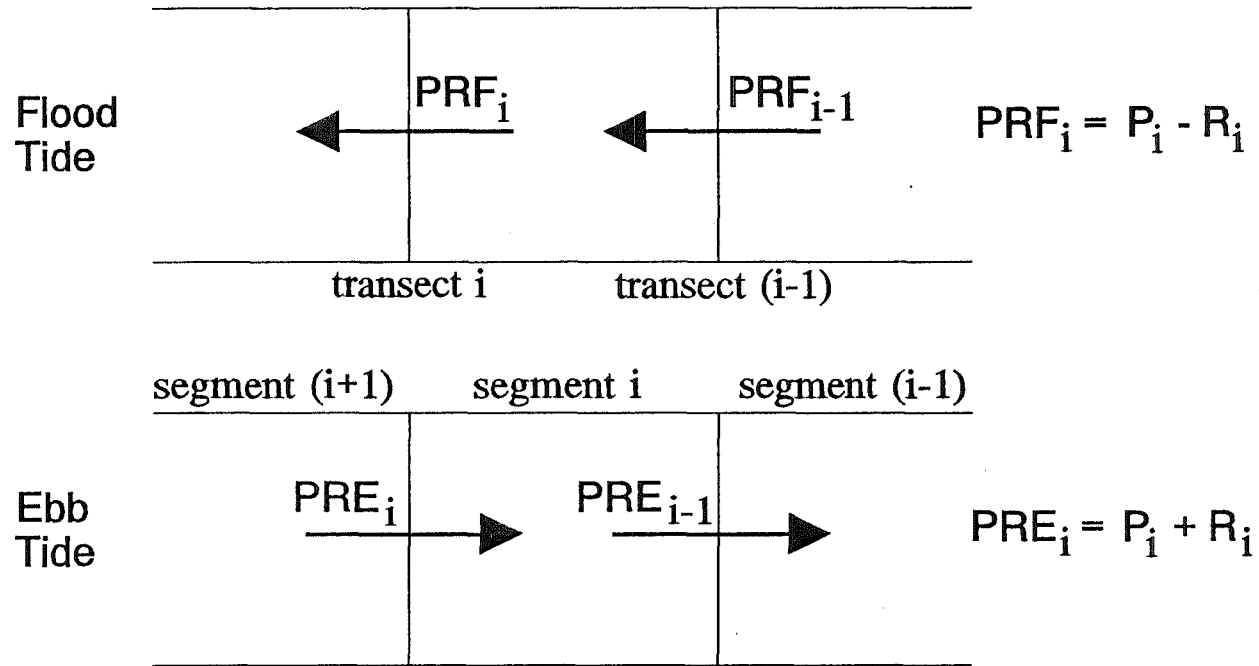


Figure 2-3. Flows across transects at flood and ebb tides.

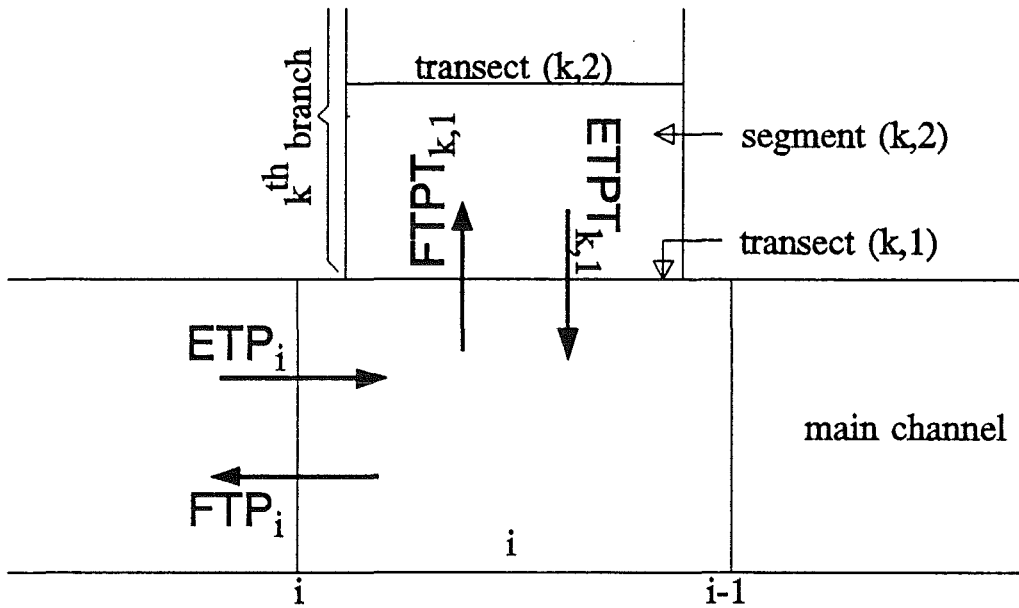


Figure 2-4. Mass transport across transects for the Type-2 segment i with branch k .

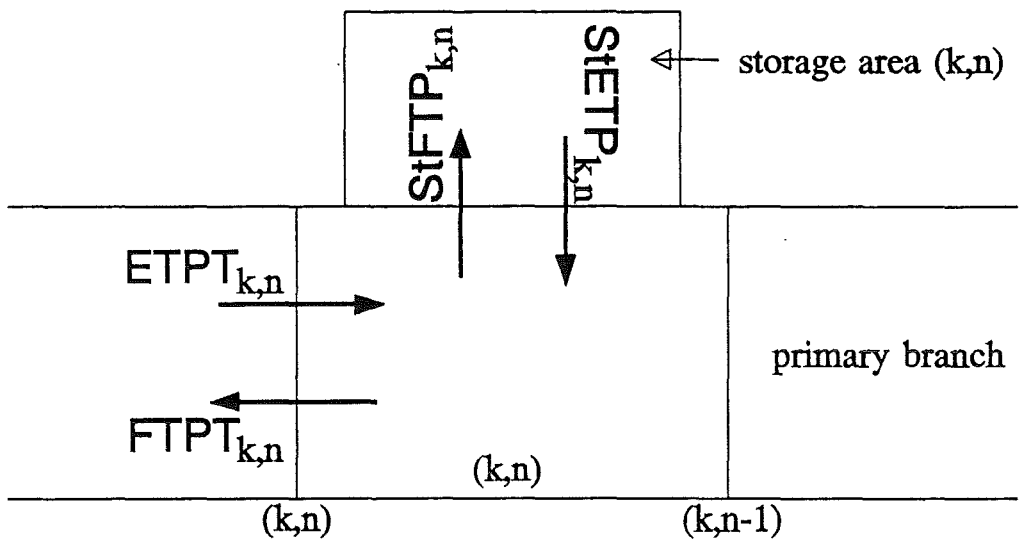


Figure 2-5. Mass transport across transects for the Type-3 segment (k,n) with storage area.

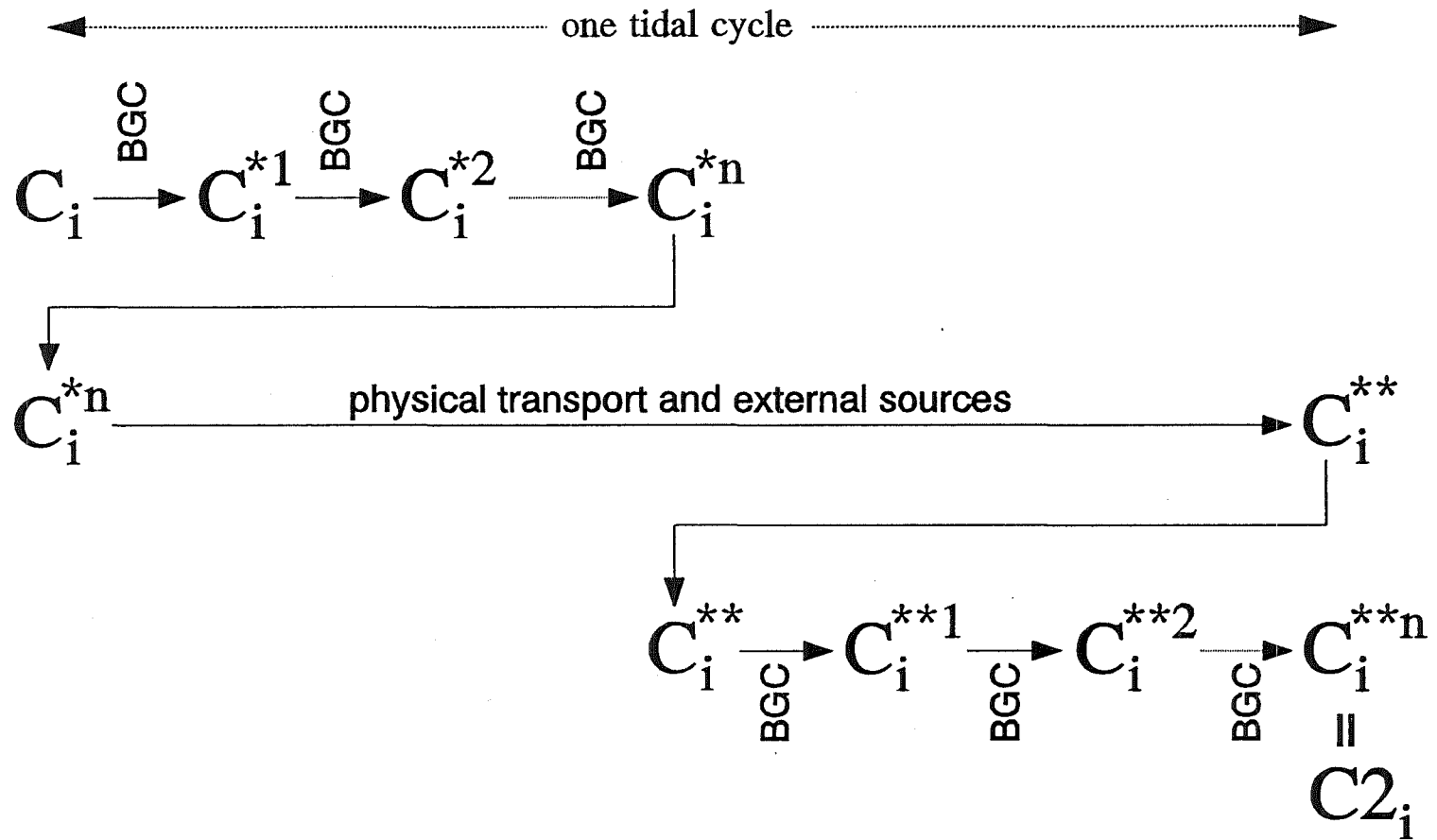


Figure 2-6. Solution method for a nonconservative substance with "n" times of BGC update for a half tidal cycle.

Chapter III. Kinetic Formulation for Water Quality State Variables

The present model has twenty three water quality related model state variables (Fig. 3-1). The kinetic processes included in the model use mostly the formulations in Chesapeake Bay three-dimensional water quality model, CE-QUAL-ICM (Cercio & Cole 1994).

- | | |
|--|--|
| 1) cyanobacteria (blue-green algae) | 2) diatoms |
| 3) green algae (others) | |
| 4) refractory particulate organic carbon | 5) labile particulate organic carbon |
| 6) dissolved organic carbon | |
| 7) refractory particulate organic phosphorus | 8) labile particulate organic phosphorus |
| 9) dissolved organic phosphorus | 10) total phosphate |
| 11) refractory particulate organic nitrogen | 12) labile particulate organic nitrogen |
| 13) dissolved organic nitrogen | 14) ammonium nitrogen |
| 15) nitrate nitrogen | |
| 16) particulate biogenic silica | 17) available silica |
| 18) chemical oxygen demand | 19) dissolved oxygen |
| 20) total suspended solid | 21) total active metal |
| 22) fecal coliform bacteria | 23) temperature |

This chapter details the kinetic sources and sinks for each state variable. Figure 3-1 shows the interactions between state variables. The external sources including point and nonpoint source inputs are taken care of in the formulations of physical transport processes (Chapter II). The exchange fluxes at the sediment-water interface including sediment oxygen demand are explained in the sediment process model (Chapter IV). An asterisk mark (*) attached to equation number denotes the kinetic formulations that are different from CE-QUAL-ICM. The solution method is described in Section III-12. The parameters values used in Chesapeake Bay modeling (Cercio & Cole 1994) are presented in Section III-13.

III-1. Algae

Algae, which occupies a central role in the model (Fig. 3-1), are grouped into three

model state variables: cyanobacteria (blue-green algae), diatoms and green algae. The subscript, x, is used to denote three algal groups: c for cyanobacteria, d for diatoms and g for green algae. Sources and sinks included in the model are

- : growth (production)
- : basal metabolism
- : predation
- : settling

Equations describing these processes are largely the same for three algal groups with differences in the values of parameters in the equations. The governing equation describing these processes is:

$$\frac{\partial B_x}{\partial t} = (P_x - BM_x - PR_x - \frac{WS_x}{h})B_x \quad (3-1)$$

B_x = algal biomass of algal group x (g C m⁻³)

t = time (day)

P_x = production rate of algal group x (day⁻¹)

BM_x = basal metabolism rate of algal group x (day⁻¹)

PR_x = predation rate of algal group x (day⁻¹)

WS_x = settling velocity of algal group x (m day⁻¹)

h = total depth (m).

III-1-1. Growth (Production)

Algal growth depends on nutrient availability, ambient light and temperature. The effects of these processes are considered to be multiplicative:

$$P_x = PM_x \cdot f_1(N) \cdot f_2(I) \cdot f_3(T) \quad (3-1a)$$

PM_x = maximum growth rate under optimal conditions for algal group x (day⁻¹)

$f_1(N)$ = effect of suboptimal nutrient concentration ($0 \leq f_1 \leq 1$)

$f_2(I)$ = effect of suboptimal light intensity ($0 \leq f_2 \leq 1$)

$f_3(T)$ = effect of suboptimal temperature ($0 \leq f_3 \leq 1$).

The freshwater cyanobacteria may undergo rapid mortality in salt water, e.g., freshwater organisms in the Potomac River (Thomann et al. 1985). For the freshwater organisms,

the increased mortality may be included in the model by retaining salinity toxicity term in the growth equation for cyanobacteria:

$$P_c = PM_c \cdot f_1(N) \cdot f_2(I) \cdot f_3(T) \cdot f_4(S) \quad (3-1b)$$

$f_4(S)$ = effect of salinity on cyanobacteria growth ($0 \leq f_4 \leq 1$).

Activation of the salinity toxicity term, $f_4(S)$, is an option in the source code.

III-1-1a. Effect of nutrients on growth

Using Liebig's "law of the minimum" (Odum 1971) that growth is determined by the nutrient in least supply, the nutrient limitation for growth of cyanobacteria and green algae is expressed as:

$$f_1(N) = \text{minimum} \left[\frac{NH4 + NO3}{KHN_x + NH4 + NO3}, \frac{PO4d}{KHP_x + PO4d} \right] \quad (3-1c)$$

NH4 = ammonium nitrogen concentration (g N m⁻³)

NO3 = nitrate nitrogen concentration (g N m⁻³)

KHN_x = half-saturation constant for nitrogen uptake for algal group x (g N m⁻³)

PO4d = dissolved phosphate phosphorus concentration (g P m⁻³)

KHP_x = half-saturation constant for phosphorus uptake for algal group x (g P m⁻³).

Some cyanobacteria, e.g., *Anabaena*, can fix nitrogen from atmosphere and thus is not limited by nitrogen. Therefore, Eq. 3-1c is not applicable to the growth of nitrogen fixers.

Since diatoms require silica as well as nitrogen and phosphorus for growth, the nutrient limitation for diatoms is expressed as:

$$f_1(N) = \text{minimum} \left[\frac{NH4 + NO3}{KHN_d + NH4 + NO3}, \frac{PO4d}{KHP_d + PO4d}, \frac{SAd}{KHS + SAd} \right] \quad (3-1d)$$

SAd = concentration of dissolved available silica (g Si m⁻³)

KHS = half-saturation constant for silica uptake for diatoms (g Si m⁻³).

III-1-1b. Effect of light on growth

The daily and vertically integrated form of Steele's equation is:

$$f_2(I) = \frac{2.718 \cdot FD}{K_{ess} \cdot h} (e^{-\alpha_B} - e^{-\alpha_T}) \quad (3-1e)$$

$$\alpha_B = \frac{I_o}{FD \cdot (I_s)_x} \cdot e^{-K_{ess} \cdot h} \quad (3-1f)$$

$$\alpha_T = \frac{I_o}{FD \cdot (I_s)_x} \quad (3-1g)$$

FD = fractional daylength ($0 \leq FD \leq 1$)

K_{ess} = total light extinction coefficient (m^{-1})

I_o = daily light intensity (langley day $^{-1}$)

$(I_s)_x$ = optimal light intensity for algal group x (langley day $^{-1}$).

Light extinction in the water column consists of three fractions in the model: a background value dependent on water color, extinction due to suspended particles and extinction due to light absorption by ambient chlorophyll:

$$K_{ess} = K_{e_b} + K_{e_{TSS}} \cdot TSS + K_{e_{chl}} \cdot \sum_{x=c,d,g} \left(\frac{B_x}{CChl_x} \right) \quad (3-1h)^*$$

K_{e_b} = background light extinction (m^{-1})

$K_{e_{TSS}}$ = light extinction coefficient for total suspended solid (m^{-1} per $g\ m^{-3}$)

TSS = total suspended solid concentration ($g\ m^{-3}$)

$K_{e_{chl}}$ = light extinction coefficient for chlorophyll 'a' (m^{-1} per $mg\ Chl\ m^{-3}$)

$CChl_x$ = carbon-to-chlorophyll ratio in algal group x ($g\ C$ per $mg\ Chl$).

For a model that does not simulate TSS, $K_{e_{TSS}}$ may be set to zero and K_{e_b} may be estimated to include light extinction due to suspended solid.

Optimal light intensity (I_s) for photosynthesis depends on algal taxonomy, duration of exposure, temperature, nutritional status and previous acclimation. Variations in I_s are largely due to adaptations by algae intended to maximize production in a variable environment. Steel (1962) noted the result of adaptations is that optimal intensity is a consistent fraction (approximately 50%) of daily intensity. Kremer & Nixon (1978) reported an analogous finding that maximum algal growth occurs at a constant depth (approximately 1 m) in the water column. Their approach is adopted so that optimal

intensity is expressed as:

$$(I_s)_x = \text{minimum} \left\{ (I_o)_{avg} \cdot e^{-K_{ess} \cdot (D_{opt})_x}, (I_s)_{min} \right\} \quad (3-1i)$$

$(D_{opt})_x$ = depth of maximum algal growth for algal group x (m)

$(I_o)_{avg}$ = adjusted surface light intensity (langleys day⁻¹).

A minimum, $(I_s)_{min}$, in Eq. 3-1i is specified so that algae do not thrive at extremely low light levels. The time required for algae to adapt to changes in light intensity is recognized by estimating $(I_s)_x$ based on a time-weighted average of daily light intensity:

$$(I_o)_{avg} = CI_a \cdot I_o + CI_b \cdot I_1 + CI_c \cdot I_2 \quad (3-1j)$$

I_1 = daily light intensity one day preceding model day (langleys day⁻¹)

I_2 = daily light intensity two days preceding model day (langleys day⁻¹)

CI_a , CI_b & CI_c = weighting factors for I_o , I_1 and I_2 , respectively: $CI_a + CI_b + CI_c = 1$.

III-1-1c. Temperature

A Gaussian probability curve is used to represent temperature dependency of algal growth:

$$\begin{aligned} f_3(T) &= \exp(-KTG1_x [T - TM_x]^2) & \text{if } T \leq TM_x \\ &= \exp(-KTG2_x [TM_x - T]^2) & \text{if } T > TM_x \end{aligned} \quad (3-1k)$$

T = temperature (°C)

TM_x = optimal temperature for algal growth for algal group x (°C)

$KTG1_x$ = effect of temperature below TM_x on growth for algal group x (°C⁻²)

$KTG2_x$ = effect of temperature above TM_x on growth for algal group x (°C⁻²).

III-1-1d. Effect of salinity on growth of freshwater cyanobacteria

The growth of freshwater cyanobacteria in salt water is limited by:

$$f_4(S) = \frac{STOX^2}{STOX^2 + S^2} \quad (3-1l)$$

STOX = salinity at which Microcystis growth is halved (ppt)

S = salinity in water column (ppt).

III-1-2. Basal Metabolism

Algal biomass in the present model decreases through basal metabolism (respiration and excretion) and predation. Basal metabolism in the present model is the sum of all internal processes that decrease algal biomass, and consists of two parts; respiration and excretion. In basal metabolism, algal matter (carbon, nitrogen, phosphorus and silica) is returned to organic and inorganic pools in the environment, mainly to dissolved organic and inorganic matter. Respiration, which may be viewed as a reversal of production, consumes dissolved oxygen. Basal metabolism is considered to be an exponentially increasing function of temperature:

$$BM_x = BMR_x \cdot \exp(KTB_x [T - TR_x]) \quad (3-1m)$$

BMR_x = basal metabolism rate at TR_x for algal group x (day^{-1})

KTB_x = effect of temperature on metabolism for algal group x ($^{\circ}\text{C}^{-1}$)

TR_x = reference temperature for basal metabolism for algal group x ($^{\circ}\text{C}$).

III-1-3. Predation

The present model does not include zooplankton. Instead, a constant rate is specified for algal predation, which implicitly assumes zooplankton biomass is a constant fraction of algal biomass. An equation similar to that for basal metabolism (Eq. 3-1m) is used for predation:

$$PR_x = PRR_x \cdot \exp(KTB_x [T - TR_x]) \quad (3-1n)$$

PRR_x = predation rate at TR_x for algal group x (day^{-1}).

The difference between predation and basal metabolism lies in the distribution of the end products of two processes. In predation, algal matter (carbon, nitrogen, phosphorus and silica) is returned to organic and inorganic pools in the environment, mainly to particulate organic matter.

III-1-4. Settling

Settling velocities for three algal groups, WS_c , WS_d and WS_g , are specified as an input. Seasonal variations in settling velocity of diatoms can be accounted for by specifying time-varying WS_d (Appendix A).

III-2. Organic Carbon

The present model has three state variables for organic carbon: dissolved, labile particulate and refractory particulate.

A. Particulate organic carbon: Labile and refractory distinctions are based on the time scale of decomposition. Labile particulate organic carbon with a decomposition time scale of days to weeks decomposes rapidly in the water column or in the sediments. Refractory particulate organic carbon with longer-than-weeks decomposition time scale decomposes slowly, primarily in the sediments, and may contribute to sediment oxygen demand years after decomposition. For labile and refractory particulate organic carbon, sources and sinks included in the model are (Fig. 3-1):

- : algal predation
- : dissolution to dissolved organic carbon
- : settling

The governing equations for refractory and labile particulate organic carbons are:

$$\frac{\partial RPOC}{\partial t} = \sum_{x=c,d,g} FCRP \cdot PR_x \cdot B_x - K_{RPOC} \cdot RPOC - \frac{WS_{RP}}{h} RPOC \quad (3-2)$$

$$\frac{\partial LPOC}{\partial t} = \sum_{x=c,d,g} FCLP \cdot PR_x \cdot B_x - K_{LPOC} \cdot LPOC - \frac{WS_{LP}}{h} LPOC \quad (3-3)$$

RPOC = concentration of refractory particulate organic carbon (g C m⁻³)

LPOC = concentration of labile particulate organic carbon (g C m⁻³)

FCRP = fraction of predated carbon produced as refractory particulate organic carbon

FCLP = fraction of predated carbon produced as labile particulate organic carbon

K_{RPOC} = dissolution rate of refractory particulate organic carbon (day⁻¹)

K_{LPOC} = dissolution rate of labile particulate organic carbon (day⁻¹)

WS_{RP} = settling velocity of refractory particulate organic matter (m day⁻¹)

WS_{LP} = settling velocity of labile particulate organic matter (m day⁻¹).

B. Dissolved organic carbon: Sources and sinks included in the model are (Fig. 3-1):

- : algal excretion (exudation) and predation
- : dissolution from refractory and labile particulate organic carbon
- : heterotrophic respiration of dissolved organic carbon (decomposition)

: denitrification

The governing equation describing these processes is:

$$\frac{\partial DOC}{\partial t} = \sum_{x=c,d,g} \left[\left[FCD_x + (1 - FCD_x) \frac{KHR_x}{KHR_x + DO} \right] BM_x + FCDP \cdot PR_x \right] \cdot B_x + K_{RPOC} \cdot RPOC + K_{LPOC} \cdot LPOC - K_{HR} \cdot DOC - Denit \cdot DOC \quad (3-4)$$

DOC = concentration of dissolved organic carbon (g C m⁻³)

FCD_x = fraction of basal metabolism exuded as dissolved organic carbon at infinite dissolved oxygen concentration for algal group x

KHR_x = half-saturation constant of dissolved oxygen for algal dissolved organic carbon excretion for group x (g O₂ m⁻³)

DO = dissolved oxygen concentration (g O₂ m⁻³)

FCDP = fraction of predated carbon produced as dissolved organic carbon

K_{HR} = heterotrophic respiration rate of dissolved organic carbon (day⁻¹)

Denit = denitrification rate (day⁻¹) given in Eq. 3-4l.

The remaining of this section explains each term in Equations 3-2 to 3-4.

III-2-1. Effect of algae on organic carbon

The terms within summation (Σ) in Equations 3-2 to 3-4 account for the effects of algae on organic carbon through basal metabolism and predation.

A. Basal metabolism: Basal metabolism, consisting of respiration and excretion, returns algal matter (carbon, nitrogen, phosphorus and silica) back to the environment.

Loss of algal biomass through basal metabolism is (Eq. 3-1):

$$\frac{\partial B_x}{\partial t} = -BM_x \cdot B_x \quad (3-4a)$$

which indicates that the total loss of algal biomass due to basal metabolism is independent of ambient dissolved oxygen concentration. In this model, it is assumed that the distribution of total loss between respiration and excretion is constant as long as there is sufficient dissolved oxygen for algae to respire. Under that condition, the losses by respiration and excretion may be written as:

$$(1 - FCD_x) \cdot BM_x \cdot B_x \quad \text{due to respiration} \quad (3-4b)$$

$$FCD_x \cdot BM_x \cdot B_x \quad \text{due to excretion} \quad (3-4c)$$

where FCD_x is a constant of value between 0 and 1. Algae cannot respire in the absence of oxygen, however. Although the total loss of algal biomass due to basal metabolism is oxygen-independent (Eq. 3-4a), the distribution of total loss between respiration and excretion is oxygen-dependent. When oxygen level is high, respiration is a large fraction of the total. As dissolved oxygen becomes scarce, excretion becomes dominant. Thus, Eq. 3-4b represents the loss by respiration only at high oxygen level. In general, Eq. 3-4b can be decomposed into two fractions as a function of dissolved oxygen availability:

$$(1 - FCD_x) \frac{DO}{KHR_x + DO} BM_x \cdot B_x \quad \text{due to respiration} \quad (3-4d)$$

$$(1 - FCD_x) \frac{KHR_x}{KHR_x + DO} BM_x \cdot B_x \quad \text{due to excretion} \quad (3-4e)$$

Equation 3-4d represents the loss of algal biomass by respiration and Eq. 3-4e represents additional excretion due to insufficient dissolved oxygen concentration. The parameter KHR_x , which is defined as half-saturation constant of dissolved oxygen for algal dissolved organic carbon excretion in Eq. 3-4, can also be defined as half-saturation constant of dissolved oxygen for algal respiration in Eq. 3-4d.

Combining Equations 3-4c and 3-4e, the total loss due to excretion is:

$$\left[FCD_x + (1 - FCD_x) \frac{KHR_x}{KHR_x + DO} \right] BM_x \cdot B_x \quad (3-4f)$$

Equations 3-4d and 3-4f combine to give the total loss of algal biomass due to basal metabolism, $BM_x \cdot B_x$ (Eq. 3-4a). The definition of FCD_x in Eq. 3-4 becomes apparent in Eq. 3-4f; i.e., fraction of basal metabolism exuded as dissolved organic carbon at infinite dissolved oxygen concentration. At zero oxygen level, 100% of total loss due to basal metabolism is by excretion regardless of FCD_x .

The end carbon product of respiration is primarily carbon dioxide, an inorganic form not considered in the present model, while the end carbon product of excretion is

primarily dissolved organic carbon. Therefore, Eq. 3-4f, that appears in Eq. 3-4, represents the contribution of excretion to dissolved organic carbon, and there is no source term for particulate organic carbon from algal basal metabolism in Equations 3-2 and 3-3.

B. Predation: Algae produce organic carbon through the effects of predation. Zooplankton take up and redistribute algal carbon through grazing, assimilation, respiration and excretion. Since zooplankton are not included in the model, routing of algal carbon through zooplankton predation is simulated by empirical distribution coefficients in Equations 3-2 to 3-4; FCRP, FCLP and FCDP. The sum of these three predation fractions should be unity.

III-2-2. Heterotrophic respiration and dissolution

The second term on the RHS of Equations 3-2 and 3-3 represents dissolution of particulate to dissolved organic carbon and the third term in the second line of Eq. 3-4 represents heterotrophic respiration of dissolved organic carbon. The oxic heterotrophic respiration is a function of dissolved oxygen: the lower the dissolved oxygen, the smaller the respiration term becomes. Heterotrophic respiration rate, therefore, is expressed using a Monod function of dissolved oxygen:

$$K_{HR} = \frac{DO}{KHOR_{DO} + DO} K_{DOC} \quad (3-4g)$$

$KHOR_{DO}$ = oxic respiration half-saturation constant for dissolved oxygen ($g\ O_2\ m^{-3}$)

K_{DOC} = heterotrophic respiration rate of dissolved organic carbon at infinite dissolved oxygen concentration (day^{-1}).

Dissolution and heterotrophic respiration rates depend on the availability of carbonaceous substrate and on heterotrophic activity. Algae produce labile carbon that fuels heterotrophic activity: dissolution and heterotrophic respiration do not require the presence of algae though, and may be fueled entirely by external carbon inputs. In the model, algal biomass, as a surrogate for heterotrophic activity, is incorporated into formulations of dissolution and heterotrophic respiration rates. Formulations of these rates require specification of algal-dependent and algal-independent rates:

$$K_{RPOC} = (K_{RC} + K_{RCalg} \sum_{x=c,d,g} B_x) \cdot \exp(KT_{HDR}[T - TR_{HDR}]) \quad (3-4h)$$

$$K_{LPOC} = (K_{LC} + K_{LCalg} \sum_{x=c,d,g} B_x) \cdot \exp(KT_{HDR}[T - TR_{HDR}]) \quad (3-4i)$$

$$K_{DOC} = (K_{DC} + K_{DCalg} \sum_{x=c,d,g} B_x) \cdot \exp(KT_{MNL}[T - TR_{MNL}]) \quad (3-4j)$$

K_{RC} = minimum dissolution rate of refractory particulate organic carbon (day^{-1})

K_{LC} = minimum dissolution rate of labile particulate organic carbon (day^{-1})

K_{DC} = minimum respiration rate of dissolved organic carbon (day^{-1})

K_{RCalg} & K_{LCalg} = constants that relate dissolution of refractory and labile particulate organic carbon, respectively, to algal biomass (day^{-1} per g C m^{-3})

K_{DCalg} = constant that relates respiration to algal biomass (day^{-1} per g C m^{-3})

KT_{HDR} = effect of temperature on hydrolysis of particulate organic matter ($^{\circ}\text{C}^{-1}$)

TR_{HDR} = reference temperature for hydrolysis of particulate organic matter ($^{\circ}\text{C}$)

KT_{MNL} = effect of temperature on mineralization of dissolved organic matter ($^{\circ}\text{C}^{-1}$)

TR_{MNL} = reference temperature for mineralization of dissolved organic matter ($^{\circ}\text{C}$).

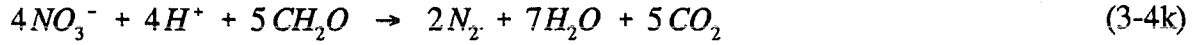
Equations 3-4h to 3-4j have exponential functions that relate rates to temperature.

In the present model, the term "hydrolysis" is defined as the process by which particulate organic matter is converted to dissolved organic form, and thus includes both dissolution of particulate carbon and hydrolysis of particulate phosphorus and nitrogen. Therefore, the parameters, KT_{HDR} and TR_{HDR} , are also used for the temperature effects on hydrolysis of particulate phosphorus (Equations 3-8f and 3-8g) and nitrogen (Equations 3-13b and 3-13c). The term "mineralization" is defined as the process by which dissolved organic matter is converted to dissolved inorganic form, and thus includes both heterotrophic respiration of dissolved organic carbon and mineralization of dissolved organic phosphorus and nitrogen. Therefore, the parameters, KT_{MNL} and TR_{MNL} , are also used for the temperature effects on mineralization of dissolved phosphorus (Eq. 3-8h) and nitrogen (Eq. 3-13d).

III-2-3. Effect of denitrification on dissolved organic carbon

As oxygen is depleted from natural systems, organic matter is oxidized by the

reduction of alternate electron acceptors. Thermodynamically, the first alternate acceptor reduced in the absence of oxygen is nitrate. The reduction of nitrate by a large number of heterotrophic anaerobes is referred to as denitrification, and the stoichiometry of this reaction is (Stumm & Morgan 1981):



The last term in Eq. 3-4 accounts for the effect of denitrification on dissolved organic carbon. The kinetics of denitrification in the model are first-order:

$$Denit = \frac{KHOR_{DO}}{KHOR_{DO} + DO} \frac{NO_3}{KHDN_N + NO_3} AANOX \cdot K_{DOC} \quad (3-4l)$$

$KHDN_N$ = denitrification half-saturation constant for nitrate ($g\ N\ m^{-3}$)

$AANOX$ = ratio of denitrification rate to oxic dissolved organic carbon respiration rate .

In Eq. 3-4l, the dissolved organic carbon respiration rate, K_{DOC} , is modified so that significant decomposition via denitrification occurs only when nitrate is freely available and dissolved oxygen is depleted. The ratio, $AANOX$, makes the anoxic respiration slower than oxic respiration. Note that K_{DOC} , defined in Eq. 3-4j, includes the temperature effect on denitrification.

III-3. Phosphorus

The present model has four state variables for phosphorus: one inorganic form (total phosphate) and three organic forms (dissolved, labile particulate and refractory particulate).

A. Particulate organic phosphorus: For refractory and labile particulate organic phosphorus, sources and sinks included in the model are (Fig. 3-1):

- : algal basal metabolism and predation
- : dissolution to dissolved organic phosphorus
- : settling

The governing equations for refractory and labile particulate organic phosphorus are:

$$\frac{\partial RPOP}{\partial t} = \sum_{x=c,d,g} (FPR_x \cdot BM_x + FPRP \cdot PR_x) APC \cdot B_x - K_{RPOP} \cdot RPOP - \frac{WS_{RP}}{h} RPOP \quad (3-5)$$

$$\frac{\partial LPOP}{\partial t} = \sum_{x=c,d,g} (FPL_x \cdot BM_x + FPLP \cdot PR_x) APC \cdot B_x - K_{LPOP} \cdot LPOP - \frac{WS_{LP}}{h} LPOP \quad (3-6)$$

RPOP = concentration of refractory particulate organic phosphorus (g P m⁻³)

LPOP = concentration of labile particulate organic phosphorus (g P m⁻³)

FPR_x = fraction of metabolized phosphorus by algal group x produced as refractory particulate organic phosphorus

FPL_x = fraction of metabolized phosphorus by algal group x produced as labile particulate organic phosphorus

FPRP = fraction of predated phosphorus produced as refractory particulate organic phosphorus

FPLP = fraction of predated phosphorus produced as labile particulate organic phosphorus

APC = mean phosphorus-to-carbon ratio in all algal groups (g P per g C)

K_{RPOP} = hydrolysis rate of refractory particulate organic phosphorus (day⁻¹)

K_{LPOP} = hydrolysis rate of labile particulate organic phosphorus (day⁻¹).

B. Dissolved organic phosphorus: Sources and sinks included in the model are (Fig. 3-1):

: algal basal metabolism and predation

: dissolution from refractory and labile particulate organic phosphorus

: mineralization to phosphate phosphorus

The governing equation describing these processes is:

$$\frac{\partial DOP}{\partial t} = \sum_{x=c,d,g} (FPD_x \cdot BM_x + FPDP \cdot PR_x) APC \cdot B_x + K_{RPOP} \cdot RPOP + K_{LPOP} \cdot LPOP - K_{DOP} \cdot DOP \quad (3-7)$$

DOP = concentration of dissolved organic phosphorus (g P m⁻³)

FPD_x = fraction of metabolized phosphorus by algal group x produced as dissolved organic phosphorus

FPDP = fraction of predated phosphorus produced as dissolved organic phosphorus

K_{DOP} = mineralization rate of dissolved organic phosphorus (day⁻¹).

C. Total phosphate: For total phosphate that includes both dissolved and sorbed

phosphate (Section III-3-1), sources and sinks included in the model are (Fig. 3-1):

- : algal basal metabolism, predation, and uptake
- : mineralization from dissolved organic phosphorus
- : settling of sorbed phosphate
- : sediment-water exchange of dissolved phosphate

The governing equation describing these processes is:

$$\frac{\partial PO4t}{\partial t} = \sum_{x=c,d,g} (FPI_x \cdot BM_x + FPIP \cdot PR_x - P_x) APC \cdot B_x + K_{DOP} \cdot DOP - \frac{WS_{TSS}}{h} PO4p + \frac{BFPO4}{h} \quad (3-8)*$$

$$PO4t = \text{total phosphate (g P m}^{-3}\text{)} = PO4d + PO4p \quad (3-8a)*$$

PO4d = dissolved phosphate (g P m⁻³)

PO4p = particulate (sorbed) phosphate (g P m⁻³)

FPI_x = fraction of metabolized phosphorus by algal group x produced as inorganic phosphorus

FPIP = fraction of predated phosphorus produced as inorganic phosphorus

WS_{TSS} = settling velocity of suspended solid (m day⁻¹)

BFPO4 = exchange flux of phosphate at sediment-water interface (g P m⁻² day⁻¹).

In Eq. 3-8, if total active metal is chosen as a measure of sorption site, the settling velocity of total suspended solid, WS_{TSS}, is replaced by that of particulate metal, WS_s, (Sections III-3-1 and III-9). The remaining of this section explains each term in Equations 3-5 to 3-8 with the total phosphate system detailed in Section III-3-1.

III-3-1. Total phosphate system

Suspended and bottom sediment particles (clay, silt and metal hydroxides) adsorb and desorb phosphate in river and estuarine waters. This adsorption-desorption process has been suggested to buffer phosphate concentration in water column and to enhance the transport of phosphate away from its external sources (Carritt & Goodgal 1954; Froelich 1988; Lebo 1991). To ease the computational complication due to the adsorption-desorption of phosphate, dissolved and sorbed phosphate are treated and transported as a

single state variable. Therefore, the model phosphate state variable, total phosphate, is defined as the sum of dissolved and sorbed phosphate (Eq. 3-8a), and the concentrations for each fraction are determined by equilibrium partitioning of their sum.

In CE-QUAL-ICM, sorption of phosphate to particulate species of metals including iron and manganese was considered based on phenomenon observed in the monitoring data from mainstem of Chesapeake Bay: phosphate was rapidly depleted from anoxic bottom waters during the autumn reaeration event (Cercio & Cole 1994). Their hypothesis was that reaeration of bottom waters caused dissolved iron and manganese to precipitate, and phosphate sorbed to newly-formed metal particles and rapidly settled to the bottom. One state variable, total active metal, in CE-QUAL-ICM was defined as the sum of all metals that act as sorption sites, and the total active metal was partitioned into particulate and dissolved fractions via an equilibrium partitioning coefficient (Section III-9). Then, phosphate was assumed to sorb to only the particulate fraction of the total active metal.

In the treatment of phosphate sorption in CE-QUAL-ICM, the particulate fraction of metal hydroxides was emphasized as a sorption site in bottom waters under anoxic conditions. Phosphorus is a highly particle-reactive element, and phosphate in solution reacts quickly with a wide variety of surfaces, being taken up by and released from particles (Froelich 1988). The present model has two options, total suspended solid and total active metal, as a measure of a sorption site for phosphate, and dissolved and sorbed fractions are determined by equilibrium partitioning of their sum as a function of total suspended solid or total active metal concentration:

$$PO4p = \frac{K_{PO4p} \cdot TSS}{1 + K_{PO4p} \cdot TSS} PO4t \quad \text{or} \quad PO4p = \frac{K_{PO4p} \cdot TAMp}{1 + K_{PO4p} \cdot TAMp} PO4t \quad (3-8b)^*$$

$$PO4d = \frac{1}{1 + K_{PO4p} \cdot TSS} PO4t \quad \text{or} \quad PO4d = \frac{1}{1 + K_{PO4p} \cdot TAMp} PO4t$$

$$= PO4t - PO4p \quad (3-8c)^*$$

K_{PO4p} = empirical coefficient relating phosphate sorption to total suspended solid (per g m^{-3}) or particulate total active metal (per mol m^{-3}) concentration

TAMp = particulate total active metal (mol m^{-3}).

Dividing Eq. 3-8b by Eq. 3-8c gives:

$$K_{PO4p} = \frac{PO4p}{PO4d} \frac{1}{TSS} \quad \text{or} \quad K_{PO4p} = \frac{PO4p}{PO4d} \frac{1}{TAMp} \quad (3-8d)$$

where the meaning of K_{PO4p} becomes apparent, i.e., the ratio of sorbed to dissolved phosphate per unit concentration of total suspended solid or particulate total active metal (i.e., per unit sorption site available).

III-3-2. Algal phosphorus-to-carbon ratio (APC)

Algal biomass is quantified in units of carbon per volume of water. In order to express the effects of algal biomass on phosphorus and nitrogen, the ratios of phosphorus-to-carbon and nitrogen-to-carbon in algal biomass must be specified. Although global mean values of these ratios are well known (Redfield et al. 1963), algal composition varies especially as a function of nutrient availability. As phosphorus and nitrogen become scarce, algae adjust their composition so that smaller quantities of these vital nutrients are required to produce carbonaceous biomass (DiToro 1980; Parsons et al. 1984). Examining the field data from the surface of upper Chesapeake Bay, Cerco & Cole (1994) showed that the variation of nitrogen-to-carbon stoichiometry was small and thus used a constant algal nitrogen-to-carbon ratio, ANC_x . Large variations, however, were observed for algal phosphorus-to-carbon ratio indicating the adaptation of algae to ambient phosphorus concentration (Cerco & Cole 1994): algal phosphorus content is high when ambient phosphorus is abundant and is low when ambient phosphorus is scarce. Thus, a variable algal phosphorus-to-carbon ratio, APC, is used in model formulation. A mean ratio for all algal group, APC, is described by an empirical approximation to the trend observed in field data (Cerco & Cole 1994):

$$APC = (CP_{pm1} + CP_{pm2} \cdot \exp[-CP_{pm3} \cdot PO4d])^{-1} \quad (3-8e)$$

CP_{pm1} = minimum carbon-to-phosphorus ratio (g C per g P)

CP_{pm2} = difference between minimum and maximum carbon-to-phosphorus ratio (g C per g P)

CP_{pm3} = effect of dissolved phosphate concentration on carbon-to-phosphorus ratio (per g P m^{-3}).

III-3-3. Effect of algae on phosphorus

The terms within summation (Σ) in Equations 3-5 to 3-8 account for the effects of algae on phosphorus. Both basal metabolism (respiration and excretion) and predation are considered, and thus formulated, to contribute to organic and phosphate phosphorus. That is, the total loss by basal metabolism ($BM_x \cdot B_x$ in Eq. 3-1) is distributed using distribution coefficients; FPR_x , FPL_x , FPD_x and FPI_x . The total loss by predation ($PR_x \cdot B_x$ in Eq. 3-1), is also distributed using distribution coefficients; $FPRP$, $FPLP$, $FPDP$ and $FPIP$. The sum of four distribution coefficients for basal metabolism should be unity, and so is that for predation. Algae take up dissolved phosphate for growth, and algae uptake of phosphate is represented by $(-\Sigma P_x \cdot APC \cdot B_x)$ in Eq. 3-8.

III-3-4. Mineralization and hydrolysis

The third term on the RHS of Equations 3-5 and 3-6 represents hydrolysis of particulate organic phosphorus and the last term in Eq. 3-7 represents mineralization of dissolved organic phosphorus. Mineralization of organic phosphorus is mediated by the release of nucleotidase and phosphatase enzymes by bacteria (Chróst & Overbek 1987) and algae (Boni et al. 1989). Since the algae themselves release the enzymes and bacterial abundance is related to algal biomass, the rate of organic phosphorus mineralization is related to algal biomass in model formulation. Another mechanism included in model formulation is that algae stimulate production of an enzyme that mineralizes organic phosphorus to phosphate when phosphate is scarce (Chróst & Overbek 1987; Boni et al. 1989). The formulations for hydrolysis and mineralization rates including these processes are:

$$K_{RPOP} = (K_{RP} + \frac{KHP}{KHP + PO4d} K_{RPalg} \sum_{x=c,d,g} B_x) \cdot \exp(KT_{HDR}[T - TR_{HDR}]) \quad (3-8f)$$

$$K_{LPOP} = (K_{LP} + \frac{KHP}{KHP + PO4d} K_{LPalg} \sum_{x=c,d,g} B_x) \cdot \exp(KT_{HDR}[T - TR_{HDR}]) \quad (3-8g)$$

$$K_{DOP} = (K_{DP} + \frac{KHP}{KHP + PO4d} K_{DPalg} \sum_{x=c,d,g} B_x) \cdot \exp(KT_{MNL}[T - TR_{MNL}]) \quad (3-8h)$$

K_{RP} = minimum hydrolysis rate of refractory particulate organic phosphorus (day^{-1})

K_{LP} = minimum hydrolysis rate of labile particulate organic phosphorus (day^{-1})
 K_{DP} = minimum mineralization rate of dissolved organic phosphorus (day^{-1})
 K_{RPaig} & K_{LPaig} = constants that relate hydrolysis of refractory and labile particulate organic phosphorus, respectively, to algal biomass (day^{-1} per g P m^{-3})
 K_{DPaig} = constant that relates mineralization to algal biomass (day^{-1} per g P m^{-3})
 KHP = mean half-saturation constant for algal phosphorus uptake (g P m^{-3})

$$= \frac{1}{3} \sum_{x=c,d,g} KHP_x \quad (3-8i)$$

When phosphate is abundant relative to KHP , the rates become to be close to the minimum values with little influence from algal biomass. When phosphate becomes scarce relative to KHP , the rates increase with the magnitude of increase depending on algal biomass. Equations 3-8f to 3-8h have exponential functions that relate rates to temperature.

III-4. Nitrogen

The present model has five state variables for nitrogen: two inorganic forms (nitrate and ammonium) and three organic forms (dissolved, labile particulate and refractory particulate). The nitrate state variable in the model represents the sum of nitrate and nitrite.

A. Particulate organic nitrogen: For refractory and labile particulate organic nitrogen, sources and sinks included in the model are (Fig. 3-1):

- : algal basal metabolism and predation
- : dissolution to dissolved organic nitrogen
- : settling

The governing equations for refractory and labile particulate organic nitrogen are:

$$\frac{\partial RPON}{\partial t} = \sum_{x=c,d,g} (FNR_x \cdot BM_x + FNRP \cdot PR_x) ANC_x \cdot B_x - K_{RPON} \cdot RPON - \frac{WS_{RP}}{h} RPON \quad (3-9)$$

$$\frac{\partial LPON}{\partial t} = \sum_{x=c,d,g} (FNL_x \cdot BM_x + FNLP \cdot PR_x) ANC_x \cdot B_x - K_{LPON} \cdot LPON - \frac{WS_{LP}}{h} LPON \quad (3-10)$$

$RPON$ = concentration of refractory particulate organic nitrogen (g N m^{-3})

LPON = concentration of labile particulate organic nitrogen (g N m^{-3})

FNR_x = fraction of metabolized nitrogen by algal group x produced as refractory particulate organic nitrogen

FNL_x = fraction of metabolized nitrogen by algal group x produced as labile particulate organic nitrogen

FNRP = fraction of predated nitrogen produced as refractory particulate organic nitrogen

FNLP = fraction of predated nitrogen produced as labile particulate organic nitrogen

ANC_x = nitrogen-to-carbon ratio in algal group x (g N per g C)

K_{RPON} = hydrolysis rate of refractory particulate organic nitrogen (day^{-1})

K_{LPON} = hydrolysis rate of labile particulate organic nitrogen (day^{-1}).

B. Dissolved organic nitrogen: Sources and sinks included in the model are (Fig. 3-1):

: algal basal metabolism and predation

: dissolution from refractory and labile particulate organic nitrogen

: mineralization to ammonium

The governing equation describing these processes is:

$$\frac{\partial DON}{\partial t} = \sum_{x=c,d,g} (FND_x \cdot BM_x + FNDP \cdot PR_x) ANC_x \cdot B_x + K_{RPON} \cdot RPON + K_{LPON} \cdot LPON - K_{DON} \cdot DON \quad (3-11)$$

DON = concentration of dissolved organic nitrogen (g N m^{-3})

FND_x = fraction of metabolized nitrogen by algal group x produced as dissolved organic nitrogen

FNDP = fraction of predated nitrogen produced as dissolved organic nitrogen

K_{DON} = mineralization rate of dissolved organic nitrogen (day^{-1}).

C. Ammonium nitrogen: Sources and sinks included in the model are (Fig. 3-1):

: algal basal metabolism, predation, and uptake

: mineralization from dissolved organic nitrogen

: nitrification to nitrate

: sediment-water exchange

The governing equation describing these processes is:

$$\frac{\partial NH4}{\partial t} = \sum_{x=c,d,g} (FNI_x \cdot BM_x + FNIP \cdot PR_x - PN_x \cdot P_x) ANC_x \cdot B_x + K_{DON} \cdot DON - Nit \cdot NH4 + \frac{BFNH4}{h} \quad (3-12)$$

FNI_x = fraction of metabolized nitrogen by algal group x produced as inorganic nitrogen

$FNIP$ = fraction of predated nitrogen produced as inorganic nitrogen

PN_x = preference for ammonium uptake by algal group x ($0 \leq PN_x \leq 1$)

Nit = nitrification rate (day^{-1}) given in Eq. 3-13g

$BFNH4$ = exchange flux of ammonium at sediment-water interface ($\text{g N m}^{-2} \text{ day}^{-1}$).

D. Nitrate nitrogen: Sources and sinks included in the model are (Fig. 3-1):

- : algal uptake
- : nitrification from ammonium
- : denitrification to nitrogen gas
- : sediment-water exchange

The governing equation describing these processes is:

$$\frac{\partial NO3}{\partial t} = - \sum_{x=c,d,g} (1 - PN_x) P_x \cdot ANC_x \cdot B_x + Nit \cdot NH4 - ANDC \cdot Denit \cdot DOC + \frac{BFNO3}{h} \quad (3-13)$$

$ANDC$ = mass of nitrate nitrogen reduced per mass of dissolved organic carbon oxidized
(0.933 g N per g C from Eq. 3-4k)

$BFNO3$ = exchange flux of nitrate at sediment-water interface ($\text{g N m}^{-2} \text{ day}^{-1}$).

The remaining of this section explains each term in Equations 3-9 to 3-13.

III-4-1. Effect of algae on nitrogen

The terms within summation (Σ) in Equations 3-9 to 3-13 account for the effects of algae on nitrogen. As in phosphorus, both basal metabolism (respiration and excretion) and predation are considered, and thus formulated, to contribute to organic and ammonium nitrogen. That is, algal nitrogen released by both basal metabolism and predation are represented by distribution coefficients; FNR_x , FNL_x , FND_x , FNI_x , $FNRP$,

FNLP, FNDP and FNIP. The sum of four distribution coefficients for basal metabolism should be unity, and so is that for predation.

Algae take up ammonium and nitrate for growth, and ammonium is preferred from thermodynamic considerations. The preference of algae for ammonium is expressed as:

$$PN_x = NH4 \frac{NO3}{(KHN_x + NH4)(KHN_x + NO3)} + NH4 \frac{KHN_x}{(NH4 + NO3)(KHN_x + NO3)} \quad (3-13a)$$

This equation forces the preference for ammonium to be unity when nitrate absent, and to be zero when ammonium is absent.

III-4-2. Mineralization and hydrolysis

The third term on the RHS of Equations 3-9 and 3-10 represents hydrolysis of particulate organic nitrogen and the last term in Eq. 3-11 represents mineralization of dissolved organic nitrogen. Including a mechanism for accelerated hydrolysis and mineralization during nutrient-limited conditions (Section III-3-4), the formulations for these processes are:

$$K_{RPN} = (K_{RN} + \frac{KHN}{KHN + NH4 + NO3} K_{RNalg} \sum_{x=c,d,g} B_x) \cdot \exp(KT_{HDR}[T - TR_{HDR}]) \quad (3-13b)$$

$$K_{LPON} = (K_{LN} + \frac{KHN}{KHN + NH4 + NO3} K_{LNalg} \sum_{x=c,d,g} B_x) \cdot \exp(KT_{HDR}[T - TR_{HDR}]) \quad (3-13c)$$

$$K_{DON} = (K_{DN} + \frac{KHN}{KHN + NH4 + NO3} K_{DNalg} \sum_{x=c,d,g} B_x) \cdot \exp(KT_{MNL}[T - TR_{MNL}]) \quad (3-13d)$$

K_{RN} = minimum hydrolysis rate of refractory particulate organic nitrogen (day^{-1})

K_{LN} = minimum hydrolysis rate of labile particulate organic nitrogen (day^{-1})

K_{DN} = minimum mineralization rate of dissolved organic nitrogen (day^{-1})

K_{RNalg} & K_{LNalg} = constants that relate hydrolysis of refractory and labile particulate organic nitrogen, respectively, to algal biomass (day^{-1} per g N m^{-3})

K_{DNalg} = constant that relates mineralization to algal biomass (day^{-1} per g N m^{-3})

KHN = mean half-saturation constant for algal nitrogen uptake (g N m^{-3})

$$= \frac{1}{3} \sum_{x=c,d,g} KHN_x \quad (3-13e)$$

Equations 3-13b to 3-13d have exponential functions that relate rates to temperature.

III-4-3. Nitrification

Nitrification is a process mediated by autotrophic nitrifying bacteria that obtain energy through the oxidation of ammonium to nitrite and of nitrite to nitrate. The stoichiometry of complete reaction is (Bowie et al. 1985):



The first term in the second line of Eq. 3-12 and its corresponding term in Eq. 3-13 represent the effect of nitrification on ammonium and nitrate, respectively. The kinetics of complete nitrification process are formulated as a function of available ammonium, dissolved oxygen and temperature:

$$Nit = \frac{DO}{KHNit_{DO} + DO} \frac{1}{KHNit_N + NH_4} Nit_m \cdot f_{Nit}(T) \quad (3-13g)$$

$$\begin{aligned} f_{Nit}(T) &= \exp(-KNit1[T - TNit]^2) && \text{if } T \leq TNit \\ &= \exp(-KNit2[TNit - T]^2) && \text{if } T > TNit \end{aligned} \quad (3-13g-1)$$

$KHNit_{DO}$ = nitrification half-saturation constant for dissolved oxygen (g O₂ m⁻³)

$KHNit_N$ = nitrification half-saturation constant for ammonium (g N m⁻³)

Nit_m = maximum nitrification rate at $TNit$ (g N m⁻³ day⁻¹)

$TNit$ = optimum temperature for nitrification (°C)

$KNit1$ = effect of temperature below $TNit$ on nitrification rate (°C⁻²)

$KNit2$ = effect of temperature above $TNit$ on nitrification rate (°C⁻²).

The Monod function of dissolved oxygen in Eq. 3-13g indicates the inhibition of nitrification at low oxygen level. The Monod function of ammonium indicates that when ammonium is abundant, the nitrification rate is limited by availability of nitrifying bacteria. The effect of suboptimal temperature is represented using Gaussian form.

III-4-4. Denitrification

The effect of denitrification on dissolved organic carbon is described in Section III-2-3. Denitrification removes nitrate from the system in stoichiometric proportion to carbon removal as determined by Eq. 3-4k. The last term in the first line of Eq. 3-13

represent this removal of nitrate.

III-5. Silica

The present model has two state variables for silica: available silica and particulate biogenic silica.

A. Particulate biogenic silica: Sources and sinks included in the model are (Fig. 3-1):

- : diatom basal metabolism and predation
- : dissolution to available silica
- : settling

The governing equation describing these processes is:

$$\frac{\partial SU}{\partial t} = (FSP_d \cdot BM_d + FSPP \cdot PR_d) ASC_d \cdot B_d - K_{SUA} \cdot SU - \frac{WS_d}{h} SU \quad (3-14)*$$

SU = concentration of particulate biogenic silica (g Si m⁻³).

FSP_d = fraction of metabolized silica by diatoms produced as particulate biogenic silica

FSPP = fraction of predated diatom silica produced as particulate biogenic silica

ASC_d = silica-to-carbon ratio of diatoms (g Si per g C)

K_{SUA} = dissolution rate of particulate biogenic silica (day⁻¹).

B. Available silica: Sources and sinks included in the model are (Fig. 3-1):

- : diatom basal metabolism, predation, and uptake
- : settling of sorbed (particulate) available silica
- : dissolution from particulate biogenic silica
- : sediment-water exchange of dissolved silica

The governing equation describing these processes is:

$$\frac{\partial SA}{\partial t} = (FSI_d \cdot BM_d + FSIP \cdot PR_d - P_d) ASC_d \cdot B_d + K_{SUA} \cdot SU - \frac{WS_{TSS}}{h} SAP + \frac{BFSA}{h} \quad (3-15)*$$

SA = concentration of available silica (g Si m⁻³) = SAd + SAP (3-15a)

SAd = dissolved available silica (g Si m⁻³)

SAP = particulate (sorbed) available silica (g Si m⁻³)

FSI_d = fraction of metabolized silica by diatoms produced as available silica

FSIP = fraction of predated diatom silica produced as available silica

BFSA = exchange flux of available silica at sediment-water interface (g Si m⁻² day⁻¹). In Eq. 3-15, if total active metal is chosen as a measure of sorption site, the settling velocity of total suspended solid, WS_{TSS}, is replaced by that of particulate metal, WS_p (Sections III-5-1 and III-9). The remaining of this section explains each term in Equations 3-14 and 3-15.

III-5-1. Available silica system

Analysis of Chesapeake Bay monitoring data indicates that silica shows similar behavior as phosphate in adsorption-desorption process (Cercio & Cole 1994). As in phosphate, therefore, available silica is defined to include both dissolved and sorbed fractions (Eq. 3-15a). Treatment of available silica is the same as total phosphate and the same method to partition dissolved and sorbed phosphate is used to partition dissolved and sorbed available silica:

$$S_{Ap} = \frac{K_{SAp} \cdot TSS}{1 + K_{SAp} \cdot TSS} SA \quad \text{or} \quad S_{Ap} = \frac{K_{SAp} \cdot TAMp}{1 + K_{SAp} \cdot TAMp} SA \quad (3-15b)^*$$

$$S_{Ad} = \frac{1}{1 + K_{SAp} \cdot TSS} SA \quad \text{or} \quad S_{Ad} = \frac{1}{1 + K_{SAp} \cdot TAMp} SA$$

$$= SA - S_{Ap} \quad (3-15c)^*$$

K_{SAp} = empirical coefficient relating available silica sorption to total suspended solid (per g m⁻³) or particulate total active metal (per mol m⁻³) concentration.

As in K_{PO₄p} in Section III-3-1, K_{SAp} is the ratio of sorbed to dissolved available silica per unit sorption site available.

III-5-2. Effect of diatoms on silica

In Equations 3-14 and 3-15, those terms expressed as a function of diatom biomass (B_d) account for the effects of diatoms on silica. As in phosphorus and nitrogen, both basal metabolism (respiration and excretion) and predation are considered, and thus formulated, to contribute to particulate biogenic and available silica. That is, diatom silica released by both basal metabolism and predation are represented by distribution coefficients; FSP_d, FSI_d, FSPP and FSIP. The sum of two distribution coefficients for

basal metabolism should be unity, and so is that for predation. Diatoms require silica as well as phosphorus and nitrogen, and diatom uptake of available silica is represented by $(-P_d \cdot ASC_d \cdot B_d)$ in Eq. 3-15.

III-5-3. Dissolution

The term $(-K_{SUA} \cdot SU)$ in Eq. 3-14 and its corresponding term in Eq. 3-15 represent dissolution of particulate biogenic silica to available silica. The dissolution rate is expressed as an exponential function of temperature:

$$K_{SUA} = K_{SU} \cdot \exp(KT_{SUA}[T - TR_{SUA}]) \quad (3-15d)$$

K_{SU} = dissolution rate of particulate biogenic silica at TR_{SUA} (day^{-1})

KT_{SUA} = effect of temperature on dissolution of particulate biogenic silica ($^{\circ}\text{C}^{-1}$)

TR_{SUA} = reference temperature for dissolution of particulate biogenic silica ($^{\circ}\text{C}$).

III-6. Chemical Oxygen Demand

In the present model, chemical oxygen demand is the concentration of reduced substances that are oxidizable through inorganic means. The source of chemical oxygen demand in saline water is sulfide released from sediments. A cycle occurs in which sulfate is reduced to sulfide in the sediments and reoxidized to sulfate in the water column. In freshwater, methane is released to water column by the sediment process model. Both sulfide and methane are quantified in units of oxygen demand and are treated with the same kinetic formulation. The governing equation is:

$$\frac{\partial COD}{\partial t} = -\frac{DO}{KH_{COD} + DO} KCOD \cdot COD + \frac{BFCOD}{h} \quad (3-16)$$

COD = concentration of chemical oxygen demand ($\text{g O}_2\text{-equivalents m}^{-3}$)

KH_{COD} = half-saturation constant of dissolved oxygen required for oxidation of chemical oxygen demand ($\text{g O}_2 \text{ m}^{-3}$)

$KCOD$ = oxidation rate of chemical oxygen demand (day^{-1})

$BFCOD$ = sediment flux of chemical oxygen demand ($\text{g O}_2\text{-equivalents m}^{-2} \text{ day}^{-1}$).

An exponential function is used to describe the temperature effect on the oxidation rate of chemical oxygen demand:

$$K_{COD} = K_{CD} \cdot \exp(KT_{COD}[T - TR_{COD}]) \quad (3-16a)$$

K_{CD} = oxidation rate of chemical oxygen demand at TR_{COD} (day^{-1})

KT_{COD} = effect of temperature on oxidation of chemical oxygen demand ($^{\circ}\text{C}^{-1}$)

TR_{COD} = reference temperature for oxidation of chemical oxygen demand ($^{\circ}\text{C}$).

III-7. Dissolved Oxygen

Sources and sinks of dissolved oxygen in the water column included in the model are (Fig. 3-1):

- : algal photosynthesis and respiration
- : nitrification
- : heterotrophic respiration of dissolved organic carbon
- : oxidation of chemical oxygen demand
- : surface reaeration
- : sediment oxygen demand

The governing equation describing these processes is:

$$\begin{aligned} \frac{\partial DO}{\partial t} = & \sum_{x=c,d,g} \left[(1.3 - 0.3 \cdot PN_x) P_x - (1 - FCD_x) \frac{DO}{K_{HR_x} + DO} BM_x \right] AOCR \cdot B_x \\ & - AONT \cdot Nit \cdot NH4 - AOCR \cdot K_{HR} \cdot DOC - \frac{DO}{K_{H_{COD}} + DO} K_{COD} \cdot COD \\ & + K_r (DO_s - DO) + \frac{SOD}{h} \end{aligned} \quad (3-17)$$

$AONT$ = mass of dissolved oxygen consumed per unit mass of ammonium nitrogen nitrified (4.33 g O_2 per g N: Section III-7-2)

$AOCR$ = dissolved oxygen-to-carbon ratio in respiration (2.67 g O_2 per g C: Section III-7-1)

K_r = reaeration coefficient (day^{-1})

DO_s = saturated concentration of dissolved oxygen ($\text{g O}_2 \text{ m}^{-3}$)

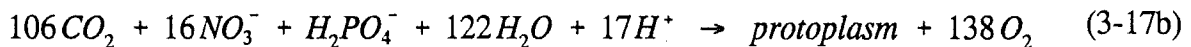
SOD = sediment oxygen demand ($\text{g O}_2 \text{ m}^{-2} \text{ day}^{-1}$): positive is to the water column.

The two sink terms in Eq. 3-17, heterotrophic respiration and chemical oxygen demand, are explained in Sections III-2-2 (Eq. 3-4g) and III-6 (Eq. 3-16), respectively. The

remaining of this section explains the effects of algae, nitrification and surface reaeration.

III-7-1. Effect of algae on dissolved oxygen

The first line on the RHS of Eq. 3-17 accounts for the effects of algae on dissolved oxygen. Algae produce oxygen through photosynthesis and consume oxygen through respiration. The quantity produced depends on the form of nitrogen utilized for growth. Equations describing production of dissolved oxygen are (Morel 1983):



When ammonium is the nitrogen source, one mole of oxygen is produced per mole of carbon dioxide fixed. When nitrate is the nitrogen source, 1.3 moles of oxygen are produced per mole of carbon dioxide fixed. The quantity, $(1.3 - 0.3 \cdot PN_x)$, in the first term of Eq. 3-17 is the photosynthesis ratio and represent the molar quantity of oxygen produced per mole of carbon dioxide fixed. It approaches unity as the algal preference for ammonium approaches unity.

The last term in the first line of Eq. 3-17 accounts for the oxygen consumption due to algal respiration (Eq. 3-4d). A simple representation of respiration process is:



from which, $AOCR = 2.67 \text{ g } O_2 \text{ per g C.}$

III-7-2. Effect of nitrification on dissolved oxygen

The stoichiometry of nitrification reaction (Eq. 3-13f) indicates that two moles of oxygen are required to nitrify one mole of ammonium into nitrate. However, cell synthesis by nitrifying bacteria is accomplished by the fixation of carbon dioxide so that less than two moles of oxygen are consumed per mole ammonium utilized (Wezernak & Gannon 1968): $AONT = 4.33 \text{ g } O_2 \text{ per g N.}$

III-7-3. Effect of surface reaeration on dissolved oxygen

The reaeration rate of dissolved oxygen at the air-water interface is proportional to

the oxygen gradient across the interface, ($DO_s - DO$), when assuming the air is saturated with oxygen. The saturated concentration of dissolved oxygen, which decreases as temperature and salinity increase, is specified using an empirical formula (Genet et al. 1974):

$$DO_s = 14.5532 - 0.38217 \cdot T + 5.4258 \times 10^{-3} \cdot T^2 - CL \cdot (1.665 \times 10^{-4} - 5.866 \times 10^{-6} \cdot T + 9.796 \times 10^{-8} \cdot T^2) \quad (3-17d)$$

CL = chloride concentration = S/1.80655.

The reaeration coefficient includes the effect of turbulence generated by bottom friction (O'Connor & Dobbins 1958) and that by surface wind stress (Banks & Herrera 1977):

$$K_r = \left[K_{ro} \sqrt{\frac{u_{eq}}{h_{eq}}} + W_{rea} \right] \frac{1}{h} \cdot KT_r^{T-20} \quad (3-17e)$$

K_{ro} = proportionality constant = 3.933 in MKS unit

u_{eq} = weighted velocity over cross-section ($m \text{ sec}^{-1}$)

h_{eq} = weighted depth over cross-section (m)

W_{rea} = wind-induced reaeration ($m \text{ day}^{-1}$)

$$= 0.728 U_w^{1/2} - 0.317 U_w + 0.0372 U_w^2 \quad (3-17f)$$

U_w = wind speed ($m \text{ sec}^{-1}$) at the height of 10 m above surface

KT_r = constant for temperature adjustment of DO reaeration rate.

III-8. Total Suspended Solid

The total suspended solid state variable is the sum of fixed (non-volatile \approx inorganic) and volatile (\approx organic) solids. The present model requires simulation of suspended solid for two processes, light attenuation, and adsorption of phosphate and silica (Fig. 3-1). One sink of suspended solid in water column is settling of solid particles. As far as phosphate adsorption and particle settling are concerned, fixed and volatile solids may behave differently. We, however, view the suspended solid to be present in natural waters as a aggregate of fixed and volatile solids, and thus do not differentiate fixed and volatile solids, which results in one model state variable, total

suspended solid.

Volatile (\approx organic) solid includes algae, particulate carbon, particulate phosphorus, particulate nitrogen and particulate biogenic silica, which makes the total suspended solid nonconservative. Examination of particulate data from lower Chesapeake Bay and York River collected in 1988 (Mo et al. 1993) indicates that five biogenic particulates (algae, particulate carbon, particulate phosphorus, particulate nitrogen and particulate biogenic silica) accounted for a mean of only 10% of total suspended solid. In the present model, therefore, the total suspended solid is assumed to be conservative, i.e., neglecting the changes caused by five biogenic particulates.

Possible sources and sinks for total suspended solid are:

- : resuspension from the bottom
- : deposition to the bottom
- : settling

A tidal average model, such as tidal prism model, does not calculate intratidal velocity, which makes the estimation of bottom shear stress unfeasible. Lack of bottom shear stress makes it difficult to represent the resuspension and deposition terms in model formulation. In the present model (one-dimensional, tidal average model), therefore, one net term is used to represent the net effect of resuspension and deposition of suspended solid. Then, the governing equation for total suspended solid may be written as:

$$\frac{\partial TSS}{\partial t} = \frac{RD_{TSS}}{h} - \frac{WS_{TSS}}{h} TSS \quad (3-18)$$

RD_{TSS} = net rate of resuspension and deposition ($\text{g m}^{-2} \text{day}^{-1}$).

The rate term, RD_{TSS} , represents the net effect of resuspension and deposition of suspended solid, and thus has to be calibrated.

III-9. Total Active Metal

The present model requires simulation of total active metal for adsorption of phosphate and silica if that option is chosen (Fig. 3-1). The total active metal state variable is the sum of iron and manganese concentrations, both particulate and dissolved. In the model, the origin of total active metal is benthic sediments. Since sediment release

of metal is not explicit in the sediment model (Chapter IV), release is specified in the kinetic portion of the water column model. The only other term included is settling of the particulate fraction. Then, the governing equation for total active metal may be written as:

$$\frac{\partial TAM}{\partial t} = \frac{KHbmf}{KHbmf + DO} \frac{BFTAM}{h} e^{K_{tam}(T - T_{tam})} - \frac{WS_s}{h} TAMp \quad (3-19)$$

$$TAM = \text{total active metal concentration (mol m}^{-3}\text{)} = TAMd + TAMp \quad (3-19a)$$

TAMd = dissolved total active metal (mol m⁻³)

TAMp = particulate total active metal (mol m⁻³)

KHbmf = dissolved oxygen concentration at which total active metal release is half the anoxic release rate (g O₂ m⁻³)

BFTAM = anoxic release rate of total active metal (mol m⁻² day⁻¹)

K_{tam} = effect of temperature on sediment release of total active metal (°C⁻¹)

T_{tam} = reference temperature for sediment release of total active metal (°C).

WS_s = settling velocity of particulate metal (m day⁻¹).

In estuaries, iron and manganese exist in particular and dissolved forms depending on dissolved oxygen concentration. In the oxygenated water, most of iron and manganese exist as particulate while under anoxic conditions, large fractions are dissolved although solid-phase sulfides and carbonates exist and may predominate. The partitioning between particulate and dissolved phases is expressed using a concept that total active metal concentration must achieve a minimum level, which is a function of dissolved oxygen, before precipitation occurs:

$$TAMd = \text{minimum}\{TAMdmx \cdot \exp(-K_{dotam} \cdot DO), TAM\} \quad (3-19b-1)$$

$$TAMp = TAM - TAMd \quad (3-19b-2)$$

TAMdmx = solubility of total active metal under anoxic conditions (mol m⁻³)

K_{dotam} = constant that relates total active metal solubility to dissolved oxygen concentration (per g O₂ m⁻³).

The behavior of Eq. 3-19b is illustrated in Fig. 4-19 of Cerco & Cole (1994).

III-10. Fecal Coliform Bacteria

Fecal coliform bacteria are indicative of organisms from the intestinal tract of humans and other animals and can be used as an indicator bacteria as a measure of public health (Thomann & Mueller 1987). In the present model, fecal coliform bacteria have no interaction with other state variables, and have only one sink term, die-off. The governing equation may be written as:

$$\frac{\partial FCB}{\partial t} = - KFCB \cdot TFCB^{T - 20} \cdot FCB \quad (3-20)$$

FCB = bacteria concentration (MPN per 100 ml)

KFCB = first order die-off rate at 20°C (day⁻¹)

TFCB = effect of temperature on decay of bacteria (°C⁻¹).

III-11. Temperature

Temperature affects most of rate coefficients. For practical purposes, in the present model, the heat balance equation is written as a conservation of mass equation for temperature. Two processes are included: exchange with atmosphere and with sediment. The rate of change due to exchange with atmosphere is considered proportional to the temperature difference between the water surface and a theoretical equilibrium temperature (Edinger et al. 1974). The rate of change due to exchange with sediment is modeled based on the diffusion of heat between the water column and sediment (Eq. 4-40). The governing equation may be written as:

$$\frac{\partial T}{\partial t} = \frac{KT}{\rho \cdot C_p \cdot h} (T_e - T) + \frac{D_T}{H^2} (T_s - T) \quad (3-21)$$

KT = heat exchange coefficient (watt m⁻² °C⁻¹)

ρ = density of water (1000 kg m⁻³)

C_p = specific heat of water (4186 watt sec kg⁻¹ °C⁻¹)

T_e = equilibrium temperature (°C)

D_T = heat diffusion coefficient between the water column and sediment (m² sec⁻¹)

H = sediment depth (m)

T_s = sediment temperature given by Eq. 4-40.

The heat exchange coefficient is a function of water temperature and wind speed, and the equilibrium temperature is defined as the hypothetical temperature at which the net rate of surface heat exchange would be zero (Edinger et al. 1974). Since KT and T_e are coupled via water temperature and meteorological conditions, these parameters are evaluated using iterative techniques described in Edinger et al. (1974) and provided as input. The last term in Eq. 3-21, that represents the heat loss to the sediment, is applied only when the sediment process model is activated.

Another option in the present model for water temperature is to use an annual sinusoidal curve:

$$T = \frac{T_{\max} + T_{\min}}{2} + \frac{T_{\max} - T_{\min}}{2} \cdot \cos \left[\frac{2\pi}{T_p} [t - t_{\max}] \right] \quad (3-21-1)$$

T_{\max} and T_{\min} = annual maximum and minimum water temperatures ($^{\circ}\text{C}$), respectively

T_p = a period = 365 days

t_{\max} = number of days since January 1 to reach T_{\max} .

III-12. Method of Solution for Kinetic Equations

This section describes the solution method of the BGC kinetic equations. The equation numbers with a \$ mark are those used in the computer program source code. As explained in Section II-4, the calculation of nonconservative water quality state variables is performed in multi-steps. First, the concentration fields are updated for the kinetic processes for a half tidal cycle. Then, the calculated concentration fields are modified by the physical transport processes and external sources for an entire tidal cycle using Eq. 2-13, 2-17 or 2-23. Finally, the calculated concentration fields are updated for the kinetic processes for the remaining half tidal cycle to give the concentration fields at the next high tide. The source code is written in such a way that one can divide the calculation of the BGC kinetic term into as many steps as needed over a half tidal cycle to prevent negative concentration. Therefore, the time step for the BGC kinetic term, Δt_{BGC} , is less than, or equal to, a half tidal cycle (Section II-4).

Finite difference solution of differential equation has a truncation error, the magnitude of which is proportional to the time step (Δt) used. For example, the second

order term that is often neglected in finite difference solution is proportional to $(K \cdot \Delta t)^2/2$ where K is a rate coefficient. In a tidal average model such as tidal prism model, the time step ($\Delta t_{\text{BGC}} \leq 6.21$ hours) may be large enough to make truncation error significant depending on the magnitude of K. To avoid truncation error, analytical solutions, rather than finite difference solutions, for the linearized differential equations of the kinetic processes are used in the present tidal prism model. When solving differential equations, it is assumed that all terms in the RHS of differential equations are known except for the state variable for which each equation is being solved, as long as this treatment does not violate mass conservation. Exceptions are explained below whenever encountered. To facilitate the analytical solution, the differential equations are solved in the following order in the source code.

A. First, temperature and total suspended solid are solved. Then, total active metal, if chosen as sorption site, is solved. The governing equation for temperature (Eq. 3-21) may be written as:

$$\frac{\partial T}{\partial t} = R_T^O - K_T^O \cdot T \quad (3-22)$$

$$K_T^O = \frac{KT}{\rho \cdot C_p \cdot h} + \frac{D_T}{H^2} \quad (3-22-1)$$

$$R_T^O = \frac{KT}{\rho \cdot C_p \cdot h} T_e + \frac{D_T}{H^2} T_s^O \quad (3-22-2)$$

The analytical solution of Eq. 3-22 is:

$$T^N = \left[T^O - \frac{R_T^O}{K_T^O} \right] e^{-K_T^O \Delta t} + \frac{R_T^O}{K_T^O} \quad (3-22\$)$$

$\Delta t = \Delta t_{\text{BGC}} =$ time increment for the kinetic processes ≤ 6.21 hours.

The superscripts O and N designates the variables before and after, respectively, being adjusted for the relevant kinetic processes. The temperature is calculated using Eq. 3-22\$ after evaluating K_T^O and R_T^O using Equations 3-22-1 and 3-22-2. Then, the average temperature between t_o and $t_o + \Delta t$ is calculated using:

$$T^A = \frac{1}{\Delta t} \int_{t^o}^{t^o + \Delta t} T \cdot dt = \frac{T^o - T^N}{\Delta t \cdot K_T^o} + \frac{R_T^o}{K_T^o} \quad (3-22\$-1)$$

The use of interval average, T^A , will become clear below.

The governing equation for total suspended solid (Eq. 3-18) may be written as:

$$\frac{\partial TSS}{\partial t} = R_{TSS}^o - K_{TSS}^o \cdot TSS \quad (3-23)$$

$$K_{TSS}^o = \frac{WS_{TSS}}{h} \quad (3-23-1)$$

$$R_{TSS}^o = \frac{RD_{TSS}}{h} \quad (3-23-2)$$

Equation 3-23 can be solved in the same manner as Eq. 3-22. The solution is the same as Eq. 3-22\$ and the interval average is the same as Eq. 3-22\$-1 after replacing K_T^o , R_T^o , T^o and T^N with K_{TSS}^o , R_{TSS}^o , TSS^o and TSS^N , respectively.

The governing equation for total active metal (Eq. 3-19) may be written as:

$$\frac{\partial TAM}{\partial t} = R_{TAM}^o - K_{TAM}^o \cdot TAM \quad (3-24)$$

$$K_{TAM}^o = \frac{WS_s}{h} \quad (3-24-1)$$

$$R_{TAM}^o = \frac{KHbmf}{KHbmf + DO^o} \frac{BFTAM^o}{h} \exp[Ktam(T^A - Ttam)] + \frac{WS_s}{h} TAMd^o \quad (3-24-2)$$

The interval average, T^A , is used in Eq. 3-24. Equation 3-24 can be solved in the same manner as Eq. 3-22. The solution is the same as Eq. 3-22\$ and the interval average is the same as Eq. 3-22\$-1 after replacing K_T^o , R_T^o , T^o and T^N with K_{TAM}^o , R_{TAM}^o , TAM^o and TAM^N , respectively.

B. Then, algal biomass is solved. The governing equation (Eq. 3-1) may be written as:

$$\frac{\partial B_x}{\partial t} = K_B^o \cdot B_x \quad (3-25)$$

$$K_B^O = P_x^O - BM_x^O - PR_x^O - \frac{WS_x^O}{h} \quad (3-25-1)$$

The analytical solution of Eq. 3-25 is:

$$B_x^N = B_x^O \cdot \exp(K_B^O \cdot \Delta t) \quad (3-25\$)$$

When calculating P_x^O , BM_x^O , PR_x^O and WS_x^O for K_B^O (Eq. 3-25-1), the temperature and light dependencies are evaluated using the interval averages, T^A and TSS^A . Then, the algal biomass at a new time step is calculated for three algal groups using Eq. 3-25\$, and the average biomass between t_o and $t_o + \Delta t$ is calculated using:

$$B_x^A = \frac{1}{\Delta t} \int_{t_o}^{t_o + \Delta t} B_x \cdot dt = \frac{B_x^O - B_x^N}{-\Delta t \cdot K_B^O} \quad (3-25\$-1)$$

C. Then, the carbon cycle is solved in the order of particulate organic and dissolved carbon. The governing equation for refractory particulate organic carbon (Eq. 3-2) may be written as:

$$\frac{\partial RPOC}{\partial t} = R_{Cl}^O - K_{Cl}^O \cdot RPOC \quad (3-26)$$

$$K_{Cl}^O = K_{RPOC}^O + \frac{WS_{RP}}{h} \quad (3-26-1)$$

$$R_{Cl}^O = \sum_{x=c,d,g} FCRP \cdot PR_x^O \cdot B_x^A \quad (3-26-2)$$

The interval averages, B_x^A and T^A , should be used in Eq. 3-26 to ensure mass conservation. Equation 3-26 can be solved in the same manner as Eq. 3-22. The solution is the same as Eq. 3-22\$ and the interval average is the same as Eq. 3-22\$-1 after replacing K_T^O , R_T^O , T^O and T^N with K_{Cl}^O , R_{Cl}^O , $RPOC^O$ and $RPOC^N$, respectively.

The governing equation for labile particulate organic carbon (Eq. 3-3) may be written as:

$$\frac{\partial LPOC}{\partial t} = R_{C2}^O - K_{C2}^O \cdot LPOC \quad (3-27)$$

$$K_{C2}^o = K_{LPOC}^o + \frac{WS_{LP}}{h} \quad (3-27-1)$$

$$R_{C2}^o = \sum_{x=c,d,g} FCLP \cdot PR_x^o \cdot B_x^A \quad (3-27-2)$$

The interval averages, B_x^A and T^A , should be used in Eq. 3-27 to ensure mass conservation. Equation 3-27 can be solved in the same manner as Eq. 3-22. The solution is the same as Eq. 3-22\$ and the interval average is the same as Eq. 3-22\$-1 after replacing K_T^o , R_T^o , T^o and T^N with K_{C2}^o , R_{C2}^o , $LPOC^o$ and $LPOC^N$, respectively.

The governing equation for dissolved organic carbon (Eq. 3-4) may be written as:

$$\frac{\partial DOC}{\partial t} = R_{C3}^o - K_{C3}^o \cdot DOC \quad (3-28)$$

$$K_{C3}^o = K_{HR}^o + Denit^o \quad (3-28-1)$$

$$R_{C3}^o = \sum_{x=c,d,g} \left[FCD_x + (1 - FCD_x) \frac{KHR_x}{KHR_x + DO^o} \right] BM_x^o + FCDP \cdot PR_x^o \cdot B_x^A + K_{RPOC}^o \cdot RPOC^A + K_{LPOC}^o \cdot LPOC^A \quad (3-28-2)$$

The interval averages, B_x^A , T^A , $RPOC^A$ and $LPOC^A$, should be used in Eq. 3-28 to ensure mass conservation. Equation 3-28 can be solved in the same manner as Eq. 3-22. The solution is the same as Eq. 3-22\$ and the interval average is the same as Eq. 3-22\$-1 after replacing K_T^o , R_T^o , T^o and T^N with K_{C3}^o , R_{C3}^o , DOC^o and DOC^N , respectively.

D. Then, the phosphorus cycle is solved in the order of particulate organic, dissolved organic and total phosphate phosphorus. The governing equation for refractory particulate organic phosphorus (Eq. 3-5) may be written as:

$$\frac{\partial RPOP}{\partial t} = R_{PI}^o - K_{PI}^o \cdot RPOP \quad (3-29)$$

$$K_{PI}^o = K_{RPOP}^o + \frac{WS_{RP}}{h} \quad (3-29-1)$$

$$R_{P1}^O = \sum_{x=c,d,g} (FPR_x \cdot BM_x^O + FPRP \cdot PR_x^O) APC^O \cdot B_x^A \quad (3-29-2)$$

The interval averages, B_x^A and T^A , should be used in Eq. 3-29 to ensure mass conservation. Equation 3-29 can be solved in the same manner as Eq. 3-22. The solution is the same as Eq. 3-22\$ and the interval average is the same as Eq. 3-22\$-1 after replacing K_T^O , R_T^O , T^O and T^N with K_{P1}^O , R_{P1}^O , $RPOP^O$ and $RPOP^N$, respectively.

The governing equation for labile particulate organic phosphorus (Eq. 3-6) may be written as:

$$\frac{\partial LPOP}{\partial t} = R_{P2}^O - K_{P2}^O \cdot LPOP \quad (3-30)$$

$$K_{P2}^O = K_{LPOP}^O + \frac{WS_{LP}}{h} \quad (3-30-1)$$

$$R_{P2}^O = \sum_{x=c,d,g} (FPL_x \cdot BM_x^O + FPLP \cdot PR_x^O) APC^O \cdot B_x^A \quad (3-30-2)$$

The interval averages, B_x^A and T^A , should be used in Eq. 3-30 to ensure mass conservation. Equation 3-30 can be solved in the same manner as Eq. 3-22. The solution is the same as Eq. 3-22\$ and the interval average is the same as Eq. 3-22\$-1 after replacing K_T^O , R_T^O , T^O and T^N with K_{P2}^O , R_{P2}^O , $LPOP^O$ and $LPOP^N$, respectively.

The governing equation for dissolved organic phosphorus (Eq. 3-7) may be written as:

$$\frac{\partial DOP}{\partial t} = R_{P3}^O - K_{P3}^O \cdot DOP \quad (3-31)$$

$$K_{P3}^O = K_{DOP}^O \quad (3-31-1)$$

$$R_{P3}^O = \sum_{x=c,d,g} (FPD_x \cdot BM_x^O + FPDP \cdot PR_x^O) APC^O \cdot B_x^A + K_{RPOP}^O \cdot RPOP^A + K_{LPOP}^O \cdot LPOP^A \quad (3-31-2)$$

The interval averages, B_x^A , T^A , $RPOP^A$ and $LPOP^A$, should be used in Eq. 3-31 to ensure mass conservation. Equation 3-31 can be solved in the same manner as Eq. 3-22. The solution is the same as Eq. 3-22\$ and the interval average is the same as Eq. 3-22\$-1

after replacing K_T^O , R_T^O , T^O and T^N with $K_{P_3}^O$, $R_{P_3}^O$, DOP^O and DOP^N , respectively.

The governing equation for total phosphate (Eq. 3-8) is nonlinear because APC is a function of PO_4t (Equations 3-8c and 3-8e). It is linearized by using known value (PO_4t^O) for APC. (The linearization of differential equation by using known values for nonlinear terms is also used for other state variables whenever needed.) Then, using the expression for PO_4p (Eq. 3-8b, for example, for total suspended solid), Eq. 3-8 may be written as:

$$\frac{\partial PO_4t}{\partial t} = R_{P_4}^O - K_{P_4}^O \cdot PO_4t \quad (3-32)$$

$$K_{P_4}^O = \frac{WS_{TSS}}{h} \frac{K_{PO_4p} \cdot TSS^A}{1 + K_{PO_4p} \cdot TSS^A} \quad (3-32-1)$$

$$R_{P_4}^O = \sum_{x=c,d,g} (FPI_x \cdot BM_x^O + FPIP \cdot PR_x^O - P_x^O) APC^O \cdot B_x^A + K_{DOP}^O \cdot DOP^A + \frac{BFPO_4^O}{h} \quad (3-32-2)$$

The interval averages, B_x^A , T^A and DOP^A , should be used in Eq. 3-32 to ensure mass conservation. Equation 3-32 can be solved in the same manner as Eq. 3-22. The solution is the same as Eq. 3-22\$ after replacing K_T^O , R_T^O , T^O and T^N with $K_{P_4}^O$, $R_{P_4}^O$, PO_4t^O and PO_4t^N , respectively. The present solution scheme does not require the calculation for the interval average, PO_4t^A .

E. Then, the nitrogen cycle is solved in the order of particulate organic, dissolved organic, ammonium and nitrate nitrogen. The governing equation for refractory particulate organic nitrogen (Eq. 3-9) may be written as:

$$\frac{\partial RPON}{\partial t} = R_{NI}^O - K_{NI}^O \cdot RPON \quad (3-33)$$

$$K_{NI}^O = K_{RPON}^O + \frac{WS_{RP}}{h} \quad (3-33-1)$$

$$R_{NI}^O = \sum_{x=c,d,g} (FNR_x \cdot BM_x^O + FNRP \cdot PR_x^O) ANC_x \cdot B_x^A \quad (3-33-2)$$

The interval averages, B_x^A and T^A , should be used in Eq. 3-33 to ensure mass conservation. Equation 3-33 can be solved in the same manner as Eq. 3-22. The solution is the same as Eq. 3-22\$ and the interval average is the same as Eq. 3-22\$-1 after replacing K_T^O , R_T^O , T^O and T^N with K_{N1}^O , R_{N1}^O , $RPON^O$ and $RPON^N$, respectively.

The governing equation for labile particulate organic nitrogen (Eq. 3-10) may be written as:

$$\frac{\partial LPON}{\partial t} = R_{N2}^O - K_{N2}^O \cdot LPON \quad (3-34)$$

$$K_{N2}^O = K_{LPON}^O + \frac{WS_{LP}}{h} \quad (3-34-1)$$

$$R_{N2}^O = \sum_{x=c,d,g} (FNL_x \cdot BM_x^O + FNLP \cdot PR_x^O) ANC_x \cdot B_x^A \quad (3-34-2)$$

The interval averages, B_x^A and T^A , should be used in Eq. 3-34 to ensure mass conservation. Equation 3-34 can be solved in the same manner as Eq. 3-22. The solution is the same as Eq. 3-22\$ and the interval average is the same as Eq. 3-22\$-1 after replacing K_T^O , R_T^O , T^O and T^N with K_{N2}^O , R_{N2}^O , $LPON^O$ and $LPON^N$, respectively.

The governing equation for dissolved organic nitrogen (Eq. 3-11) may be written as:

$$\frac{\partial DON}{\partial t} = R_{N3}^O - K_{N3}^O \cdot DON \quad (3-35)$$

$$K_{N3}^O = K_{DON}^O \quad (3-35-1)$$

$$R_{N3}^O = \sum_{x=c,d,g} (FND_x \cdot BM_x^O + FNDP \cdot PR_x^O) ANC_x \cdot B_x^A + K_{RPON}^O \cdot RPON^A + K_{LPON}^O \cdot LPON^A \quad (3-35-2)$$

The interval averages, B_x^A , T^A , $RPON^A$ and $LPON^A$, should be used in Eq. 3-35 to ensure mass conservation. Equation 3-35 can be solved in the same manner as Eq. 3-22. The solution is the same as Eq. 3-22\$ and the interval average is the same as Eq. 3-22\$-1 after replacing K_T^O , R_T^O , T^O and T^N with K_{N3}^O , R_{N3}^O , DON^O and DON^N , respectively.

The governing equation for ammonium nitrogen (Eq. 3-12) is nonlinear because of

Monod function of ammonium in PN_x (Eq. 3-13a) and Nit (Eq. 3-13g). Equation 3-12 is linearized by using known value for ammonium ($NH4^0$) in Eq. 3-13a and in denominator of Monod function in Eq. 3-13g. Then, Eq. 3-12 may be written as:

$$\frac{\partial NH4}{\partial t} = R_{N4}^0 - K_{N4}^0 \cdot NH4 \quad (3-36)$$

$$K_{N4}^0 = \frac{DO^0}{KHNit_{DO} + DO^0} \frac{Nit_m}{KHNit_N + NH4^0} \exp(-KNit[T^A - TNit]^2) = Nit^0 \quad (3-36-1)$$

$$R_{N4}^0 = \sum_{x=c,d,g} (FNI_x \cdot BM_x^0 + FNIP \cdot PR_x^0 - PN_x^0 \cdot P_x^0) ANC_x \cdot B_x^A + K_{DON}^0 \cdot DON^A + \frac{BFNH4^0}{h} \quad (3-36-2)$$

The interval averages, B_x^A , T^A and DON^A , should be used in Eq. 3-36 to ensure mass conservation. Equation 3-36 can be solved in the same manner as Eq. 3-22. The solution is the same as Eq. 3-22\$ and the interval average is the same as Eq. 3-22\$-1 after replacing K_T^0 , R_T^0 , T^0 and T^N with K_{N4}^0 , R_{N4}^0 , $NH4^0$ and $NH4^N$, respectively.

The governing equation for nitrate nitrogen (Eq. 3-13) is nonlinear because of Monod function of nitrate in PN_x (Eq. 3-13a) and Denit (Eq. 3-4l). Equation 3-13 is linearized by using known value for nitrate ($NO3^0$) in Eq. 3-13a and in denominator of Monod function in Eq. 3-4l: the latter conserves mass-balance compared to dissolved organic carbon equation (Eq. 3-28). Then, Eq. 3-13 may be written as:

$$\frac{\partial NO3}{\partial t} = R_{NS}^0 \quad (3-37)$$

$$R_{NS}^0 = - \sum_{x=c,d,g} (1 - PN_x^0) P_x^0 \cdot ANC_x \cdot B_x^A + Nit^0 \cdot NH4^A - ANDC \cdot Denit^0 \cdot DOC^A + \frac{BFNO3^0}{h} \quad (3-37-1)$$

When evaluating the nitrification term in Eq. 3-37-1, Nit^0 (Eq. 3-36-1) should be used to conserve mass-balance compared to ammonium nitrogen equation (Eq. 3-26). Also note the interval averages, B_x^A , T^A , $NH4^A$ and DOC^A , should be used in Eq. 3-37 to ensure mass conservation. The solution of Eq. 3-37 may be expressed as:

$$NO3^N = NO3^O + R_{NS}^O \cdot \Delta t \quad (3-37\$)$$

The present solution scheme does not require the calculation for the interval average, $NO3^A$.

F. Then, the silica cycle is solved in the order of particulate biogenic silica and available silica. The governing equation for particulate biogenic silica (Eq. 3-14) may be written as:

$$\frac{\partial SU}{\partial t} = R_{SI}^O - K_{SI}^O \cdot SU \quad (3-38)$$

$$K_{SI}^O = K_{SUA}^O + \frac{WS_d^O}{h} \quad (3-38-1)$$

$$R_{SI}^O = (FSP_d \cdot BM_d^O + FSPP \cdot PR_d^O) ASC_d \cdot B_d^A \quad (3-38-2)$$

The interval averages, B_x^A and T^A , should be used in Eq. 3-38 to ensure mass conservation. Equation 3-38 can be solved in the same manner as Eq. 3-22. The solution is the same as Eq. 3-22\$ and the interval average is the same as Eq. 3-22\$-1 after replacing K_T^O , R_T^O , T^O and T^N with K_{SI}^O , R_{SI}^O , SU^O and SU^N , respectively.

The governing equation for available silica (Eq. 3-15), using the expression for SAP (Eq. 3-15b, for example, for total suspended solid), may be written as:

$$\frac{\partial SA}{\partial t} = R_{S2}^O - K_{S2}^O \cdot SA \quad (3-39)$$

$$K_{S2}^O = \frac{WS_{TSS}}{h} \frac{K_{SAP} \cdot TSS^A}{1 + K_{SAP} \cdot TSS^A} \quad (3-39-1)$$

$$R_{S2}^O = (FSI_d \cdot BM_d^O + FSIP \cdot PR_d^O - P_d^O) ASC_d \cdot B_d^A + K_{SUA}^O \cdot SU^A + \frac{BFSA^O}{h} \quad (3-39-2)$$

The interval averages, B_x^A , T^A and SU^A , should be used in Eq. 3-39 to ensure mass conservation. Equation 3-39 can be solved in the same manner as Eq. 3-22. The solution is the same as Eq. 3-22\$ after replacing K_T^O , R_T^O , T^O and T^N with K_{S2}^O , R_{S2}^O , SA^O and SA^N , respectively. The present solution scheme does not require the calculation

for the interval average, SA^A .

G. Then, chemical oxygen demand is solved. The governing equation (Eq. 3-16) may be written as:

$$\frac{\partial COD}{\partial t} = R_{COD}^o - K_{COD}^o \cdot COD \quad (3-40)$$

$$K_{COD}^o = \frac{DO^o}{KH_{COD} + DO^o} K_{COD}^o \quad (3-40-1)$$

$$R_{COD}^o = \frac{BFCOD^o}{h} \quad (3-40-2)$$

As in all other sediment-water exchange terms, the sediment flux of chemical oxygen demand is evaluated before Eq. 3-40 is solved. Equation 3-40 can be solved in the same manner as Eq. 3-22. The solution is the same as Eq. 3-22\$ and the interval average is the same as Eq. 3-22\$-1 after replacing K_T^o , R_T^o , T^o and T^N with K_{COD}^o , R_{COD}^o , COD^o and COD^N , respectively.

H. Then, dissolved oxygen is solved. In the governing equation (Eq. 3-17), almost all terms are a function of dissolved oxygen. To linearize the equation and to conserve mass-balance, the known value (DO^o) is used for algal respiration (Eq. 3-4d), nitrification (Eq. 3-13g), heterotrophic respiration (Eq. 3-4g), and chemical oxygen demand (Eq. 3-16). Then, Eq. 3-17 may be written as:

$$\frac{\partial DO}{\partial t} = R_{DO}^o - K_{DO}^o \cdot DO \quad (3-41)$$

$$K_{DO}^o = K_r^o \quad (3-41-1)$$

$$R_{DO}^o = \sum_{x=c,d,g} \left[(1.3 - 0.3 \cdot PN_x^o) P_x^o - (1 - FCD_x) \frac{DO^o}{KHR_x + DO^o} BM_x^o \right] AOCR \cdot B_x^A - AONT \cdot Nit^o \cdot NH4^A - AOCR \cdot K_{HR}^o \cdot DOC^A$$

$$- \frac{DO^o}{KH_{COD} + DO^o} K_{COD}^o \cdot COD^A + K_r^o \cdot DO_s^o + \frac{SOD^o}{h} \quad (3-41-2)$$

The interval averages, B_x^A , T^A , NH_4^A , DOC^A and COD^A should be used in Eq. 3-41 to ensure mass conservation. Equation 3-41 can be solved in the same manner as Eq. 3-22. The solution is the same as Eq. 3-22\$ after replacing K_T^o , R_T^o , T^o and T^N with K_{DO}^o , R_{DO}^o , DO^o and DO^N , respectively. The present solution scheme does not require the calculation for the interval average, DO^A .

I. Finally, fecal coliform bacteria is solved. The governing equation (Eq. 3-20) may be written as:

$$\frac{\partial FCB}{\partial t} = - K_{FCB}^o \cdot FCB \quad (3-42)$$

$$K_{FCB}^o = K_{FCB} \cdot T_{FCB}^{T^A - 20} \quad (3-42-1)$$

The interval average, T^A , is used in Eq. 3-41. Equation 3-42 can be solved in the same manner as Eq. 3-25. The solution is the same as Eq. 3-25\$ after replacing K_B^o , B_x^o and B_x^N with $- K_{FCB}^o$, FCB^o and FCB^N , respectively. The present solution scheme does not require the calculation for the interval average, FCB^A .

III-12. Parameter Evaluation

The present water quality model involves many parameters that need to be evaluated from field data or through model calibration. The parameter values found from the model application to the Chesapeake Bay (Cercó & Cole 1994) are listed in Tables 3-1 to 3-7. These values, that were established after analyzing extensive data sets and model calibration, may serve as an excellent starting point for model application to estuaries of the eastern United States.

Table 3-1. Parameters related to algae in water column.

Parameter	Value ^a	Equation Number ^b
*PM _c (day ⁻¹)	2.5 (upper Potomac only)	3-1a
*PM _d (day ⁻¹)	2.25	3-1a
*PM _g (day ⁻¹)	2.5	3-1a
KHN _x (g N m ⁻³)	0.01 (all groups)	3-1c
KHP _x (g P m ⁻³)	0.001 (all groups)	3-1c
KHS (g Si m ⁻³)	0.05	3-1d
FD	temporally-varying input	3-1e
I _o (langley days day ⁻¹)	temporally-varying input	3-1f
*Ke _b (m ⁻¹)	spatially-varying input	3-1h
Ke _{TSS} (m ⁻¹ per g m ⁻³)	NA ^c	3-1h
Ke _{chl} (m ⁻¹ per mg Chl m ⁻³)	0.017	3-1h
CChl _x (g C per mg Chl)	0.06 (all groups)	3-1h
(D _{opt}) _x (m)	1.0 (all groups)	3-1i
(I _s) _{min} (langley days day ⁻¹)	40.0	3-1i
CI _a , CI _b & CI _c	0.7, 0.2 & 0.1	3-1j
TM _c , TM _d & TM _g (°C)	27.5, 20.0 & 25.0	3-1k
KTG1 _c & KTG2 _c (°C ⁻²)	0.005 & 0.004	3-1k
KTG1 _d & KTG2 _d (°C ⁻²)	0.004 & 0.006	3-1k
KTG1 _g & KTG2 _g (°C ⁻²)	0.008 & 0.01	3-1k
STOX (ppt)	1.0	3-1l
*BMR _c (day ⁻¹)	0.04	3-1m
*BMR _d (day ⁻¹)	0.01	3-1m
	0.003 (Jan. - May in saltwater only)	
*BMR _g (day ⁻¹)	0.01	3-1m
TR _x (°C)	20.0 (all groups)	3-1m
KTB _x (°C ⁻¹)	0.069 (all groups)	3-1m
*PRR _c (day ⁻¹)	0.01	3-1n
*PRR _d (day ⁻¹)	0.215	3-1n
	0.065 (Jan. - May in saltwater only)	
*PRR _g (day ⁻¹)	0.215	3-1n
*WS _c (m day ⁻¹)	0.0	3-1
*WS _d (m day ⁻¹)	0.35 (January - May)	3-1
	0.1 (June - December)	
*WS _g (m day ⁻¹)	0.1	3-1

^a The evaluation of these values are detailed in Chapter IX of Cerco & Cole (1994).

^b The equation number where the corresponding parameter is first appeared and defined.

^c Not available in Cerco & Cole (1994) since their formulations do not include these parameters.

* The parameters declared as an array in the source code.

Table 3-2. Parameters related to organic carbon in water column.

Parameter	Value ^a	Equation Number ^b
FCRP	0.35	3-2
FCLP	0.55	3-3
FCDP	0.10	3-4
FCD _x	0.0 (all groups)	3-4
*WS _{RP} (m day ⁻¹)	1.0	3-2
*WS _{LP} (m day ⁻¹)	1.0	3-3
KHR _x (g O ₂ m ⁻³)	0.5 (all groups)	3-4
KHOR _{DO} (g O ₂ m ⁻³)	0.5	3-4g
K _{RC} (day ⁻¹)	0.005	3-4h
K _{LC} (day ⁻¹)	0.075	3-4i
K _{DC} (day ⁻¹)	0.01	3-4j
K _{RCalg} (day ⁻¹ per g C m ⁻³)	0.0	3-4h
K _{LCalg} (day ⁻¹ per g C m ⁻³)	0.0	3-4i
K _{DCalg} (day ⁻¹ per g C m ⁻³)	0.0	3-4j
TR _{HDR} (°C)	20.0	3-4h
TR _{MNL} (°C)	20.0	3-4j
KT _{HDR} (°C ⁻¹)	0.069	3-4h
KT _{MNL} (°C ⁻¹)	0.069	3-4j
KHDN _N (g N m ⁻³)	0.1	3-4i
AANOX	0.5	3-4i

^a The evaluation of these values are detailed in Chapter IX of Cerco & Cole (1994).

^b The equation number where the corresponding parameter is first appeared and defined.

* The parameters declared as an array in the source code.

Table 3-3. Parameters related to phosphorus in water column.

Parameter	Value ^a	Equation Number ^b
FPRP	0.1	3-5
FPLP	0.2	3-6
FPDP	0.5	3-7
FPIP	0.2 ^c	3-8
FPR _x	0.0 (all groups)	3-5
FPL _x	0.0 (all groups)	3-6
FPD _x	1.0 (all groups)	3-7
FPI _x	0.0 ^c (all groups)	3-8
*WS _{TSS} (m day ⁻¹)	NA ^c	3-8
*WS _s (m day ⁻¹)	1.0	3-8
K _{PO4p} (per g m ⁻³) for TSS	NA ^c	3-8b
K _{PO4p} (per mol m ⁻³) for TAM	6.0	3-8b
CP _{pm1} (g C per g P)	42.0	3-8e
CP _{pm2} (g C per g P)	85.0	3-8e
CP _{pm3} (per g P m ⁻³)	200.0	3-8e
K _{RP} (day ⁻¹)	0.005	3-8f
K _{LP} (day ⁻¹)	0.075	3-8g
K _{DP} (day ⁻¹)	0.1	3-8h
K _{RPalg} (day ⁻¹ per g C m ⁻³)	0.0	3-8f
K _{LPalg} (day ⁻¹ per g C m ⁻³)	0.0	3-8g
K _{DPalg} (day ⁻¹ per g C m ⁻³)	0.2	3-8h

^a The evaluation of these values are detailed in Chapter IX of Cerco & Cole (1994).

^b The equation number where the corresponding parameter is first appeared and defined.

^c Not available in Cerco & Cole (1994) since their formulations do not include these parameters

: FPI_x is estimated from FPR_x+FPL_x+FPD_x+FPI_x = 1.

* The parameters declared as an array in the source code.

Table 3-4. Parameters related to nitrogen in water column.

Parameter	Value ^a	Equation Number ^b
FNRP	0.35	3-9
FNLP	0.55	3-10
FNDP	0.10	3-11
FNIP	0.0	3-12
FNR _x	0.0 (all groups)	3-9
FNL _x	0.0 (all groups)	3-10
FND _x	1.0 (all groups)	3-11
FNI _x	0.0 (all groups)	3-12
ANC _x (g N per g C)	0.167 (all groups)	3-9
ANDC (g N per g C)	0.933	3-13
K _{RN} (day ⁻¹)	0.005	3-13b
K _{LN} (day ⁻¹)	0.075	3-13c
K _{DN} (day ⁻¹)	0.015	3-13d
K _{RNalg} (day ⁻¹ per g C m ⁻³)	0.0	3-13b
K _{LNalg} (day ⁻¹ per g C m ⁻³)	0.0	3-13c
K _{DNalg} (day ⁻¹ per g C m ⁻³)	0.0	3-13d
Nit _m (g N m ⁻³ day ⁻¹)	0.07	3-13g
KHNit _{DO} (g O ₂ m ⁻³)	1.0	3-13g
KHNit _N (g N m ⁻³)	1.0	3-13g
TNit (°C)	27.0	3-13g-1
KNit1 (°C ⁻²)	0.0045	3-13g-1
KNit2 (°C ⁻²)	0.0045	3-13g-1

^a The evaluation of these values are detailed in Chapter IX of Cerco & Cole (1994).

^b The equation number where the corresponding parameter is first appeared and defined.

Table 3-5. Parameters related to silica in water column.

Parameter	Value ^a	Equation Number ^b
FSPP	1.0 ^c	3-14
FSIP	0.0 ^c	3-15
FSP _d	1.0 ^c	3-14
FSI _d	0.0 ^c	3-15
ASC _d (g Si per g C)	0.5	3-14
K _{SAP} (per g m ⁻³) for TSS	NA ^c	3-15b
K _{SAP} (per mol m ⁻³) for TAM	6.0	3-15b
K _{SU} (day ⁻¹)	0.03	3-15d
TR _{SUA} (°C)	20.0	3-15d
KT _{SUA} (°C ⁻¹)	0.092	3-15d

^a The evaluation of these values are detailed in Chapter IX of Cerco & Cole (1994).

^b The equation number where the corresponding parameter is first appeared and defined.

^c Not available in Cerco & Cole (1994) since their formulations do not include these parameters

: FSPP and FSIP are estimated from $FSPP + FSIP = 1$

: FSP_d and FSI_d are estimated from $FSP_d + FSI_d = 1$.

Table 3-6. Parameters related to chemical oxygen demand and dissolved oxygen in water column.

Parameter	Value ^a	Equation Number ^b
KH _{COD} (g O ₂ m ⁻³)	1.5	3-16
K _{CD} (day ⁻¹)	20.0	3-16a
TR _{COD} (°C)	20.0	3-16a
KT _{COD} (°C ⁻¹)	0.041	3-16a
AOCR (g O ₂ per g C)	2.67	3-17
AONT (g O ₂ per g N)	4.33	3-17
K _{ro} (in MKS unit)	3.933 ^c	3-17e
KT _r	1.024 ^c (1.005 - 1.030)	3-17e

^a The evaluation of these values are detailed in Chapter IX of Cerco & Cole (1994).

^b The equation number where the corresponding parameter is first appeared and defined.

^c Not available in Cerco & Cole (1994) since their formulations do not include these parameters

: K_{ro} is from O'Connor & Dobbins (1958)

: KT_r is from Thomann & Mueller (1987).

Table 3-7. Parameters related to total suspended solid, total active metal, fecal coliform bacteria and temperature in water column.

Parameter	Value ^a	Equation Number ^b
RD _{TSS} (g m ⁻² day ⁻¹)	NA ^c	3-18
KHbmf (g O ₂ m ⁻³)	0.5	3-19
BFTAM (mol m ⁻² day ⁻¹)	0.01	3-19
T _{tam} (°C)	20.0	3-19
K _{tam} (°C ⁻¹)	0.2	3-19
TAMdmx (mol m ⁻³)	0.015	3-19b-1
K _{dotam} (per g O ₂ m ⁻³)	1.0	3-19b-1
KFCB (day ⁻¹)	0.0 - 3.0 ^c	3-20
TFCB (°C ⁻¹)	1.07 ^c	3-20
C _p (watt sec kg ⁻¹ °C ⁻¹)	4200.0 (4186.0 ^c)	3-21
KT (watt m ⁻² °C ⁻¹)	temporally-varying input	3-21
T _e (°C)	temporally-varying input	3-21

^a The evaluation of these values are detailed in Chapter IX of Cerco & Cole (1994).

^b The equation number where the corresponding parameter is first appeared and defined.

^c Not available in Cerco & Cole (1994) since their formulations do not include these parameters

: RD_{TSS} has to be calibrated with field data

: KFCB and TFCB are from Thomann & Mueller (1987)

: C_p = 4186.0 in Edinger et al. (1974) and Thomann & Mueller (1987).

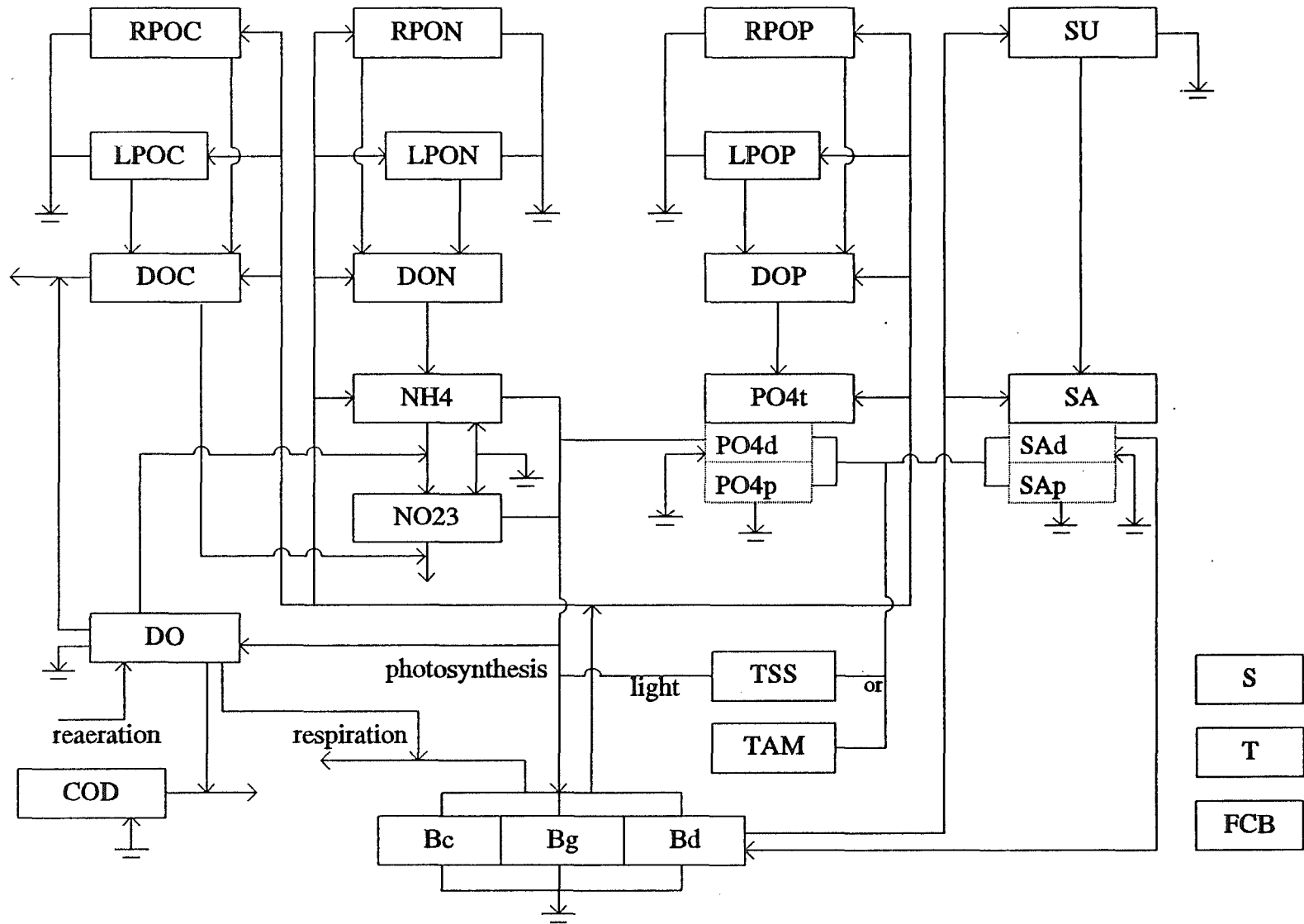


Figure 3-1. A schematic diagram for water column water quality model.

Chapter IV. Sediment Process Model

The sediment process model developed by DiToro & Fitzpatrick (1993) was coupled with CE-QUAL-ICM for Chesapeake Bay water quality modeling (Cerco & Cole 1994). This sediment model is slightly modified and included in the present model package. An asterisk mark (*) attached to equation number denotes formulations that are different from the model in DiToro & Fitzpatrick (1993): hereinafter this report is referred to as D&F. The sediment process model has sixteen water quality related model state variables and fluxes.

- | | |
|-----------------------------------|---------------------------------------|
| 1) particulate organic carbon | 2) particulate organic nitrogen |
| 3) particulate organic phosphorus | 4) particulate biogenic silica |
| 5) sulfide/methane | 6) ammonium nitrogen |
| 7) nitrate nitrogen | 8) phosphate phosphorus |
| 9) available silica | |
| 10) ammonium nitrogen flux | 11) nitrate nitrogen flux |
| 12) phosphate phosphorus flux | 13) silica flux |
| 14) sediment oxygen demand | 15) release of chemical oxygen demand |
| 16) sediment temperature | |

In the sediment model, benthic sediments are represented as two layers (Fig. 4-1). The upper layer (Layer 1) is in contact with the water column and may be oxic or anoxic depending on dissolved oxygen concentration in the overlying water. The lower layer (Layer 2) is permanently anoxic. The upper layer depth, which is determined by the penetration of oxygen into the sediments, is at its maximum only a small fraction of the total. Because H_1 (~ 0.1 cm) $\ll H_2$,

$$H = H_1 + H_2 \approx H_2 \quad (4-1)$$

where H is the total depth (approximately 10 cm: see Section IV-7-2D), H_1 is the upper layer depth and H_2 is the lower layer depth.

The model incorporates three basic processes (Fig. 4-2): 1) depositional flux of particulate organic matter (POM), 2) their diagenesis and 3) resulting sediment flux. The sediment model is driven by net settling of particulate organic carbon, nitrogen,

phosphorus and silica from the overlying water to the sediments (**depositional flux**). Because of the negligible thickness of the upper layer (Eq. 4-1), deposition is considered to be proceeded from the water column directly to the lower layer. Within the lower layer, the model simulates the diagenesis (mineralization or decay) of deposited POM, which produces oxygen demand and inorganic nutrients (**diagenesis flux**). The third basic process is the flux of substances produced by diagenesis (**sediment flux**). Oxygen demand, as sulfide (in saltwater) or methane (in freshwater), takes three paths out of the sediments: 1) oxidation at the sediment-water interface as sediment oxygen demand, 2) export to the water column as chemical oxygen demand or 3) burial to deep, inactive sediments. Inorganic nutrients produced by diagenesis takes two paths out of the sediments: 1) release to the water column or 2) burial to deep, inactive sediments (Fig. 4-2).

This chapter describes the three basic processes with reactions and sources/sinks for each state variable. The method of solution including finite difference equations, solution scheme, boundary and initial conditions, and stand alone model are explained in Section IV-6. Parameter evaluation and some limitations of the model formulations found in D&F are described in Section IV-7. Complete model documentation can be found in D&F.

IV-1. Depositional Flux

Deposition is one process that couples the water column model with the sediment model. Consequently, deposition is represented in both the water column and sediment models. In the water column model, the governing mass-balance equations for the following state variables:

- : three algal groups, cyanobacteria, diatoms and green algae (Eq. 3-1)
- : refractory and labile particulate organic carbon (Equations 3-2 and 3-3)
- : refractory and labile particulate organic phosphorus (Equations 3-5 and 3-6) and total phosphate (Eq. 3-8)
- : refractory and labile particulate organic nitrogen (Equations 3-9 and 3-10)
- : particulate biogenic silica (Eq. 3-14) and available silica (Eq. 3-15)

contain settling terms, which represent the depositional fluxes.

The sediment model receives these depositional fluxes of particulate organic carbon (POC), particulate organic nitrogen (PON), particulate organic phosphorus (POP) and particulate biogenic silica (PSi). Because of the negligible thickness of the upper layer (Eq. 4-1), deposition is considered to proceed from the water column directly to the lower layer. Since the sediment model has three G classes of POM, G_i ($i = 1, 2$ or 3), depending on the time scales of reactivity (Section IV-2), the POM fluxes from the water column should be mapped into three G classes based on their reactivity. Then, the depositional fluxes for the i^{th} G class ($i = 1, 2$ or 3) may be expressed as:

$$J_{POC,i} = FCLP_i \cdot WS_{LP} \cdot LPOC^A + FCRP_i \cdot WS_{RP} \cdot RPOC^A + \sum_{x=c,d,g} FCB_{x,i} \cdot WS_x \cdot B_x^A \quad (4-2)$$

$$J_{PON,i} = FNLP_i \cdot WS_{LP} \cdot LPON^A + FNRP_i \cdot WS_{RP} \cdot RPON^A + \sum_{x=c,d,g} FNB_{x,i} \cdot ANC_x \cdot WS_x \cdot B_x^A \quad (4-3)$$

$$J_{POP,i} = FPLP_i \cdot WS_{LP} \cdot LPOP^A + FPRP_i \cdot WS_{RP} \cdot RPOP^A + \sum_{x=c,d,g} FPB_{x,i} \cdot APC \cdot WS_x \cdot B_x^A + \lambda_i \cdot WS_{TSS} \cdot PO4p^A \quad (4-4)$$

$$J_{PSi} = WS_d \cdot SU^A + ASC_d \cdot WS_d \cdot B_d^A + WS_{TSS} \cdot SAP^A \quad (4-5)$$

$J_{POM,i}$ = depositional flux of POM ($M = C, N$ or P) routed into the i^{th} G class ($\text{g m}^{-2} \text{ day}^{-1}$)

J_{PSi} = depositional flux of PSi ($\text{g Si m}^{-2} \text{ day}^{-1}$)

$FCLP_i, FNLP_i$ & $FPLP_i$ = fraction of water column labile POC, PON and POP, respectively, routed into the i^{th} G class in sediment

$FCRP_i, FNRP_i$ & $FPRP_i$ = fraction of water column refractory POC, PON and POP, respectively, routed into the i^{th} G class in sediment

$FCB_{x,i}, FNB_{x,i}$ & $FPB_{x,i}$ = fraction of POC, PON and POP, respectively, in the algal group x routed into the i^{th} G class in sediment

$\lambda_i = 1$ for $i = 1$

0 for $i = 2$ or 3 .

The superscript A indicates the interval average as defined in Eq. 3-22-1. The settling of sorbed phosphate is considered to contribute to the labile G_1 pool in Eq. 4-4, and settling of sorbed silica contributes to J_{PSi} in Eq. 4-5 to avoid creation of additional

depositional fluxes for inorganic particulates. The sum of distribution coefficients should be unity: $\sum_i FCLP_i = \sum_i FNLP_i = \sum_i FPLP_i = \sum_i FCRP_i = \sum_i FNRP_i = \sum_i FPRP_i = \sum_i FCB_{x,i} = \sum_i FNB_{x,i} = \sum_i FPB_{x,i} = 1$. The settling velocities, WS_{LP} , WS_{RP} , WS_x and WS_{TSS} , as defined in the water column model (Chapter III), are net settling velocities.

IV-2. Diagenesis Flux

Another coupling point of the sediment model to the water column model is the sediment flux, which is described in Section IV-3. The computation of sediment flux requires that the magnitude of the diagenesis flux be known. The diagenesis flux is explicitly computed using mass-balance equations for deposited POC, PON and POP. (Dissolved silica is produced in the sediments as the result of the dissolution of PSi. Since the dissolution process is different from bacterial-mediated diagenesis process, it is presented separately in Section IV-4.) In the mass-balance equations, the depositional fluxes of POM are the source terms and the decay of POM in the sediments produces the diagenesis fluxes. The integration of the mass-balance equations for POM provides the diagenesis fluxes that are the inputs for the mass-balance equations for ammonium, nitrate, phosphate and sulfide/methane in the sediments (Section IV-3).

The difference in decay rates of POM is accounted for by assigning a fraction of POM to various decay classes (Westrich & Berner 1984). POM in the sediments is divided into three G classes, or fractions, representing three scales of reactivity. The G_1 (labile) fraction has a half life of 20 days, and the G_2 (refractory) fraction has a half life of one year. The G_3 (inert) fraction is non-reactive, i.e., undergoes no significant decay before burial into deep, inactive sediments. The varying reactivity of the G classes controls the time scale over which changes in depositional flux will be reflected in changes in diagenesis flux. If the G_1 class would dominate the POM input into the sediments, then there would be no significant time lag introduced by POM diagenesis and any changes in depositional flux would be readily reflected in diagenesis flux.

Because the upper layer thickness is negligible (Eq. 4-1) and thus depositional flux is considered to proceed directly to the lower layer (Equations 4-2 to 4-5), diagenesis is considered to occur in the lower layer only. The mass-balance equations are similar for POC, PON and POP, and for different G classes. The mass-balance equation in the

anoxic lower layer for the i^{th} G class ($i = 1, 2$ or 3) may be expressed as:

$$H_2 \frac{\partial G_{POM,i}}{\partial t} = - K_{POM,i} \cdot \theta_{POM,i}^{T-20} \cdot G_{POM,i} \cdot H_2 - W \cdot G_{POM,i} + J_{POM,i} \quad (4-6)$$

$G_{POM,i}$ = concentration of POM ($M = C, N$ or P) in the i^{th} G class in Layer 2 (g m^{-3})

$K_{POM,i}$ = decay rate of the i^{th} G class POM at 20°C in Layer 2 (day^{-1})

$\theta_{POM,i}$ = constant for temperature adjustment for $K_{POM,i}$

T = sediment temperature ($^\circ\text{C}$)

W = burial rate (m day^{-1}).

Since the G_3 class is inert, $K_{POM,3} = 0$.

Once the mass-balance equations for $G_{POM,1}$ and $G_{POM,2}$ are solved, the diagenesis fluxes are computed from the rate of mineralization of the two reactive G classes:

$$J_M = \sum_{i=1}^2 K_{POM,i} \cdot \theta_{POM,i}^{T-20} \cdot G_{POM,i} \cdot H_2 \quad (4-7)$$

J_M = diagenesis flux ($\text{g m}^{-2} \text{day}^{-1}$) of carbon ($M = C$), nitrogen ($M = N$) or phosphorus ($M = P$).

IV-3. Sediment Flux

The mineralization of POM produces soluble intermediates, which are quantified as diagenesis fluxes in the previous section. The intermediates react in the oxic and anoxic layers, and portions are returned to the overlying water as sediment fluxes. Computation of sediment fluxes requires mass-balance equations for ammonium, nitrate, phosphate, sulfide/methane and available silica. This section describes the flux portion for ammonium, nitrate, phosphate and sulfide/methane of the model. Available silica is described in Section IV-4.

In the upper layer, the processes included in the flux portion are (Fig. 4-1)

- : exchange of dissolved fraction between Layer 1 and the overlying water
- : exchange of dissolved fraction between Layer 1 and 2 via diffusive transport
- : exchange of particulate fraction between Layer 1 and 2 via particle mixing
- : loss by burial to the lower layer (Layer 2)
- : removal (sink) by reaction

: internal sources.

Since the upper layer is quite thin, $H_1 \sim 0.1$ cm (Eq. 4-1) and the surface mass transfer coefficient (s) is on the order of 0.1 m day⁻¹, then the residence time in the upper layer is: $H_1/s \sim 10^{-2}$ days. Hence, a steady-state approximation is made in the upper layer. Then, the mass-balance equation for ammonium, nitrate, phosphate or sulfide/methane in the upper layer is:

$$H_1 \frac{\partial C_{t_1}}{\partial t} = 0 = s(fd_o \cdot C_{t_o} - fd_1 \cdot C_{t_1}) + KL(fd_2 \cdot C_{t_2} - fd_1 \cdot C_{t_1}) + \omega(fp_2 \cdot C_{t_2} - fp_1 \cdot C_{t_1}) - W \cdot C_{t_1} - \frac{\kappa_1^2}{s} C_{t_1} + J_1 \quad (4-8)$$

C_{t_1} & C_{t_2} = total concentrations in Layer 1 and 2, respectively (g m⁻³)

C_{t_o} = total concentration in the overlying water (g m⁻³)

s = surface mass transfer coefficient (m day⁻¹)

KL = diffusion velocity for dissolved fraction between Layer 1 and 2 (m day⁻¹)

ω = particle mixing velocity between Layer 1 and 2 (m day⁻¹)

fd_o = dissolved fraction of total substance in the overlying water ($0 \leq fd_o \leq 1$)

fd_1 = dissolved fraction of total substance in Layer 1 ($0 \leq fd_1 \leq 1$)

fp_1 = particulate fraction of total substance in Layer 1 ($= 1 - fd_1$)

fd_2 = dissolved fraction of total substance in Layer 2 ($0 \leq fd_2 \leq 1$)

fp_2 = particulate fraction of total substance in Layer 2 ($= 1 - fd_2$)

κ_1 = reaction velocity in Layer 1 (m day⁻¹)

J_1 = sum of all internal sources in Layer 1 (g m⁻² day⁻¹).

The first term on the RHS of Eq. 4-8 represents the exchange across sediment-water interface. Then, the sediment flux from Layer 1 to the overlying water, which couples the sediment model to the water column model, may be expressed as:

$$J_{aq} = s(fd_1 \cdot C_{t_1} - fd_o \cdot C_{t_o}) \quad (4-9)$$

J_{aq} = sediment flux of ammonium, nitrate, phosphate or sulfide/methane to the overlying water (g m⁻² day⁻¹).

The convention used in Eq. 4-9 is that positive flux is from the sediment to the overlying water.

- In the lower layer, the processes included in the flux portion are (Fig. 4-1)
- : exchange of dissolved fraction between Layer 1 and 2 via diffusive transport
 - : exchange of particulate fraction between Layer 1 and 2 via particle mixing
 - : deposition from Layer 1, and burial to the deep inactive sediments
 - : removal (sink) by reaction
 - : internal sources including diagenetic source.

The mass-balance equation for ammonium, nitrate, phosphate or sulfide/methane in the lower layer is:

$$H_2 \frac{\partial Ct_2}{\partial t} = -KL(fd_2 \cdot Ct_2 - fd_1 \cdot Ct_1) - \omega(fp_2 \cdot Ct_2 - fp_1 \cdot Ct_1) + W(Ct_1 - Ct_2) - \kappa_2 \cdot Ct_2 + J_2 \quad (4-10)$$

κ_2 = reaction velocity in Layer 2 (m day⁻¹)

J_2 = sum of all internal sources including diagenesis in Layer 2 (g m⁻² day⁻¹).

The substances produced by mineralization of POM in sediments may be present in both dissolved and particulate phases. This distribution directly affects the magnitude of the substance that is returned to the overlying water. In Equations 4-8 to 4-10, the distribution of a substance between the dissolved and particulate phases in a sediment is parameterized using a linear partitioning coefficient. The dissolved and particulate fractions are computed from the partitioning equations:

$$fd_1 = \frac{1}{1 + m_1 \cdot \pi_1} \quad fp_1 = 1 - fd_1 \quad (4-11-1)$$

$$fd_2 = \frac{1}{1 + m_2 \cdot \pi_2} \quad fp_2 = 1 - fd_2 \quad (4-11-2)$$

m_1 & m_2 = solid concentrations in Layer 1 and 2, respectively (kg L⁻¹)

π_1 & π_2 = partition coefficients in Layer 1 and 2, respectively (per kg L⁻¹).

The partition coefficient is the ratio of particulate to dissolved fraction per unit solid concentration (i.e., per unit sorption site available).

All terms, except the last two terms, in Equations 4-8 and 4-10 are common to all state variables and are described in Section IV-3-1. The last two terms represent the

reaction and source/sink terms, respectively. These terms, which take different mathematical formulations for different state variables, are described in Sections IV-3-2 to IV-3-5 for ammonium, nitrate, phosphate and sulfide/methane, respectively.

IV-3-1. Common parameters for sediment flux

Parameters that are needed for the sediment fluxes are s , ω , KL , W , H_2 , m_1 , m_2 , π_1 , π_2 , κ_1 , κ_2 , J_1 and J_2 in Equations 4-8 to 4-11. Of these, κ_1 , κ_2 , J_1 and J_2 are variable-specific. Among the other common parameters, W (Section IV-7-2C), H_2 (Section IV-7-2D), and m_1 and m_2 (Section IV-7-3B), are specified as input. The modeling of the remaining three parameters, s , ω , KL , are described in this section.

A. Surface mass transfer coefficient: Owing to the observation that the surface mass transfer coefficient, s , can be related to the sediment oxygen demand, SOD (DiToro et al. 1990), s can be estimated from the ratio of SOD and overlying water oxygen concentration:

$$s = \frac{D_1}{H_1} = \frac{SOD}{DO_0} \quad (4-12)$$

D_1 = diffusion coefficient in Layer 1 ($m^2 \text{ day}^{-1}$).

Knowing s , it is possible to estimate the other model parameters.

B. Particulate phase mixing coefficient: The particle mixing velocity between Layer 1 and 2 is parameterized as:

$$\omega = \frac{D_p \cdot \theta_{Dp}^{T-20}}{H_2} \frac{G_{POC,1}}{G_{POC,R}} \frac{DO_0}{KM_{Dp} + DO_0} \quad (4-13)$$

D_p = apparent diffusion coefficient for particle mixing ($m^2 \text{ day}^{-1}$)

θ_{Dp} = constant for temperature adjustment for D_p

$G_{POC,R}$ = reference concentration for $G_{POC,1}$ ($g \text{ C } m^{-3}$)

KM_{Dp} = particle mixing half-saturation constant for oxygen ($g \text{ O}_2 \text{ m}^{-3}$).

The enhanced mixing of sediment particles by macrobenthos (bioturbation) is quantified by estimating D_p . The particle mixing appears to be proportional to the benthic biomass

(Matisoff 1982), which is correlated to the carbon input to the sediment (Robbins et al. 1989). This is parameterized by assuming that benthic biomass is proportional to the available labile carbon, $G_{POC,1}$, and $G_{POC,R}$ is the reference concentration at which the particle mixing velocity is at its nominal value. The Monod-type oxygen dependency accounts for the oxygen dependency of benthic biomass.

It has been observed that a hysteresis exists in the relationship between the bottom water oxygen and benthic biomass. Benthic biomass increases as the summer progresses. However, the occurrence of anoxia/hypoxia reduces the biomass drastically and also imposes stress on benthic activities. After full overturn, the bottom water oxygen increases but the population does not recover immediately. Hence, the particle mixing velocity, which is proportional to the benthic biomass, does not increase in response to the increased bottom water oxygen. Recovery of benthic biomass following hypoxic events depends on many factors including severity and longevity of hypoxia, constituent species and salinity (Diaz & Rosenberg, submitted).

This phenomenon of reduced benthic activities and hysteresis is parameterized based on the idea of stress that low oxygen imposes on the benthic population. It is analogous to the modeling of the toxic effect of chemicals on organisms (Mancini 1983). A first order differential equation is employed, in which the benthic stress 1) accumulates only when overlying oxygen is below KM_{Dp} and 2) is dissipated at a first order rate (Fig. 4-3a):

$$\begin{aligned} \frac{\partial ST}{\partial t} &= -K_{ST} \cdot ST + \left[1 - \frac{DO_0}{KM_{Dp}} \right] && \text{if } DO_0 < KM_{Dp} \\ \frac{\partial ST}{\partial t} &= -K_{ST} \cdot ST && \text{if } DO_0 > KM_{Dp} \end{aligned} \quad (4-14)^*$$

ST = accumulated benthic stress (day)

K_{ST} = first order decay rate for ST (day^{-1}).

The behavior of this formulation can be understood by evaluating the steady-state stresses at two extreme conditions of overlying water oxygen, DO_0 :

as $DO_0 = 0$	$K_{ST} \cdot ST = 1$	$f(ST) = (1 - K_{ST} \cdot ST) = 0$
as $DO_0 \geq KM_{Dp}$	$K_{ST} \cdot ST = 0$	$f(ST) = (1 - K_{ST} \cdot ST) = 1$

The unitless expression, $f(ST) = 1 - K_{ST} \cdot ST$, appears to be the proper variable to quantify the effect of benthic stress on benthic biomass and thus particle mixing (Fig. 4-3b).

The final formulation for the particle mixing velocity including the benthic stress is:

$$\omega = \frac{D_p \cdot \theta_{Dp}^{T-20}}{H_2} \frac{G_{POC,1}}{G_{POC,R}} \frac{DO_0}{KM_{Dp} + DO_0} f(ST) + \frac{Dp_{min}}{H_2} \quad (4-15)$$

Dp_{min} = minimum diffusion coefficient for particle mixing ($m^2 \text{ day}^{-1}$).

The reduction in particle mixing due to the benthic stress, $f(ST)$, is estimated by employing the following procedure. The stress, ST , is normally calculated with Eq. 4-14. Once DO_0 drops below a critical concentration, $DO_{ST,c}$, for $NC_{hypoxia}$ consecutive days or more, the calculated stress is not allowed to decrease until t_{MBS} days of $DO_0 > DO_{ST,c}$. That is, only when hypoxic days are longer than critical hypoxia days ($NC_{hypoxia}$), the maximum stress, or minimum $(1 - K_{ST} \cdot ST)$, is retained for a specified period (t_{MBS} days) after DO_0 recovery (Fig. 4-3). No hysteresis occurs if DO_0 does not drop below $DO_{ST,c}$ or if hypoxia lasts shorter than $NC_{hypoxia}$ days. When applying maximum stress for t_{MBS} days, the subsequent hypoxic days are not included in t_{MBS} . This parametrization of hysteresis essentially assumes seasonal hypoxia, i.e., one or two major hypoxic events during summer, and might be unsuitable for systems with multiple hypoxic events throughout a year.

Three parameters relating to hysteresis, $DO_{ST,c}$, $NC_{hypoxia}$ and t_{MBS} , are functions of many factors including severity and longevity of hypoxia, constituent species and salinity, and thus have site-specific variabilities (Diaz & Rosenberg, submitted). The critical overlying oxygen concentration, $DO_{ST,c}$, also depends on the distance from the bottom of the location of DO_0 measurement, which is discussed in section for parameter evaluation (Section IV-7-3B). The critical hypoxia days, $NC_{hypoxia}$, depends on tolerance of benthic organisms to hypoxia and thus on benthic community structure (Diaz & Rosenberg, submitted). The time lag for the recovery of benthic biomass following hypoxic events, t_{MBS} , tends to be longer for higher salinity. Since the present tidal prism model is intended to be applied to relatively small systems, the above three parameters are considered to be spatially constant input parameters.

C. Dissolved phase mixing coefficient: Dissolved phase mixing between Layer 1 and 2 is via passive molecular diffusion, which is enhanced by the mixing activities of the benthic organisms (bio-irrigation). This is modeled by increasing the diffusion coefficient relative to the molecular diffusion coefficient:

$$KL = \frac{D_d \cdot \theta_{Dd}^{T-20}}{H_2} + R_{BI,BT} \cdot \omega \quad (4-16)$$

D_d = diffusion coefficient in pore water ($m^2 \text{ day}^{-1}$)

θ_{Dd} = constant for temperature adjustment for D_d

$R_{BI,BT}$ = ratio of bio-irrigation to bioturbation.

The last term in Eq. 4-16 accounts for the enhanced mixing by organism activities.

IV-3-2. Ammonium nitrogen

Diagenesis is assumed not to occur in the upper layer because of its shallow depth, and ammonium is produced by diagenesis in the lower layer:

$$J_{1,NH4} = 0 \quad J_{2,NH4} = J_N \quad (\text{from Eq. 4-7}) \quad (4-17)$$

Ammonium is nitrified to nitrate in the presence of oxygen. A Monod-type expression is used for the ammonium and oxygen dependency of the nitrification rate. Then, the oxic layer reaction velocity in Eq. 4-8 for ammonium may be expressed as:

$$\kappa_{1,NH4}^2 = \frac{DO_0}{2 \cdot KM_{NH4,O2} + DO_0} \frac{KM_{NH4}}{KM_{NH4} + NH4_1} \kappa_{NH4}^2 \theta_{NH4}^{T-20} \quad (4-18)$$

and then the nitrification flux becomes:

$$J_{Nit} = \frac{\kappa_{1,NH4}^2}{S} \cdot NH4_1 \quad (4-19)$$

$KM_{NH4,O2}$ = nitrification half-saturation constant for dissolved oxygen ($g \text{ O}_2 \text{ m}^{-3}$)

$NH4_1$ = total ammonium nitrogen concentration in Layer 1 ($g \text{ N m}^{-3}$)

KM_{NH4} = nitrification half-saturation constant for ammonium ($g \text{ N m}^{-3}$)

κ_{NH4} = optimal reaction velocity for nitrification at 20°C ($m \text{ day}^{-1}$)

θ_{NH4} = constant for temperature adjustment for κ_{NH4}

J_{Nit} = nitrification flux ($g \text{ N m}^{-2} \text{ day}^{-1}$).

Nitrification does not occur in the anoxic lower layer:

$$\kappa_{2,NH4} = 0 \quad (4-20)$$

Once Equations 4-8 and 4-10 are solved for $NH4_1$ and $NH4_2$, the sediment flux of ammonium to the overlying water, $J_{aq,NH4}$, can be calculated using Eq. 4-9. Note that it is not $NH4_1$ and $NH4_2$ that determine the magnitude of $J_{aq,NH4}$ (Section X-B-2 in D&F). The magnitude is determined by 1) the diagenesis flux, 2) the fraction that is nitrified and 3) surface mass transfer coefficient (s) that mixes the remaining portion.

IV-3-3. Nitrate nitrogen

Nitrification flux is the only source of nitrate in the upper layer, and there is no diagenetic source for nitrate in both layers:

$$J_{1,NO3} = J_{Ni} \quad (\text{from Eq. 4-19}) \quad J_{2,NO3} = 0 \quad (4-21)$$

Nitrate is present in sediments as dissolved substance, i.e., $\pi_{1,NO3} = \pi_{2,NO3} = 0$, making $fd_{1,NO3} = fd_{2,NO3} = 1$ (Eq. 4-11): it also makes ω meaningless, hence $\omega = 0$. Nitrate is removed by denitrification in both oxic and anoxic layers with the carbon required for denitrification supplied by carbon diagenesis. The reaction velocities in Equations 4-8 and 4-10 for nitrate may be expressed as:

$$\kappa_{1,NO3}^2 = \kappa_{NO3,1}^2 \cdot \theta_{NO3}^{T-20} \quad (4-22-1)$$

$$\kappa_{2,NO3} = \kappa_{NO3,2} \cdot \theta_{NO3}^{T-20} \quad (4-22-2)$$

and the denitrification flux out of sediments as a nitrogen gas becomes:

$$J_{N2(g)} = \frac{\kappa_{1,NO3}^2}{s} NO3_1 + \kappa_{2,NO3} \cdot NO3_2 \quad (4-23)$$

$\kappa_{NO3,1}$ = reaction velocity for denitrification in Layer 1 at 20°C (m day⁻¹)

$\kappa_{NO3,2}$ = reaction velocity for denitrification in Layer 2 at 20°C (m day⁻¹)

θ_{NO3} = constant for temperature adjustment for $\kappa_{NO3,1}$ and $\kappa_{NO3,2}$

$J_{N2(g)}$ = denitrification flux (g N m⁻² day⁻¹)

$NO3_1$ = total nitrate nitrogen concentration in Layer 1 (g N m⁻³)

$NO3_2$ = total nitrate nitrogen concentration in Layer 2 (g N m⁻³).

Once Equations 4-8 and 4-10 are solved for NO_3_1 and NO_3_2 , the sediment flux of nitrate to the overlying water, $J_{\text{aq,NO}_3}$, can be calculated using Eq. 4-9. The steady-state solution for nitrate showed that the nitrate flux is a linear function of NO_3_0 (Eq. III-15 in D&F): the intercept quantifies the amount of ammonium in the sediment that is nitrified but not denitrified (thus releases as $J_{\text{aq,NO}_3}$), and the slope quantifies the extent to which overlying water nitrate is denitrified in the sediment. It also revealed that if the internal production of nitrate is small relative to the flux of nitrate from the overlying water, the normalized nitrate flux to the sediment, $-J_{\text{aq,NO}_3}/\text{NO}_3_0$, is linear in s for small s and constant for large s (Section III-C in D&F). For small s ($\sim 0.01 \text{ m day}^{-1}$), H_1 is large (Eq. 4-12) so that oxic layer denitrification predominates and $J_{\text{aq,NO}_3}$ is essentially zero independent of NO_3_0 (Fig. III-4 in D&F).

IV-3-4. Phosphate phosphorus

Phosphate is produced by the diagenetic breakdown of POP in the lower layer:

$$J_{1,\text{PO}_4} = 0 \quad J_{2,\text{PO}_4} = J_p \quad (\text{from Eq. 4-7}) \quad (4-24)$$

A portion of the liberated phosphate remains in the dissolved form and a portion becomes particulate phosphate, either via precipitation of phosphate-containing minerals (Troup 1974), e.g., vivianite, $\text{Fe}_3(\text{PO}_4)_2(\text{s})$, or by partitioning to phosphate sorption sites (Lijklema 1980; Barrow 1983; Giordani & Astorri 1986). The extent of particulate formation is determined by the magnitude of the partition coefficients, π_{1,PO_4} and π_{2,PO_4} , in Eq. 4-11. Phosphate flux is strongly affected by DO_0 , the overlying water oxygen concentration. As DO_0 approaches zero, the phosphate flux from the sediments increases. This mechanism is incorporated by making π_{1,PO_4} larger, under oxic conditions, than π_{2,PO_4} . In the model, when DO_0 exceeds a critical concentration, $(\text{DO}_0)_{\text{crit,PO}_4}$, sorption in the upper layer is enhanced by an amount $\Delta\pi_{\text{PO}_4,1}$:

$$\pi_{1,\text{PO}_4} = \pi_{2,\text{PO}_4} \cdot (\Delta\pi_{\text{PO}_4,1}) \quad \text{DO}_0 > (\text{DO}_0)_{\text{crit,PO}_4} \quad (4-25-1)$$

When oxygen falls below $(\text{DO}_0)_{\text{crit,PO}_4}$, then:

$$\pi_{1,\text{PO}_4} = \pi_{2,\text{PO}_4} \cdot (\Delta\pi_{\text{PO}_4,1})^{\text{DO}_0/(\text{DO}_0)_{\text{crit,PO}_4}} \quad \text{DO}_0 \leq (\text{DO}_0)_{\text{crit,PO}_4} \quad (4-25-2)$$

which smoothly reduces π_{1,PO_4} to π_{2,PO_4} as DO_0 goes to zero. There is no removal

reaction for phosphate in both layers:

$$\kappa_{1,PO4} = \kappa_{2,PO4} = 0 \quad (4-26)$$

Once Equations 4-8 and 4-10 are solved for $PO4_1$ and $PO4_2$, the sediment flux of phosphate to the overlying water, $J_{aq,PO4}$, can be calculated using Eq. 4-9.

IV-3-5. Sulfide/methane and oxygen demand

A. Sulfide: No diagenetic production of sulfide occurs in the upper layer. In the lower layer, sulfide is produced by carbon diagenesis (Eq. 4-7) decremented by the organic carbon consumed by denitrification (Eq. 4-23). Then:

$$J_{1,H2S} = 0 \quad J_{2,H2S} = a_{O2,C} \cdot J_C - a_{O2,NO3} \cdot J_{N2(g)} \quad (4-27)$$

$a_{O2,C}$ = stoichiometric coefficient for carbon diagenesis consumed by sulfide oxidation
(2.6667 g O₂-equivalents per g C)

$a_{O2,NO3}$ = stoichiometric coefficient for carbon diagenesis consumed by denitrification
(2.8571 g O₂-equivalents per g N).

A portion of the dissolved sulfide that is produced in the anoxic layer reacts with the iron to form particulate iron monosulfide, FeS(s) (Morse et al. 1987). The particulate fraction is mixed into the oxic layer where it can be oxidized to ferric oxyhydroxide, Fe₂O₃(s). The remaining dissolved fraction also diffuses into the oxic layer where it is oxidized to sulfate. Partitioning between dissolved and particulate sulfide in the model represents the formation of FeS(s), which is parameterized using partition coefficients, $\pi_{1,H2S}$ and $\pi_{2,H2S}$, in Eq. 4-11.

The present sediment model has three pathways for sulfide, the reduced end product of carbon diagenesis: 1) sulfide oxidation, 2) aqueous sulfide flux and 3) burial. The distribution of sulfide among the three pathways is controlled by the partitioning coefficients and the oxidation reaction velocities (Section V-E in D&F). Both dissolved and particulate sulfide are oxidized in the oxic layer, consuming oxygen in the process. In the oxic upper layer, the oxidation rate that is linear in oxygen concentration is used (Cline & Richards 1969; Millero 1986; Boudreau 1991). In the anoxic lower layer, no oxidation can occur. Then, the reaction velocities in Equations 4-8 and 4-10 may be expressed as:

$$\kappa_{1,H2S}^2 = (\kappa_{H2S,d1}^2 \cdot fd_{1,H2S} + \kappa_{H2S,p1}^2 \cdot fp_{1,H2S}) \theta_{H2S}^{T-20} \frac{DO_0}{2 \cdot KM_{H2S,O2}} \quad (4-28-1)$$

$$\kappa_{2,H2S} = 0 \quad (4-28-2)$$

$\kappa_{H2S,d1}$ = reaction velocity for dissolved sulfide oxidation in Layer 1 at 20°C (m day⁻¹)

$\kappa_{H2S,p1}$ = reaction velocity for particulate sulfide oxidation in Layer 1 at 20°C (m day⁻¹)

θ_{H2S} = constant for temperature adjustment for $\kappa_{H2S,d1}$ and $\kappa_{H2S,p1}$

$KM_{H2S,O2}$ = constant to normalize the sulfide oxidation rate for oxygen (g O₂ m⁻³).

The constant, $KM_{H2S,O2}$, which is included for convenience only, is used to scale the oxygen concentration in the overlying water. At $DO_0 = KM_{H2S,O2}$, the reaction velocity for sulfide oxidation rate is at its nominal value.

The oxidation reactions in the oxic upper layer cause oxygen flux to the sediment, which exerts SOD. By convention, SOD is positive: $SOD = -J_{aq,O2}$. The SOD in the model consists of two components, carbonaceous sediment oxygen demand (CSOD) due to sulfide oxidation and nitrogenous sediment oxygen demand (NSOD) due to nitrification:

$$SOD = CSOD + NSOD = \frac{\kappa_{1,H2S}^2}{s} H2S_1 + a_{O2,NH4} \cdot J_{Nit} \quad (4-29)$$

$H2S_1$ = total sulfide concentration in Layer 1 (g O₂-equivalents m⁻³)

$a_{O2,NH4}$ = stoichiometric coefficient for oxygen consumed by nitrification (4.33 g O₂ per g N: Section III-7-2).

Equation 4-29 is nonlinear for SOD because the RHS contains s ($= SOD/DO_0$) so that SOD appears on both sides of the equation: note that J_{Nit} (Eq. 4-19) is also a function of s . A simple back substitution method is used, as explained in Section IV-6-1.

If the overlying water oxygen is low, then the sulfide that is not completely oxidized in the upper layer can diffuse into the overlying water. This aqueous sulfide flux out of the sediments, which contributes to the chemical oxygen demand in the water column model, is modeled using

$$J_{aq,H2S} = s(fd_{1,H2S} \cdot H2S_1 - COD) \quad (4-30)*$$

The sulfide released from the sediment reacts very quickly in the water column when

oxygen is available, but can accumulate in the water column under anoxic conditions. The COD, quantified as oxygen equivalents, is entirely supplied by benthic release in the water column model (Eq. 3-16). Since sulfide also is quantified as oxygen equivalents, COD is used as a measure of sulfide in the water column in Eq. 4-30.

B. Methane: When sulfate is used up, methane can be produced by carbon diagenesis and methane oxidation consumes oxygen (DiToro et al. 1990). Owing to the abundant sulfate in the saltwater, only the aforementioned sulfide production and oxidation are considered to occur in the saltwater. Since the sulfate concentration in the freshwater is generally insignificant, methane production is considered to replace sulfide production in the freshwater. In the freshwater, methane is produced by carbon diagenesis in the lower layer decremented by the organic carbon consumed by denitrification, and no diagenetic production of methane occurs in the upper layer (Eq. 4-27):

$$J_{1,CH_4} = 0 \quad J_{2,CH_4} = a_{O_2,C} \cdot J_C - a_{O_2,NO_3} \cdot J_{N_2(g)} \quad (4-31)$$

The dissolved methane produced takes two pathways: 1) oxidation in the oxic upper layer causing CSOD or 2) escape from the sediment as aqueous flux or as gas flux:

$$J_{2,CH_4} = CSOD + J_{aq,CH_4} + J_{CH_4(g)} \quad (4-32)$$

J_{aq,CH_4} = aqueous methane flux (g O₂-equivalents m⁻² day⁻¹)

$J_{CH_4(g)}$ = gaseous methane flux (g O₂-equivalents m⁻² day⁻¹).

A portion of dissolved methane that is produced in the anoxic layer diffuses into the oxic layer where it is oxidized. This methane oxidation causes CSOD in the freshwater sediment (DiToro et al. 1990):

$$CSOD = CSOD_{max} \cdot \left[1 - \operatorname{sech} \left[\frac{\kappa_{CH_4} \cdot \theta_{CH_4}^{T-20}}{S} \right] \right] \quad (4-33)$$

$$CSOD_{max} = \operatorname{minimum} \left\{ \sqrt{2 \cdot KL \cdot CH_{4,sat} \cdot J_{2,CH_4}}, J_{2,CH_4} \right\} \quad (4-33-1)$$

$$CH_{4,sat} = 100 \left[1 + \frac{h + H_2}{10} \right] 1.024^{20 - T} \quad (4-33-2)$$

$CSOD_{max}$ = maximum CSOD occurring when all the dissolved methane transported to

the oxic layer is oxidized

κ_{CH_4} = reaction velocity for dissolved methane oxidation in Layer 1 at 20°C (m day⁻¹)

θ_{CH_4} = constant for temperature adjustment for κ_{CH_4}

CH_4_{sat} = saturation concentration of methane in the pore water (g O₂-equivalents m⁻³).

The term, $(h + H_2)/10$ where h and H_2 are in meters, in Eq. 4-33-2 is the depth from the water surface that corrects for the in situ pressure. Equation 4-33-2 is accurate to within 3% of the reported methane solubility between 5 and 20°C (Yamamoto et al. 1976).

If the overlying water oxygen is low, the methane that is not completely oxidized can escape the sediment into the overlying water either as aqueous flux or as gas flux. The aqueous methane flux, which contributes to the chemical oxygen demand in the water column model, is modeled using (DiToro et al. 1990):

$$J_{aq,CH_4} = CSOD_{max} \cdot \operatorname{sech}\left[\frac{\kappa_{CH_4} \cdot \theta_{CH_4}^{T-20}}{s}\right] = CSOD_{max} - CSOD \quad (4-34)$$

Methane is only slightly soluble in water. If its solubility, CH_4_{sat} given by Eq. 4-33-2, is exceeded in the pore water, it forms a gas phase that escapes as bubbles. The loss of methane as bubbles, i.e., the gaseous methane flux, is modeled using Eq. 4-32 with J_{2,CH_4} from Eq. 4-31, CSOD from Eq. 4-33 and J_{aq,CH_4} from Eq. 4-34 (DiToro et al. 1990).

IV-4. Silica

The production of ammonium, nitrate and phosphate in sediments is the result of the mineralization of POM by bacteria. The production of dissolved silica in sediments is the result of the dissolution of particulate biogenic or opaline silica, which is thought to be independent of bacterial processes.

The depositional flux of particulate biogenic silica from the overlying water to the sediments is modeled using Eq. 4-5. With this source, the mass-balance equation for particulate biogenic silica may be written as:

$$H_2 \frac{\partial PSi}{\partial t} = - S_{Si} \cdot H_2 - W \cdot PSi + J_{PSi} + J_{DSi} \quad (4-35)$$

PSi = concentration of particulate biogenic silica in the sediment (g Si m⁻³)

S_{Si} = dissolution rate of PSi in Layer 2 (g Si m⁻³ day⁻¹)

J_{PSi} = depositional flux of PSi ($\text{g Si m}^{-2} \text{ day}^{-1}$) given by Eq. 4-5

J_{DSi} = detrital flux of PSi ($\text{g Si m}^{-2} \text{ day}^{-1}$) to account for PSi settling to the sediment that is not associated with the algal flux of biogenic silica (??).

The processes included in Eq. 4-35 are dissolution (i.e., production of dissolved silica), burial, and depositional and detrital fluxes from the overlying water. Equation 4-35 can be viewed as the analog of the diagenesis equations for POM (Eq. 4-6). The dissolution rate is formulated using a reversible reaction that is first order in silica solubility deficit and follows a Monod-type relationship in particulate silica:

$$S_{Si} = K_{Si} \cdot \theta_{Si}^{T-20} \frac{PSi}{PSi + KM_{PSi}} (Si_{sat} - f_{d2,Si} \cdot Si_2) \quad (4-36)$$

K_{Si} = first order dissolution rate for PSi at 20°C in Layer 2 (day^{-1})

θ_{Si} = constant for temperature adjustment for K_{Si}

KM_{PSi} = silica dissolution half-saturation constant for PSi (g Si m^{-3})

Si_{sat} = saturation concentration of silica in the pore water (g Si m^{-3}).

The mass-balance equations for mineralized silica can be formulated using the general forms, Equations 4-8 and 4-10. There is no source/sink term and no reaction in the upper layer:

$$J_{1,Si} = \kappa_{1,Si} = 0 \quad (4-37)$$

In the lower layer, silica is produced by the dissolution of particulate biogenic silica, which is modeled using Eq. 4-36. The two terms in Eq. 4-36 correspond to the source term and reaction term in Eq. 4-10:

$$J_{2,Si} = K_{Si} \cdot \theta_{Si}^{T-20} \frac{PSi}{PSi + KM_{PSi}} Si_{sat} \cdot H_2 \quad (4-38-1)$$

$$\kappa_{2,Si} = K_{Si} \cdot \theta_{Si}^{T-20} \frac{PSi}{PSi + KM_{PSi}} f_{d2,Si} \cdot H_2 \quad (4-38-2)$$

A portion of silica dissolved from particulate silica sorbs to solids and a portion remains in the dissolved form. Partitioning using the partition coefficients, $\pi_{1,Si}$ and $\pi_{2,Si}$, in Eq. 4-11 controls the extent to which dissolved silica sorbs to solids. Since silica shows similar behavior as phosphate in adsorption-desorption process, the same

partitioning method as applied to phosphate (Section IV-3-4) is used for silica. That is, when DO_0 exceeds a critical concentration, $(DO_0)_{crit,Si}$, sorption in the upper layer is enhanced by an amount $\Delta\pi_{Si,1}$:

$$\pi_{1,Si} = \pi_{2,Si}(\Delta\pi_{Si,1}) \quad DO_0 > (DO_0)_{crit,Si} \quad (4-39-1)$$

When oxygen falls below $(DO_0)_{crit,Si}$, then:

$$\pi_{1,Si} = \pi_{2,Si}(\Delta\pi_{Si,1})^{DO_0/(DO_0)_{crit,Si}} \quad DO_0 \leq (DO_0)_{crit,Si} \quad (4-39-2)$$

which smoothly reduces $\pi_{1,Si}$ to $\pi_{2,Si}$ as DO_0 goes to zero.

Once Equations 4-8 and 4-10 are solved for Si_1 and Si_2 , the sediment flux of silica to the overlying water, $J_{aq,Si}$, can be calculated using Eq. 4-9.

IV-5. Sediment temperature

All rate coefficients in the aforementioned mass-balance equations are expressed as a function of sediment temperature, T . The sediment temperature is modeled based on the diffusion of heat between the water column and sediment:

$$\frac{\partial T}{\partial t} = \frac{D_T}{H^2}(T_w - T) \quad (4-40)$$

D_T = heat diffusion coefficient between the water column and sediment ($m^2 \text{ sec}^{-1}$)

T_w = temperature in the overlying water column ($^{\circ}\text{C}$) calculated by Eq. 3-21.

The model application in D&F and Cerco & Cole (1994) used $D_T = 1.8 \times 10^{-7} \text{ m}^2 \text{ sec}^{-1}$.

IV-6. Method of Solution

IV-6-1. Finite difference equations and solution scheme

An implicit integration scheme is used to solve the governing mass-balance equations. The finite difference form of Eq. 4-8 may be expressed as:

$$\begin{aligned} 0 = & s(fd_0 \cdot Ct_0' - fd_1 \cdot Ct_1') + KL(fd_2 \cdot Ct_2' - fd_1 \cdot Ct_1') + \omega(fp_2 \cdot Ct_2' - fp_1 \cdot Ct_1') \\ & - W \cdot Ct_1' - \frac{\kappa_1^2}{s} Ct_1' + J_1' \end{aligned} \quad (4-41)$$

where the primed variables designate the values evaluated at $t + \Delta t$ and the unprimed variables are those at t . The finite difference form of Eq. 4-10 may be expressed as:

$$0 = -KL(fd_2 \cdot Ct_2' - fd_1 \cdot Ct_1') - \omega(fp_2 \cdot Ct_2' - fp_1 \cdot Ct_1') + W(Ct_1' - Ct_2') - (\kappa_2 + \frac{H_2}{\Delta t})Ct_2' + \left[J_2' + \frac{H_2}{\Delta t} Ct_2 \right] \quad (4-42)$$

The two terms, $-(H_2/\Delta t)Ct_2'$ and $(H_2/\Delta t)Ct_2$, are from the derivative term, $H_2(\partial Ct_2/\partial t)$ in Eq. 4-10, each of which simply adds to the Layer 2 removal rate and the forcing function, respectively. Setting these two terms equal to zero results in the steady-state model. The two unknowns, Ct_1' and Ct_2' , can be calculated at every time step using:

$$\begin{bmatrix} s \cdot fd_1 + a_1 + \frac{\kappa_1^2}{s} & -a_2 \\ -a_1 & a_2 + W + \kappa_2 + \frac{H_2}{\Delta t} \end{bmatrix} \begin{bmatrix} Ct_1' \\ Ct_2' \end{bmatrix} = \begin{bmatrix} J_1' + s \cdot fd_0 \cdot Ct_0' \\ J_2' + \frac{H_2}{\Delta t} Ct_2 \end{bmatrix} \quad (4-43)$$

$$a_1 = KL \cdot fd_1 + \omega \cdot fp_1 + W \quad a_2 = KL \cdot fd_2 + \omega \cdot fp_2 \quad (4-43-1)$$

The solution of Eq. 4-43 requires an iterative method since the surface mass transfer coefficient, s , is a function of the SOD (Eq. 4-12), which also is a function of s (Eq. 4-29). A simple back substitution method is used:

- (1) Start with an initial estimate of SOD: for example, $SOD = a_{O_2,C} \cdot J_C$ or the previous time step SOD.
- (2) Solve Eq. 4-43 for ammonium, nitrate and sulfide/methane.
- (3) Compute the SOD using Eq. 4-29.
- (4) Refine the estimate of SOD: a root finding method (Brent's method in Press et al. 1986) is used to make the new estimate.
- (5) Go to (2) if no convergence.
- (6) Solve Eq. 4-43 for phosphate and silica.

For the sake of symmetry, the equations for diagenesis, particulate biogenic silica and sediment temperature are also solved in implicit form. The finite difference form of the diagenesis equation (Eq. 4-6) may be expressed as:

$$G'_{POM,i} = \left[G_{POM,i} + \frac{\Delta t}{H_2} J_{POM,i} \right] \left[1 + \Delta t \cdot K_{POM,i} \cdot \theta_{POM,i}^{T-20} + \frac{\Delta t}{H_2} W \right]^{-1} \quad (4-44)$$

The finite difference form of the PSi equation (Eq. 4-35) may be expressed as:

$$PSi' = \left[PSi + \frac{\Delta t}{H_2} (J_{PSi} + J_{DSi}) \right] \left[1 + \Delta t \cdot K_{Si} \cdot \theta_{Si}^{T-20} \frac{Si_{sat} - f_{d2, Si} \cdot Si_2}{PSi + KM_{PSi}} + \frac{\Delta t}{H_2} W \right]^{-1} \quad (4-45)$$

using Eq. 4-32 for the dissolution term, in which PSi in the Monod-type term has been kept at time level t to simplify the solution. The finite difference form of the sediment temperature equation (Eq. 4-40) may be expressed as:

$$T' = \left[T + \frac{\Delta t}{H^2} D_T \cdot T_w \right] \left[1 + \frac{\Delta t}{H^2} D_T \right]^{-1} \quad (4-46)$$

IV-6-2. Boundary and initial conditions

The above finite difference equations constitute an initial boundary-value problem. The boundary conditions are the depositional fluxes ($J_{POM,i}$ and J_{PSi}) and the overlying water conditions (C_{t0} and T_w) as a function of time, which are provided from the water column water quality model. The initial conditions are the concentrations at $t = 0$, $G_{POM,i}(0)$, $PSi(0)$, $C_{t1}(0)$, $C_{t2}(0)$ and $T(0)$, to start the computations. Strictly speaking, these initial conditions should reflect the past history of the overlying water conditions and depositional fluxes, which often is impractical because of lack of field data for these earlier years. The procedure to evaluate the initial conditions using the stand-alone model is described in Section IV-6-3.

IV-6-3. Stand-alone model

For the purposes of estimating initial conditions and "stand alone" application (Section IV-7), a stand-alone version of sediment model is included in the present model package. The stand-alone model application also requires initial and boundary conditions. The steady-state solution for the average conditions on the first year, for which the field data are available, is obtained and used as an arbitrary set of initial conditions. The solution scheme in Section IV-6-1 becomes the steady-state one as $\Delta t \rightarrow \infty$.

The boundary conditions are the overlying water conditions including temperature and the depositional fluxes. The overlying water conditions in the stand-alone model have to be based on observations collected at the time sediment-water fluxes are

measured. These conditions as a function of time can be obtained using a four-term Fourier series:

$$Cd_0(t) = a_0 + \sum_{k=1}^4 \left\{ a_k \cdot \sin \left[\frac{2\pi kt}{T_p} \right] + b_k \cdot \cos \left[\frac{2\pi kt}{T_p} \right] \right\} \quad (4-47)$$

Since the field data are often sampled at irregular intervals, the nine coefficients, $a_0 \dots a_4$ and $b_1 \dots b_4$, may be estimated using a multiple linear regression. For multiple year data, the data for each year may be fitted separately so that the period, T_p , is one year.

The stand-alone model may use the observed depositional fluxes, if available, as boundary conditions. If the depositional flux of nitrogen, J_{PON} ($= \sum_i J_{PON,i}$), is measured, the depositional fluxes of carbon, phosphorus and silica can be established using suitable stoichiometric ratios. However, the measurements of J_{PON} for the entire model simulation period are impractical and hardly exist. Two possibilities are available. One is to derive J_{POM} using the observed water column POM and estimate of settling velocity of POM. The other is to assume that the depositional fluxes are constant within a year and that seasonal variations in diagenesis fluxes are accounted for by the temperature dependency of the diagenesis rate constants (Section VIII-E in D&F). Yearly average depositional fluxes can be derived from the observed J_{aq,NH_4} , DO_0 , SOD and NH_4_0 by estimating the ammonium diagenesis flux, J_N . The procedure is described below.

From the observed J_{aq,NH_4} , J_N can be estimated using (Sections II-D and VIII-E in D&F):

$$\begin{aligned} J_N &= J_{aq,NH_4} + \frac{\kappa_{1,NH_4}^2}{s} NH_4_1 \\ &= J_{aq,NH_4} + \frac{DO_0}{2 \cdot KM_{NH_4,O_2} + DO_0} \frac{KM_{NH_4} \cdot \theta_{KM,NH_4}^{T-20}}{KM_{NH_4} \cdot \theta_{KM,NH_4}^{T-20} + NH_4_1} \frac{\kappa_{NH_4}^2 \cdot \theta_{NH_4}^{T-20}}{s} NH_4_1 \end{aligned} \quad (4-48)$$

where θ_{KM,NH_4} , a constant for temperature adjustment for KM_{NH_4} , accounts for the effect of temperature on KM_{NH_4} : $\theta_{KM,NH_4} = 1.125$ is used in D&F. Equation 4-48, which can be obtained by adding Equations 4-8 and 4-10 assuming steady-state and no burial, states that J_N is the sum of J_{aq,NH_4} and the quantity of ammonium that is nitrified to nitrate.

Rearrangement of Eq. 4-9 gives the oxic layer ammonium concentration:

$$NH4_1 = \frac{1}{fd_{1,NH4}} \left[\frac{J_{aq,NH4}}{s} + NH4_0 \right] \quad (4-49)$$

Equations 4-48 and 4-49 can be applied pointwise to each measurement of $J_{aq,NH4}$, and the resulting time series estimates of J_N serve as the calibration data for estimating J_{PON} .

With the initial conditions estimated from the steady-state solution for the average conditions on the first year, the diagenesis portion of the model (Equations 4-6 and 4-7) is solved to compute J_N for an assumed J_{PON} . Through the comparison of the model calculated J_N to the time series estimates, yearly average J_{PON} can be evaluated. The location-specific, yearly average J_{PON} estimated using the Chesapeake Bay data set (1985-1988) ranged 0.03 to 0.125 g N m⁻² day⁻¹ (Table 8-6 in D&F). The other depositional fluxes, J_{POC} , J_{POP} and J_{PSi} , can be established using constant stoichiometric ratios:

$$J_{POC} = a_{C,N} \cdot J_{PON} \quad J_{POP} = \frac{1}{a_{C,P}} \cdot J_{POC} \quad J_{PSi} = \frac{1}{a_{C,Si}} \cdot J_{POC} \quad (4-50)$$

$a_{C,N}$ = stoichiometric ratio of carbon to nitrogen in POM (g C per g N)

$a_{C,P}$ = stoichiometric ratio of carbon to phosphorus in POM (g C per g P)

$a_{C,Si}$ = stoichiometric ratio of carbon to silica in POM (g C per g Si).

The above procedure may be viewed as being indexed by $J_{aq,NH4}$, since it starts from an observed $J_{aq,NH4}$.

Once the depositional fluxes are evaluated to reproduce the estimated J_N , they are distributed into the three G classes. Then, using the initial and boundary conditions evaluated above for the first year average conditions, the stand-alone model is solved for one year. The final concentrations at the end of the first year are then used as the initial conditions and the stand-alone mode is solved again for the first year. This procedure is repeated until the final concentrations at the end of the year are equal, within a tolerance, the initial conditions at the beginning of the year. The final conditions represent the situation that would be reached if the conditions for the first year repeatedly occurred and the sediment had equilibrated to these conditions. When the kinetic coefficients need to be changed to improve the calibration, the initial conditions are recalculated with the new coefficients.

IV-7. Parameter Evaluation

The present sediment model involves many parameters that need to be evaluated from field data or through model calibration. The parameter evaluation, which is at least as important as model formulations, is described in this section. Some limitations of the model formulations and the parameter values found from the model application to the Chesapeake Bay are also presented.

As in Chesapeake Bay water quality modeling effort (Cercio & Cole 1994), it is desirable that the sediment model is operated in a "stand alone" model during initial application. Spatially-constant values are to be evaluated for model parameters in a "stand alone" application. Then, the parameters not employed or only roughly evaluated in the "stand alone" application are to be determined through the application of the coupled sediment-water column model. The sediment model application in a coupled model, which receives spatially-varying water column conditions, may require spatially-varying sediment model parameters.

IV-7-1. Parameters for depositional flux

The "stand alone" sediment model application determines the depositional fluxes of POM sufficient to reproduce the diagenesis rates that drive the stand-alone sediment model (Section IV-6-3). Constant stoichiometric ratios used in Eq. 4-50 are required to estimate J_{POC} , J_{POP} and J_{PSi} from J_{PON} . These ratios can be estimated using the pore water profiles of ammonium, phosphate and sulfate (Section VIII-C in D&F). The values used in D&F are:

$$a_{\text{C,N}} = 5.68 \text{ g C per g N}$$

$$a_{\text{C,P}} = 41.0 \text{ g C per g P}$$

$$a_{\text{C,Si}} = 2.0 \text{ g C per g Si.}$$

where $a_{\text{C,N}}$ and $a_{\text{C,P}}$ are Redfield ratios, and $a_{\text{C,Si}}$ is based on a limited amount of overlying water PSi data (Section VIII-E in D&F). The distribution coefficients of POM into three G classes are described in Section IV-7-2A.

In the coupled model application, parameters that need to be estimated for the depositional fluxes are the settling velocities in Equations 4-2 to 4-5: WS_{LP} , WS_{RP} , WS_{TSS} and WS_x . These settling velocities, in principle, are determined from the water column model application. The values determined for the Chesapeake Bay water quality

modeling (Cercó & Cole 1994) are listed in Tables 3-1 and 3-2. The depositional fluxes determined from the "stand alone" application may help determining the settling velocities in the water column model application.

IV-7-2. Parameters for diagenesis flux

Parameters that need to be estimated for the diagenesis fluxes are $FMLP_i$, $FMRP_i$ and $FMB_{x,i}$ in Equations 4-2 to 4-5, and $K_{POM,i}$, $\theta_{POM,i}$, W and H_2 in Eq. 4-6 for carbon ($M = C$), nitrogen ($M = N$) and phosphorus ($M = P$). The data from the kinetic experiments, measuring the rate at which reactants are consumed and end-products accumulate in a closed reaction vessel (Section VIII-D in D&F), can be used to confirm the determination of the reactive fractions ($FMLP_i$, $FMRP_i$ and $FMB_{x,i}$) and decay rates ($K_{POM,i}$).

A. Assignment to G classes: The sediment model has three classes: G_1 (labile), G_2 (refractory) and G_3 (inert). In the "stand alone" application, the depositional fluxes are estimated using the ammonium diagenesis flux and constant stoichiometric ratios. The distribution of the depositional fluxes into the three G classes used for the "stand alone" application (D&F) is listed in Table 4-1.

In the coupled model application, the deposited POM expressed in terms of the water column model state variables, upon deposition in the sediments, needs to be converted to the sediment model state variables. The water column model has two classes of POM based on the time scale of decomposition, labile and refractory (Section III-2A). Labile POM from the water column model is transferred directly into the G_1 class in the sediment model owing to the similar time scales of their reactivity, e.g., $FMLP_1 = 1$ and $FMLP_2 = FMLP_3 = 0$. Experiments by Westrich & Berner (1984) noted even split of refractory POC in the water column into G_2 and G_3 classes in the sediment. The initial even distribution may be further modified from model calibration.

The results from the Chesapeake Bay water quality modeling (Cercó & Cole 1994) are listed in Table 4-1. The observed carbon enrichment of sediment particles relative to the water column was reflected by making nitrogen to be slightly more reactive than carbon or phosphorus. Splits of refractory POM were spatially-varying. To reproduce

the observed water column nutrient concentrations, POM immediately below the fall lines (Bay and Tributary Zones 1) was considered largely inert. Routing of algae settled to the sediments into the sediment state variables also is listed in Table 4-1. The algal fraction assigned to the G₁ class was equivalent to the fraction of algal matter assigned to the labile particles following mortality in the water column (Tables 3-2 to 3-5). Split of refractory algae into G₂ and G₃ classes was equivalent to the split employed for refractory POM for most of the Bay away from the fall lines (i.e., except Bay Zones 1, 2 and 10, and Tributary Zone 1).

B. Decay rate: Differences in reactivity of deposited POM are accounted for by assigning them to three G classes: e.g., FNRP₂ > FCRP₂ and FNB_{x,2} > FCB_{x,2} in Table 4-1. For any G class, the same values, that are representative of reported literature values, may be used for the decay of POC, PON and POP. The values used in D&F are:

$$\begin{array}{ll}
 K_{\text{POC},1} = K_{\text{PON},1} = K_{\text{POP},1} = 0.035 \text{ day}^{-1} & \theta_{\text{POC},1} = \theta_{\text{PON},1} = \theta_{\text{POP},1} = 1.10 \\
 K_{\text{POC},2} = K_{\text{PON},2} = K_{\text{POP},2} = 0.0018 \text{ day}^{-1} & \theta_{\text{POC},2} = \theta_{\text{PON},2} = \theta_{\text{POP},2} = 1.15 \\
 K_{\text{POC},3} = K_{\text{PON},3} = K_{\text{POP},3} = 0.0 \text{ day}^{-1} & \theta_{\text{POC},3} = \theta_{\text{PON},3} = \theta_{\text{POP},3} = \text{not available.}
 \end{array}$$

C. Burial (sedimentation) rate: Burial rates can be measured using a number of methods (²¹⁰Pb, ²³⁹Pu, ¹³⁷Cs, Pollen, etc). The measurements tend to have considerable variability since the rate at which solids are sedimented can depend on site specific features. From the "stand alone" calibration, an average value of W = 0.25 cm yr⁻¹ was determined (D&F). For the coupled model application, spatially-varying values listed in Table 4-2 were used (Cercio & Cole 1994). The values were calibrated, within the range of observations, for the concentrations of sediment organic particles. In the Bay, burial rates were highest near the Susquehanna, least in the central Bay and moderate near the Bay mouth, in general agreement with Officer et al. (1984). In tributaries, burial rates had the decreasing trend with distance away from the fall lines in general agreement with Brush (1984).

D. Active layer depth: The active layer depth, H, controls the volume of the anoxic layer reservoir. From Eq. 4-1, H ≈ H₂. The mechanisms that influence the depth to

which solids are mixed determine H . These mixing mechanisms establish a homogeneous layer within which the diagenesis and other reactions take place. The principal agents of deep sediment mixing are the larger benthic organisms, and H is chosen to represent the depth of organism mixing. Active layer depths of 5 to 15 cm have been reported for estuaries (Aller 1982). A value of $H_2 = 10$ cm was used in D&F.

E. Comparisons with field data

The most important validation of the diagenesis portion of the model is the comparison to ammonium diagenesis. However, the composition of sediment POM is also important. The gross sediment composition is almost entirely due to G_3 class POM since the reactive fractions, G_1 and G_2 , have decayed to produce the diagenesis flux: the median reactive fraction has been shown to be on the order of 10% of the sediment POM in Chesapeake Bay (Section VIII-D in D&F). Therefore, if measurements of the sediment composition are available, they can be compared to model predictions of G_3 class organic matter (Section VIII-F in D&F).

The G_2 class POM dominates the reactive portion: the G_2 class has been shown to be on the order of 90% of the reactive portion of sediment POM, i.e., $G_1 + G_2$ (Section VIII-D in D&F). Hence, the data from anoxic mineralization experiments can be used to estimate the quantity of G_2 fraction (Section VIII-D in D&F).

The primary source of POC in the sediments of Chesapeake Bay is algal POC. The decay kinetics of algal chlorophyll in the sediments has been found to be relatively independent of temperature with a first order decay constant of approximately 0.03 day^{-1} . Since this decay rate coincides with the mean mineralization rate of G_1 class carbon (Section IV-7-2B), the concentration of sediment chlorophyll should be a direct measure of the concentration of G_1 class carbon in the sediment (Section VIII-G in D&F).

The above three comparisons using measurements of sediment composition and algal POC may serve as additional measures of the reliability of the diagenesis portion of the model.

IV-7-3. Common Parameters for sediment flux

Parameters that need to be estimated for the sediment fluxes are s , KL , ω , m_1 , m_2 ,

π_1 , π_2 , W , H_2 , κ_1 , κ_2 , J_1 and J_2 in Equations 4-8 to 4-11 for ammonium, nitrate, phosphate and sulfide/methane. Among these, s , KL , ω , m_1 , m_2 , W and H_2 are the same for different variables. The parameter s is estimated using Eq. 4-12. The estimation of the parameters, W and H_2 , has been described in Section IV-7-2.

A. Particulate and dissolved phase mixing coefficients: Evaluation of ω involves six new parameters (Eq. 4-15). The values used in D&F are:

$$\begin{aligned} D_p &= 1.2 \times 10^{-4} \text{ m}^2 \text{ day}^{-1} \text{ (from calibration)} & D_{p_{\min}} &= 3.0 \times 10^{-6} \text{ m}^2 \text{ day}^{-1} \\ \theta_{Dp} &= 1.117 \text{ (from data)} & KM_{Dp} &= 4.0 \text{ g O}_2 \text{ m}^{-3} \text{ (from data)} \\ G_{\text{POC,R}} &= 100 \text{ g C m}^{-3} & K_{\text{ST}} &= 0.03 \text{ day}^{-1}. \end{aligned}$$

Detailed vertical profiles of sediment chlorophyll can be used to quantify the rate of particle mixing by estimating the ratio of surface to depth averaged chlorophyll (Section VIII-G in D&F). Large ratio indicates little particle mixing, while the ratio approaching unity indicates intense mixing.

Three more parameters, $DO_{\text{ST,c}}$, NC_{hypoxia} and t_{MBS} , need to be evaluated to account for the benthic stress and hysteresis explained in Section IV-3-1B. These parameters depend on severity and longevity of hypoxia, constituent species and salinity (Diaz & Rosenberg, submitted). Benthic infaunal mortality was suggested to be initiated when the oxygen concentration drops below about $2.8 \text{ g O}_2 \text{ m}^{-3}$ (Rosenberg 1980). However, Diaz & Rosenberg (submitted) pointed out that the oxygen measurements in several of the field studies referred to in Rosenberg (1980) were made at some distance above the bottom. In areas with seasonal hypoxia (e.g., estuaries), the critical oxygen concentration for benthic organisms is closer to about $1 \text{ g O}_2 \text{ m}^{-3}$ (Llansó 1992). The present model simulates segment mean dissolved oxygen concentration and thus oxygen concentration immediately above bottom is not available. Hence, $DO_{\text{ST,c}} = 3 \text{ g O}_2 \text{ m}^{-3}$ may be used as an initial estimate when DO_0 is vertical mean. The critical hypoxia days, NC_{hypoxia} , depends on tolerance of benthic organisms to hypoxia (Diaz & Rosenberg, submitted): $NC_{\text{hypoxia}} = 1$ week will be used as an initial estimate. The time lag, t_{MBS} , for the recovery of benthic biomass following hypoxic events tends to be longer for higher salinity and shorter for lower salinity: about 3 to 4 weeks for low salinity water, e.g., < 20 ppt, and about 3 to 4 months for high salinity water, e.g., > 20 ppt (Diaz, personal

communication).

Evaluation of KL involves three new parameters (Eq. 4-16). The values used in D&F are:

$$D_d = 0.001 \text{ m}^2 \text{ day}^{-1} \text{ (from calibration)} \quad \theta_{Dd} = 1.08$$

$$R_{BI,BT} = 0.0.$$

The value of D_d was estimated directly using observed J_{aq,NH_4} , NH_4_0 , NH_4_2 and estimated J_N and s (Eq. III-42 in D&F). The resulting diffusion coefficient, which is roughly ten times the molecular diffusivity, indicates the importance of benthic enhancement. The temperature coefficient was chosen to be typical of biological reactions.

B. Solids concentration: The dissolved and particulate fractions are computed from the partitioning equations (Eq. 4-11), which require the concentration of sorbing solids. After analyzing field data, D&F used a solids concentration of $m_1 = m_2 = 0.5 \text{ kg L}^{-1}$, which are representative of the upper Bay conditions. This solids concentration is equivalent to approximately 81% porosity assuming dry sediment density of 2.65 kg L^{-1} (Mackin & Aller, 1984).

IV-7-4. Parameters for ammonium flux

The parameters that need to be estimated specifically for the ammonium flux are J_{1,NH_4} , J_{2,NH_4} , κ_{1,NH_4} , κ_{2,NH_4} , π_{1,NH_4} and π_{2,NH_4} in Equations 4-8 to 4-11. As described in Section IV-3-2:

$$J_{1,NH_4} = 0$$

$$J_{2,NH_4} = J_N \text{ (Eq. 4-7)}$$

$$\kappa_{1,NH_4} \text{ from Eq. 4-18}$$

$$\kappa_{2,NH_4} = 0$$

$$\pi_{1,NH_4} = \pi_{2,NH_4} = 1.0 \text{ L kg}^{-1}.$$

Partitioning is included although it has a negligible effect on the computation: from $m_1 = m_2 = 0.5 \text{ kg L}^{-1}$ (Section IV-7-3B) and Eq. 4-11, the partition coefficients, $\pi = 1$, indicate that approximately 67% of ammonium exists as dissolved form in sediments. For the parameters in Eq. 4-18 for κ_{1,NH_4} , the median values from a number of previous studies were used for the "stand alone" application in D&F:

$$\kappa_{NH_4} = 0.131 \text{ m day}^{-1}$$

$$\theta_{NH_4} = 1.08$$

$$KM_{NH_4} = 1.5 \text{ g N m}^{-3}$$

$$KM_{NH_4,O_2} = 3.68 \text{ g O}_2 \text{ m}^{-3}.$$

The parameters κ_{NH_4} and J_{N} (Eq. 4-48) can be estimated from observed DO_0 , SOD, $J_{\text{aq,NH}_4}$, NH_4 (or NH_4 and Eq. 4-49) and T, and estimated KM_{NH_4} , $\text{KM}_{\text{NH}_4,\text{O}_2}$ and θ_{NH_4} (Section II-D in D&F). If direct measurements of the nitrification rate in the sediments are available, these can be compared to model predictions for J_{Nit} computed using Eq. 4-19. This comparison may be used to confirm the estimated model parameters as well as model formulation for nitrification (Section II-F in D&F). The "stand alone" application in D&F showed that approximately 76% of the depositional nitrogen flux was returned to the water column as ammonium flux, and the remaining 24% was lost either as PON burial or became nitrate via nitrification (Section X-B-3 in D&F).

In the coupled model application, predicted ammonium flux from the sediment during hypoxic/anoxic intervals often exceeded observations (Cercio & Cole 1994). The excess anoxic release, which was due to blocking of the nitrification portion of the nitrification-denitrification process that removes nitrogen from the sediments, was reduced by lowering $\text{KM}_{\text{NH}_4,\text{O}_2}$ to a value consistent with that for the water column model, KHNit_{DO} in Table 3-4. In saltwater, a significant portion of the nitrogen is released as ammonium, while in freshwater, most of the mineralized nitrogen is often released from the sediments as nitrogen gas (Gardner et al 1991). Sediments adjacent to fall lines appeared to retain larger fractions of deposited phosphorus than sediments elsewhere. These variations were parameterized in the coupled model by assigning larger values for nitrification and denitrification rates, and phosphorus sorption coefficient in freshwater relative to saltwater (Cercio & Cole 1994). The division between two regimes was set at 1 ppt salinity, the same salinity that separates sulfide or methane in the SOD kinetics (Section IV-3-5). Small adjustment was made for κ_{NH_4} in the final calibration of the coupled model. The coupled model had (Cercio & Cole 1994):

$$\begin{aligned} \kappa_{\text{NH}_4} &= 0.14 \text{ m day}^{-1} \text{ for saltwater } (S > S_{\text{crit,NH}_4}) & \text{KM}_{\text{NH}_4,\text{O}_2} &= 1.0 \text{ g O}_2 \text{ m}^{-3} \\ &= 0.20 \text{ m day}^{-1} \text{ for freshwater } (S < S_{\text{crit,NH}_4}) & S_{\text{crit,NH}_4} &= 1 \text{ ppt.} \end{aligned}$$

IV-7-5. Parameters for nitrate flux

The parameters that need to be estimated specifically for the nitrate flux are J_{1,NO_3} , J_{2,NO_3} , κ_{1,NO_3} , κ_{2,NO_3} , π_{1,NO_3} and π_{2,NO_3} in Equations 4-8 to 4-11. As described in Section IV-3-3:

$$J_{1,\text{NO}_3} = J_{\text{Nit}} \text{ from Eq. 4-19}$$

$$J_{2,\text{NO}_3} = 0$$

$$\kappa_{\text{NO}_3,1} \text{ from Eq. 4-22-1}$$

$$\kappa_{\text{NO}_3,2} \text{ from Eq. 4-22-2}$$

$$\omega = 0$$

$$\pi_{1,\text{NO}_3} = \pi_{2,\text{NO}_3} = 0.$$

The parameters for κ_{1,NO_3} (Eq. 4-22-1) and κ_{2,NO_3} (Eq. 4-22-2) can be estimated from observed NO_3_1 (or NO_3_0 and Eq. 4-9), $J_{\text{aq},\text{NO}_3}$ and $J_{\text{aq},\text{NH}_4}$, and estimated s , J_{N} (Eq. 4-48) and θ_{NO_3} (Section III-H in D&F). If direct measurements of the denitrification rate in the sediments are available, these may be compared to model predictions for $J_{\text{N}_2(\text{g})}$ (Eq. 4-23): estimation of NO_3_1 and NO_3_2 is described in Section III-I in D&F. This comparison may be used to confirm the estimated model parameters as well as model formulation for denitrification (Section III-I in D&F). The "stand alone" model (D&F) had:

$$\kappa_{\text{NO}_3,1} = 0.10 \text{ m day}^{-1}$$

$$\kappa_{\text{NO}_3,2} = 0.25 \text{ m day}^{-1}$$

$$\theta_{\text{NO}_3} = 1.08 \text{ (median value from previous studies).}$$

The "stand alone" application showed that 76% of J_{N} is returned as $J_{\text{aq},\text{NH}_4}$, and the rest is either denitrified or returned as $J_{\text{aq},\text{NO}_3}$ (Section III-K in D&F). Large fraction of the nitrate produced by nitrification escapes as $J_{\text{N}_2(\text{g})}$ while small fraction is returned as $J_{\text{aq},\text{NO}_3}$: 22% of J_{N} escapes as $J_{\text{N}_2(\text{g})}$ but this includes the denitrification of overlying water nitrate as well (Sections III-J and III-K in D&F). For large NO_3_0 , $J_{\text{aq},\text{NO}_3}$ is negative (to the sediment) and $J_{\text{N}_2(\text{g})}$ is large owing to the denitrification of overlying water nitrate transported to the sediment (Section III-J in D&F). One surprising result was that the primary site of denitrification is in the oxic layer: mass transfer of nitrate to the anoxic lower layer is insufficient for significant denitrification to occur in that layer (Section III-H in D&F). This finding, which contradicts some measurements (e.g., Sørensen & Revsbech 1990), may be resulted from an artifact of the two layer segmentation and deserves further investigation.

As in nitrification rate in Section IV-7-4, spatially-varying values, larger in freshwater, were used for $\kappa_{\text{NO}_3,1}$ in the final calibration of the coupled model (Cercó & Cole 1994):

$$\kappa_{\text{NO}_3,1} = 0.125 \text{ m day}^{-1} \text{ for saltwater } (S > S_{\text{crit},\text{NO}_3})$$

$$S_{\text{crit},\text{NO}_3} = 1 \text{ ppt}$$

$$= 0.300 \text{ m day}^{-1} \text{ for freshwater } (S < S_{\text{crit},\text{NO}_3}).$$

IV-7-6. Parameters for phosphate flux

The parameters that need to be estimated specifically for the phosphate flux are $J_{1,PO4}$, $J_{2,PO4}$, $\kappa_{1,PO4}$, $\kappa_{2,PO4}$, $\pi_{1,PO4}$ and $\pi_{2,PO4}$ in Equations 4-8 to 4-11. As described in Section IV-3-4:

$$J_{1,PO4} = 0$$

$$J_{2,PO4} = J_p \text{ from Eq. 4-7}$$

$$\kappa_{1,PO4} = \kappa_{2,PO4} = 0.$$

Evaluation of the partition coefficients involves three parameters (Eq. 4-25). The "stand alone" model (D&F) had:

$$\pi_{2,PO4} = 100.0 \text{ L kg}^{-1}$$

$$\Delta\pi_{PO4,1} = 300.0$$

$$(\text{DO}_0)_{\text{crit},PO4} = 2.0 \text{ g O}_2 \text{ m}^{-3}.$$

Any set of laboratory or field measurements that include simultaneous measurements of ammonium and phosphate fluxes can be compared to model predictions using the stand-alone model (Section IV-6-3, and Section VI-E in D&F). It has been shown in D&F (Section VI-E), the steady-state model cannot produce the excess anoxic $J_{\text{aq},PO4}$, which is due to the phosphate stored in the sediment during oxic periods. In time-varying "stand alone" application, D&F noted that the formulation for phosphate partitioning (Eq. 4-25) was not complete although the phosphate cycle still was representative (Section X-F-2 in D&F). A number of cases occurred where the model predicted a negative phosphate flux whereas the observation was positive. This discrepancy occurred just after turnover when the overlying water oxygen increased. The model recreated the oxic layer immediately with its high partition coefficient and the resulting phosphate concentration in the oxic layer caused a flux to the sediment. They suggested that a more realistic formulation would involve a model of the iron cycle, in which the formation of iron oxyhydroxide would take place more slowly and the oxic layer partition coefficient would increase more slowly.

Spatial variation in the ratio of dissolved to particulate sediment phosphate was observed in the mainstem Chesapeake Bay: at the most upriver station, pore water phosphate was lowest while particulate inorganic phosphate was highest (Fig. X-22 in D&F). It suggests that the partition coefficient was largest at the upriver station and decreased in the downriver direction (Fig. X-23 in D&F). Thus, as in nitrification rate in Section IV-7-4, spatially-varying values, larger in freshwater, were used for $\Delta\pi_{PO4,1}$ in

the final calibration of the coupled model (Cercio & Cole 1994):

$$\begin{aligned} \Delta\pi_{\text{PO4},1} &= 300.0 \text{ for saltwater } (S > S_{\text{crit,PO4}}) & S_{\text{crit,PO4}} &= 1 \text{ ppt} \\ &= 3000.0 \text{ for freshwater } (S < S_{\text{crit,PO4}}). \end{aligned}$$

IV-7-7. Parameters for sulfide/methane flux and SOD

The parameters that need to be estimated specifically for the sulfide flux and SOD are $J_{1,\text{H2S}}$, $J_{2,\text{H2S}}$, $\kappa_{1,\text{H2S}}$, $\kappa_{2,\text{H2S}}$, $\pi_{1,\text{H2S}}$ and $\pi_{2,\text{H2S}}$ in Equations 4-8 to 4-11. As described in Section IV-3-5:

$$\begin{aligned} J_{1,\text{H2S}} &= 0 & J_{2,\text{H2S}} &\text{ from Eq. 4-27} \\ \kappa_{2,\text{H2S}} &= 0. \end{aligned}$$

Evaluation of $\kappa_{1,\text{H2S}}$ involves six parameters (Eq. 4-28). The values used in D&F are:

$$\begin{aligned} \pi_{1,\text{H2S}} &= 100.0 \text{ L kg}^{-1} & \pi_{2,\text{H2S}} &= 100.0 \text{ L kg}^{-1} \\ \kappa_{\text{H2S,d1}} &= 0.2 \text{ m day}^{-1} & \kappa_{\text{H2S,p1}} &= 0.4 \text{ m day}^{-1} \\ \theta_{\text{H2S}} &= 1.08 & \text{KM}_{\text{H2S,O2}} &= 4.0 \text{ g O}_2 \text{ m}^{-3}. \end{aligned}$$

No adjustment was made for the parameters in the final calibration of the coupled model application.

The methane flux in the freshwater (Equations 4-31 to 4-34) requires the following parameters:

$$\begin{aligned} J_{1,\text{CH4}} &= 0 & J_{2,\text{CH4}} &\text{ from Eq. 4-31} \\ \kappa_{\text{CH4}} &= 0.2 \text{ m day}^{-1} & \theta_{\text{CH4}} &= 1.08. \end{aligned}$$

The "stand alone" application in D&F showed that approximately 18% of the depositional carbon flux was not returned as either CSOD or as a $J_{\text{aq,H2S}}$. Among 18% loss, 15% was due to the burial of the G_3 class carbon (Table 4-1) and 3% was lost by burial of particulate sulfide. The "stand alone" application also noted that neither data nor the model show any strong temperature dependency of SOD (Fig. X-19 in D&F). As in phosphate flux, simultaneous measurements of ammonium and oxygen fluxes can be used to compare to model predictions using the stand-alone model (Section IV-6-3, and Section V-G in D&F).

It has been shown in D&F (Fig. V-4A), the steady-state model cannot produce the excess SOD, which is due to the oxidation of particulate sulfide stored in the sediment during periods where carbon diagenesis exceeds SOD. In time-varying "stand alone"

application, D&F noted that the sulfur cycle in the model was not complete although it still was representative (Section X-D-2 in D&F). The model calculated particulate sulfide concentrations higher than the observed FeS (acid volatile sulfide) but lower than the observed FeS+FeS₂ (chromate reducible sulfide) (Fig. X-13B in D&F). The model forms FeS(s) only using a partitioning equilibria, which is considered to be reactive and oxidized. However, FeS can also react with elemental sulfur to form iron pyrite, FeS₂, which is much less reactive and thus builds up in the sediment. They suggested that inclusion of the reaction for FeS₂ formation would lower the computed FeS concentrations, thus improving the agreement with the observations, and would increase the computed total sulfide owing to the build-up of FeS₂. Another limitation of the model found in D&F was that the model predicted almost no seasonal variation whereas the pore water sulfide data appeared to indicate a seasonal variation (Fig. X-16 in D&F). It was both due to omission of FeS₂ formation process and to use of constant linear partitioning.

IV-7-8. Parameters for silica

The parameters that need to be estimated for the particulate biogenic silica are S_{Si} , H_2 , W , J_{PSi} and J_{DSi} in Eq. 4-35. The parameters, H_2 and W , are described in Section IV-7-2, and J_{PSi} is estimated from Eq. 4-5. D&F had:

$$J_{DSi} = 0.1 \text{ g Si m}^{-2} \text{ day}^{-1}.$$

Evaluation of S_{Si} involves five parameters (Eq. 4-36). The values used in D&F are:

$$K_{Si} = 0.5 \text{ day}^{-1}$$

$$\theta_{Si} = 1.1$$

$$Si_{sat} = 40.0 \text{ g Si m}^{-3}$$

$$\pi_{2,Si} = 100.0 \text{ L kg}^{-1}$$

$$KM_{PSi} = 5 \times 10^4 \text{ g Si m}^{-3}.$$

The KM_{PSi} value is equivalent to 0.1 g Si g^{-1} if solid concentration is 0.5 kg L^{-1} (Section IV-7-3B).

The parameters that need to be estimated specifically for the silica flux are $J_{1,Si}$, $J_{2,Si}$, $\kappa_{1,Si}$, $\kappa_{2,Si}$, $\pi_{1,Si}$ and $\pi_{2,Si}$ in Equations 4-8 to 4-11. As described in Section IV-4:

$$J_{1,Si} = 0$$

$$J_{2,Si} \text{ from Eq. 4-38-1}$$

$$\kappa_{1,Si} = 0$$

$$\kappa_{2,Si} \text{ from Eq. 4-38-2.}$$

Evaluation of the partition coefficients involves three parameters, $\pi_{2,Si}$, $\Delta\pi_{Si,1}$ and $(DO_0)_{crit,Si}$ (Eq. 4-39). The values used in D&F are:

$$\Delta\pi_{\text{Si},1} = 10.0$$

$$(\text{DO}_0)_{\text{crit,Si}} = 1.0 \text{ g O}_2 \text{ m}^{-3}.$$

Evaluation of $J_{2,\text{Si}}$ (Eq. 4-38-1) and $\kappa_{2,\text{Si}}$ (Eq. 4-38-2) requires five parameters, K_{Si} , θ_{Si} , KM_{PSi} , Si_{sat} and $\pi_{2,\text{Si}}$. The values used in D&F are given above. All the above values were estimated from field data, previous studies or model calibration. No adjustment was made for the parameters in the final calibration of the coupled model application.

As in phosphate flux and SOD, simultaneous measurements of ammonium and silica fluxes can be used to compare to model predictions using the stand-alone model (Section IV-6-3, and Section VII-D in D&F). In the "stand alone" application, D&F showed that approximately 76% of the depositional nitrogen flux was returned as a $J_{\text{aq,NH}_4}$ (Section IV-7-4) and approximately 82% of the depositional carbon flux was returned as either CSOD or as a $J_{\text{aq,H}_2\text{S}}$ (Section IV-7-7). However, the fraction of recycled silica ($J_{\text{aq,Si}}$) to the total silica input ($J_{\text{PSi}} + J_{\text{DSi}}$) was quite variable and did not appear to be strongly related to the total input (Section X-G-2 in D&F). This is because there is a limitation to the quantity of silica that can be recycled, which is determined by the silica solubility.

IV-7-9. Comments

The parameter values presented in this section were established after analyzing extensive data sets and model calibration (D&F; Cerco & Cole 1994). These values may serve as an excellent starting point for model application to estuaries of the eastern United States. However, since no two systems are exactly the same, it might be necessary to alter the values of some parameters when applying this sediment model for different systems. The parameters that one may want to alter include

- : split of POM settling from the overlying water to three G classes (FMLP_i , FMRP_i and $\text{FMB}_{x,i}$ in Equations 4-2 to 4-4)
- : burial rate (W in Eq. 4-6)
- : nitrification rate (κ_{NH_4} in Eq. 4-19) and denitrification rate ($\kappa_{\text{NO}_3,1}$ and $\kappa_{\text{NO}_3,2}$ in Eq. 4-22), particularly as a function of salinity
- : phosphate sorption in oxic upper layer (π_{2,PO_4} , $\Delta\pi_{\text{PO}_4,1}$ and $(\text{DO}_0)_{\text{crit,PO}_4}$ in Eq. 4-25).

Table 4-1. Assignment of water column particulate organic matter (POM) to sediment G classes used in Cerco & Cole (1994).

WCM Variable	Carbon & Phosphorus			Nitrogen		
	G ₁	G ₂	G ₃	G ₁	G ₂	G ₃
A. "stand alone" model	0.65	0.20	0.15	0.65	0.25	0.10
B. coupled model						
Labile Particulate	1.0	0.0	0.0	1.0	0.0	0.0
Refractory Particulate ^a						
: Bay and Tributary Zones 1	0.0	0.11	0.89	0.0	0.26	0.74
: Bay Zones 2 and 10	0.0	0.43	0.57	0.0	0.54	0.46
: All Other Zones	0.0	0.73	0.27	0.0	0.82	0.18
Algae	0.65	0.255	0.095	0.65	0.28	0.07

^a See Figure 10-6 in Cerco & Cole (1994) for the definition of Zones.

Table 4-2. Sediment burial rates (W) used in Cerco & Cole (1994).

Bay Zones ^a	Rate (cm yr ⁻¹)	Tributary Zones ^a	Rate (cm yr ⁻¹)
1, 2, 10	0.50	1	0.50
3, 6, 9	0.25	2, 3	0.25
7, 8	0.37		

^a See Figure 10-6 in Cerco & Cole (1994) for the definition of Zones.

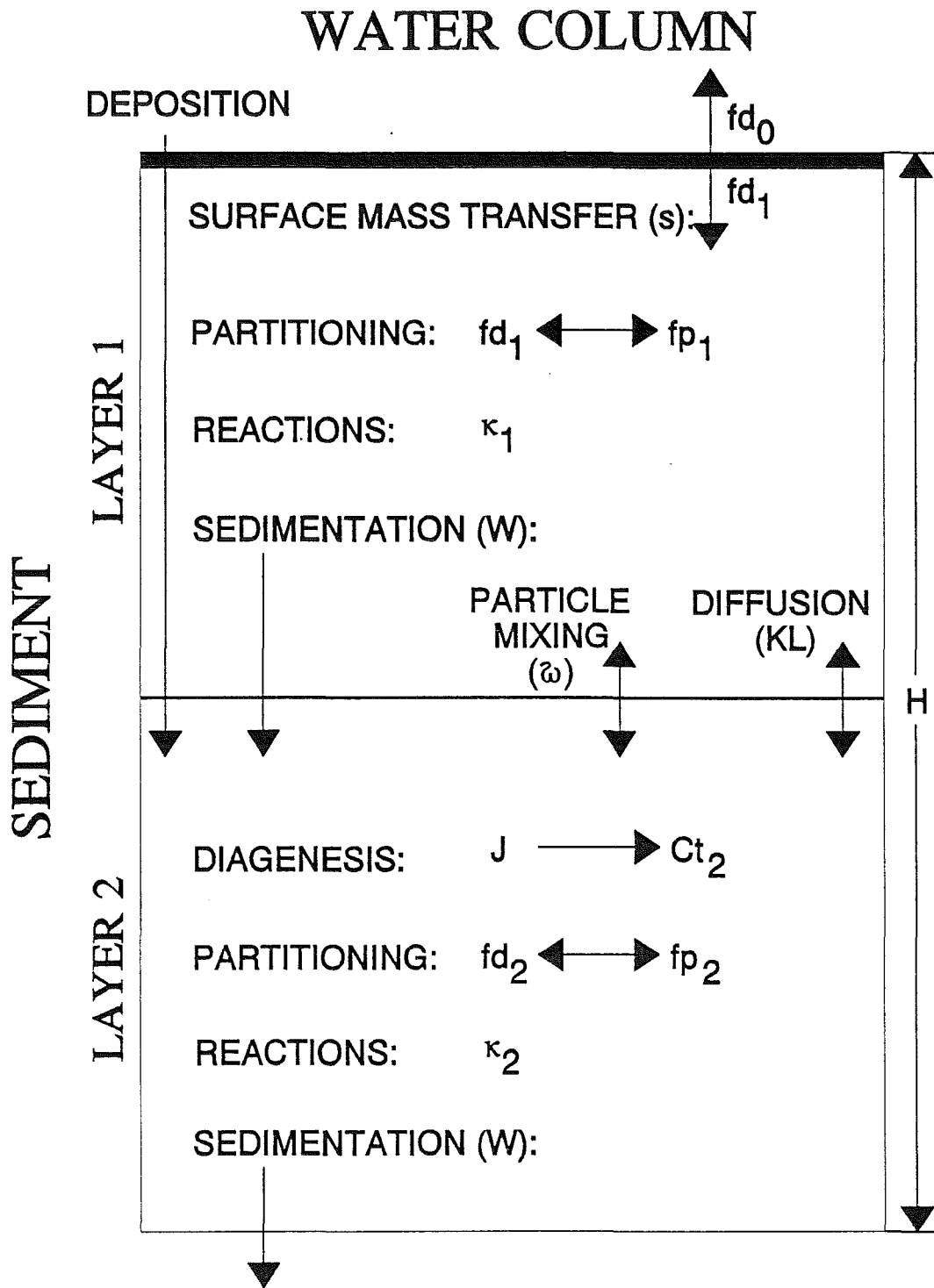


Figure 4-1. Sediment layers and processes included in sediment process model.

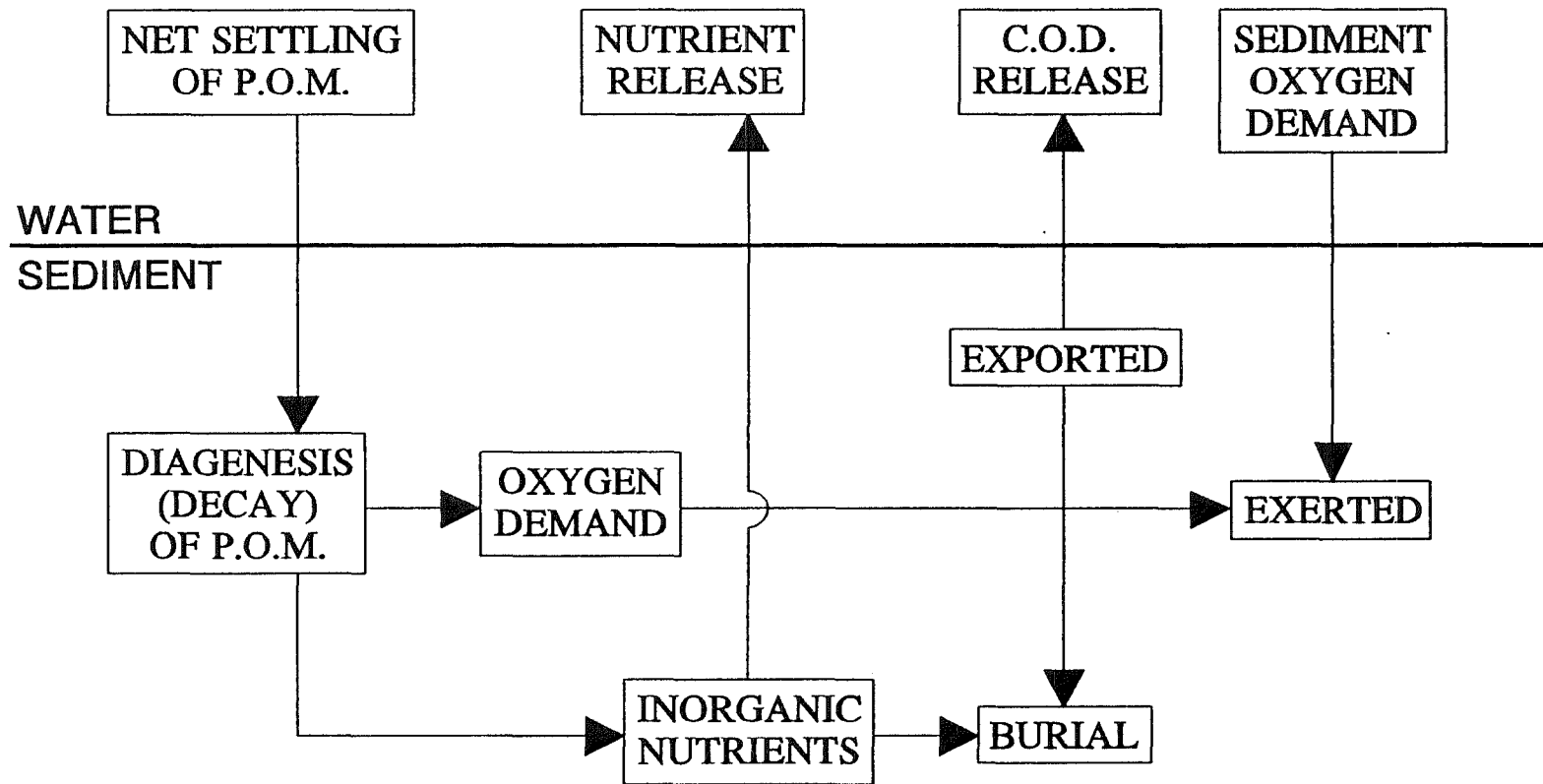


Figure 4-2. A schematic diagram for sediment process model.

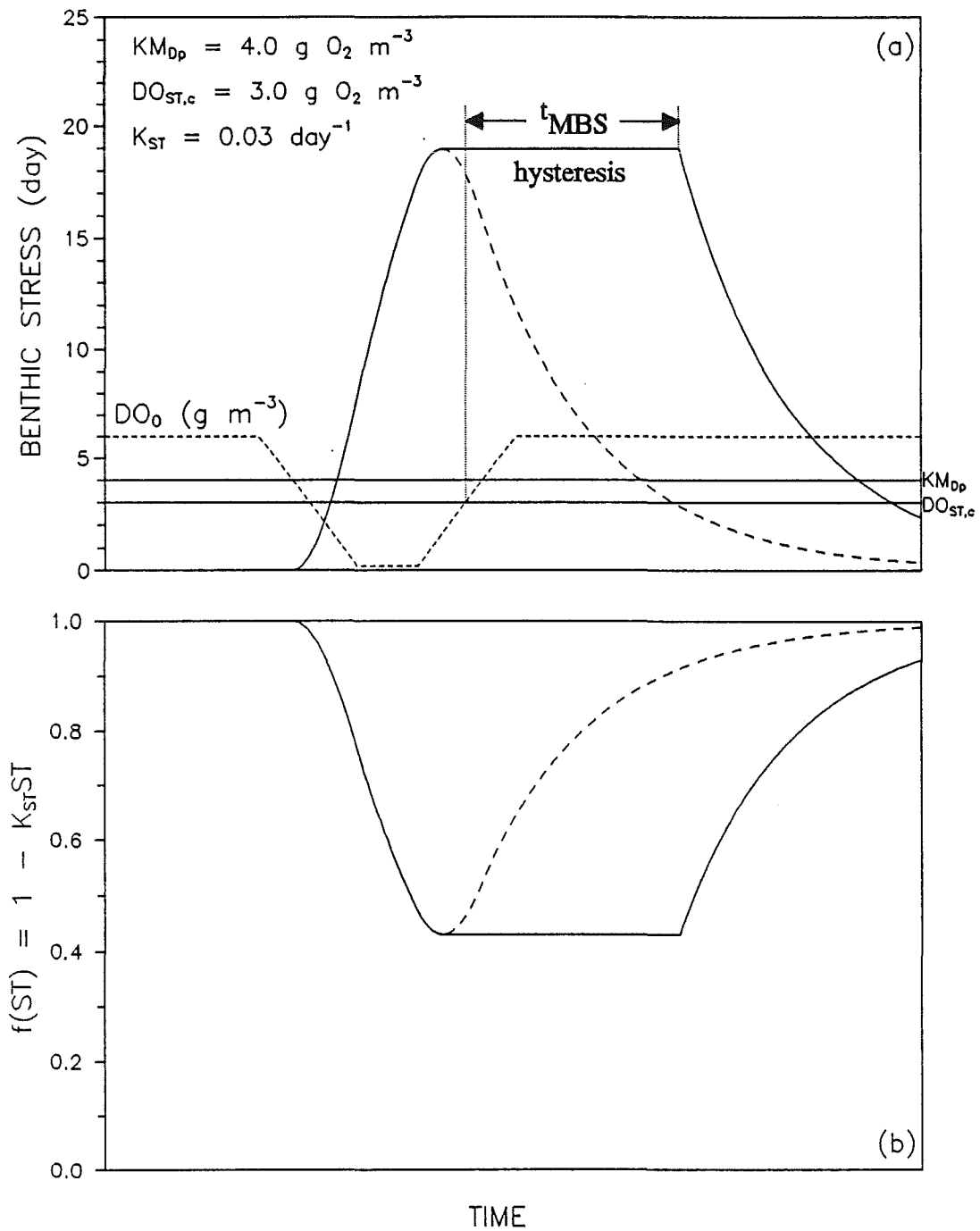


Figure 4-3. Benthic stress (a) and its effect on particle mixing (b) as a function of overlying dissolved oxygen concentration.

Chapter V. Model Operation (Execution)

This chapter gives the general description of what the present model does when one prepares the input data files and runs the model. When applying the model to any system, data for geometry and calibrated constants are required. The geometric data include identification of main channel and branches, segmentation and evaluation of high tide volume, inter-tidal volume (tidal prism), depth, etc (see Chapter II and Appendix A-1-1). The calibrated constants include return ratio (Section II-3-2) and a number of biogeochemical coefficients described in Chapters III and IV, and Appendix A.

In addition, for each model simulation, initial and boundary conditions are required. Initial conditions, the conditions at the beginning of a model simulation, need to be specified for all state variables both in water column and in sediment. When the model runs, it starts with initial conditions and calculates water column and sediment state variables at each segment at each time step until the time that one specifies to stop the model run. It takes some time for mass state variables to be stabilized, i.e., for the model solution to be independent of initial conditions. Considerable effort, hence, is required to specify the initial conditions, evaluation of initial conditions for the sediment process model is described in Section IV-6.

To drive the model, the following external forcing variables are needed as boundary conditions:

- (a) concentrations for all water column state variables at downriver boundary, i.e., 1st segment in main channel (see Section II-1),
- (b) discharge rates from point and nonpoint source inputs,
- (c) point and nonpoint source loadings for all water column state variables,
- (d) solar radiation including heat exchange coefficient and equilibrium temperature (see Eq. 3-21).

As the model calculation proceeds, it is constrained by the specified boundary conditions. The boundary conditions, with accounting for the physical transport using tidal flushing, drive the model to solve mass balance equations for state variables, and calculate spatial and temporal distributions.

The present model implementation allows two types of output generation: snapshot

spatial distribution and time-series output. At each time that one specifies to generate the snapshot output (Appendix A-1-2), the model writes instantaneous values of all state variables at all segments. At each segment, up to ten segments, that one specifies to generate the time-series output, the model writes the time-series information of all state variables. Detailed description of input and output file organization is given in Appendix A.

References

- Aller, R.C. 1982. The effects of macrobenthos on chemical properties of marine sediment and overlying water, pp. 53-102. In: P.L. McCall & M.J.S. Tevesz (eds.), *Animal-Sediment Relations: The Biogenic Alteration of Sediments*, Plenum Press, NY.
- Banks, R.B. & Herrera, F.F. 1977. Effect of wind and rain on surface reaeration. *J. of the Environmental Engineering Division, ASCE*, 103(EE3): 489-504.
- Barrow, N.J. 1983. A mechanistic model for describing the sorption and desorption of phosphate by soil. *J. of Soil Science*, 34: 733-750.
- Boni, L., Carpené, E., Wynne, D., & Reti, M. 1989. Alkaline phosphatase activity in *Protogonyaulax tamarensis*. *J. of Plankton Research*, 11(5): 879-885.
- Boudreau, B.P. 1991. Modelling the sulfide-oxygen reaction and associated pH gradients in porewaters. *Geochimica et Cosmochimica Acta*, 55: 145-159.
- Bowie, G.L., Mills, W.B., Porcella, D.B., Campbell, C.L., Pagenkopf, J.R., Rupp, G.L., Johnson, K.M., Chan, P.W.H., Gherini, S.A. & Chamberlin, C.E. 1985. Rates, constants and kinetics formulations in surface water quality modeling (second edition). EPA/600/3-85/040, Environmental Research Lab., US EPA, 455 pp.
- Brush, G.S. 1984. Patterns of recent sediment accumulation in Chesapeake Bay (Virginia-Maryland, U.S.A.) tributaries. *Chemical Geology*, 44: 227-242.
- Carritt, D.E. & Goodgal, S. 1954. Sorption reactions and some ecological implications. *Deep-Sea Research*, 1: 224-243.
- Cerco, C.F. & Kuo, A.Y. 1981. Water quality in a small tidal creek: Parker Creek, Virginia. Special Report in Applied Marine Science and Ocean Engineering (SRAMSOE) #145, Virginia Institute of Marine science (VIMS), The College of William and Mary, VA, 112 pp.
- Cerco, C.F. & Cole, T.M. 1994. Three-dimensional eutrophication model of Chesapeake Bay: Volume 1, main report. Technical Report EL-94-4, US Army Engineer Waterways Experiment Station, Vicksburg, MS.
- Chróst, R.J. & Overbek, J. 1987. Kinetics of alkaline phosphatase activity and phosphorus availability for phytoplankton and bacterioplankton in Lake Plußsee (North German eutrophic lake). *Microbial Ecology*, 13: 229-248.
- Cline, J.D. & Richards, F.A. 1969. Oxygenation of hydrogen sulfide in seawater at constant salinity, temperature and pH. *Environmental Science & Technology*, 3(9): 838-843.

- Diaz, R.J. & Rosenberg, R. submitted. Marine benthichypoxia - review of ecological effects and behavioral responses of benthic macrofauna. *Oceanography Marine Biology Annual Review*.
- DiToro, D.M. 1980. Applicability of cellular equilibrium and Monod theory to phytoplankton growth kinetics. *Ecological Modelling*, 8: 201-218.
- DiToro, D.M., Paquin, P.R., Subburamu, K. & Gruber, D.A. 1990. Sediment oxygen demand model: methane and ammonia oxidation. *J. of Environmental Engineering, ASCE*, 116(5): 945-986.
- DiToro, D.M. & Fitzpatrick, J.J. 1993. Chesapeake bay sediment flux model. Contract Report EL-93-2, US Army Engineer Waterways Experiment Station, Vicksburg, MS, 316 pp.
- Edinger, J.E., Brady, D.K. & Geyer, J.C. 1974. Heat exchange and transport in the environment. Report No. 14, The Johns Hopkins University, Electric Power Research Institute Publication No. 74-049-00-3, 125 pp.
- Froelich, P.N. 1988. Kinetic control of dissolved phosphate in natural rivers and estuaries: a primer on the phosphate buffer mechanism. *Limnology and Oceanography*, 33(4, part 2): 649-668.
- Gardner, W.S., Seitzinger, S.P. & Malczyk, J.M. 1991. The effects of sea salts on the forms of nitrogen released from estuarine and freshwater sediments: does ion pairing affect ammonium flux? *Estuaries*, 14(2): 157-166.
- Genet, L.A., Smith, D.J. & Sonnen, M.B. 1974. Computer program documentation for the dynamic estuary model. Prepared for US EPA, Systems Development Branch, Washington, D.C.
- Giordani, P. & Astorri, M. 1986. Phosphate analysis of marine sediments. *Chemistry in Ecology*, 2: 103-112.
- Ho, G.C., Kuo, A.Y. & Neilson, B.J. 1977. Mathematical models of Little Creek Harbor and the Lynnhaven Bay system. SRAMSOE #145, VIMS, The College of William and Mary, VA, 100 pp.
- Johnson, B.H., Kim, K.W., Heath, R.H., Butler, H.L. & Hsieh, B.B. 1991. User's guide for a three-dimensional numerical hydrodynamic, salinity and temperature model of Chesapeake Bay. Technical Report HL-91-20, US Army Engineer Waterways Experiment Station, Vicksburg, MS, 41 pp.
- Ketchum, B.H. 1951. The exchanges of fresh and salt waters in tidal estuaries. *J. of Marine Research*, 10(1): 18-38.

- Kremer, J.N. & Nixon, S.W. 1978. A coastal marine ecosystem: simulation and analysis. *Ecological Studies* 24, Springer-Verlag, New York, 217 pp.
- Kuo, A.Y. & Hyer, P.V. 1979. A water quality study of the Eastern Branch of the Lynnhaven Bay, Virginia. A Report to the Norfolk District, US Army Corps of Engineers, Prepared by VIMS, The College of William and Mary, VA, 29 pp.
- Kuo, A.Y. & Neilson, B.J. 1988. A modified tidal prism model for water quality in small coastal embayments. *Water Science Technology*, 20(6/7): 133-142.
- Kuo, A.Y. & Park, K. 1992. Transport of hypoxic waters: an estuary-subestuary exchange, pp. 599-615. In: D. Prandle (ed.), *Dynamics and Exchanges in Estuaries and the Coastal Zone*, Coastal and Estuarine Sciences 40, AGU, Washington D.C.
- Lebo, M.E. 1991. Particle-bound phosphorus along an urbanized coastal plain estuary. *Marine Chemistry*, 34: 225-246.
- Lijklema, L. 1980. Interaction of ortho-phosphate with iron (III) and aluminum hydroxides. *Environmental Science & Technology*, 14(5): 537-541.
- Llansó, R.J. 1992. Effects of hypoxia on estuarine benthos: the lower Rappahannock River (Chesapeake Bay), a case study. *Estuarine, Coastal and Shelf Science*, 35: 491-515.
- Mackin, J.E. & Aller, R.C. 1984. Ammonium adsorption in marine sediments. *Limnology and oceanography*, 29(2): 250-257.
- Mancini, J.L. 1983. A method for calculating effects, on aquatic organisms, of time varying concentrations. *Water Research*, 17(10): 1355-1362.
- Matisoff, G. 1982. Mathematical models of bioturbation, pp. 289-330. In: P.L. McCall & M.J.S. Tevesz (eds.), *Animal-Sediment Relations: The Biogenic Alteration of Sediments*, Plenum Press, NY.
- Millero, F.J. 1986. The thermodynamics and kinetics of the hydrogen sulfide system in natural waters. *Marine Chemistry*, 18: 121-147.
- Mo, C., Neilson, B.J. & Wetzel, R.L. 1993. Sediment processes monitoring data report for calendar year 1989. Data Report No. 48, VIMS, The College of William and Mary, VA, 39 pp.
- Morel, F. 1983. *Principles of Aquatic Chemistry*. John Wiley & Sons, New York, NY, 446 pp.
- Morse, J.W., Millero, F.J., Cornwell, J.C. & Rickard, D. 1987. The chemistry of the hydrogen sulfide and iron sulfide systems in natural waters. *Earth-Science Reviews*, 24:

1-42.

O'Connor, D.J. & Dobbins, W.E. 1958. Mechanism of reaeration in natural streams. *Transactions of the American Society of Civil Engineers*, 123(2934): 641-684.

Odum, E.P. 1971. *Fundamentals of ecology* (third edition). W.B. Saunders Co., Philadelphia, PA, 574pp.

Officer, C.B., Lynch, D.R., Setlock, G.H. & Helz, G.R. 1984. Recent sedimentation rates in Chesapeake Bay, pp. 131-157. In: V.S. Kennedy (ed.), *The Estuary as a Filter*, Academic Press.

Parsons, T.R., Takahashi, M. & Hargrave, B. 1984. *Biological oceanographic processes* (third edition). Pergamon Press, 330 pp.

Press, W.H., Flannery, B.P., Teukolsky, S.A. & Vetterling, W.T. 1986. *Numerical recipes: the art of scientific computing*. Cambridge University Press, 818 pp.

Redfield, A.C., Ketchum, B.H. & Richards, F.A. 1963. The influence of organisms on the composition of sea-water (Chapter 2) pp 26-77. In: M.N. Hill (ed.), *The Sea - Ideas and Observations on Progress in the Study of the Seas: Vol. 2, Composition of Sea Water, Comparative and Descriptive Oceanography*, Interscience Publishers.

Robbins, J.A., Keilty, T., White, D.S. & Edgington, D.N. 1989. Relationships among tubificid abundances, sediment composition and accumulation rates in Lake Erie. *Canadian J. of Fisheries & Aquatic Sciences*, 46(2): 223-231.

Rosenberg, R. 1980. Effect of oxygen deficiency on benthic macrofauna in fjords, pp. 499-514. In: H.J. Freeland, D.M. Farmer & C.D. Levings (eds.), *Fjord Oceanography*, Plenum Press, NY.

Smolarkiewicz, P.K. & Margolin, L.G. 1993. On forward-in-time differencing for fluids: extension to a curvilinear framework. *Monthly Weather Review*, 121: 1847-1859.

Sørensen, J. & Revsbech, N.P. 1990. Denitrification in stream biofilm and sediment: in situ variation and control factors, pp. 277-289. In: N.P. Revsbech & J. Sørensen (eds.), *Denitrification in Soil and Sediment*, FEMS Symposium No. 56, Plenum Press, NY.

Steele, J.H. 1962. Environmental control of photosynthesis in the sea. *Limnology and Oceanography*, 7(2): 137-150.

Stumm, W. & Morgan, J.J. 1981. *Aquatic chemistry, an introduction emphasizing chemical equilibria in natural waters* (second edition). John Wiley & Sons, Inc., 780 pp.

Thomann, R.V., Jaworski, N.J., Nixon, S.W., Paerl, H.W. & Taft, J. 1985. The 1983 algal bloom in the Potomac Estuary. *The Algal Bloom Expert Panel*, Prepared for the

Potomac Strategy State/EPA Management Committee, US EPA Region III, Philadelphia, PA.

Thomann, R.V. & Mueller, J.A. 1987. Principles of surface water quality modeling and control. Harper & Row, Publishers, Inc., 644 pp.

Thomann, R.V., Collier, J.R., Butt, A.R., Casman, E. & Linker, L.C. 1994. Technical analysis of response of Chesapeake Bay water quality model to loading scenarios. CBP/TRS 101/94, Modeling Subcommittee of the Chesapeake Bay Program, US EPA.

Troup, R. 1974. The interaction of iron with phosphate, carbonate and sulfide in Chesapeake Bay interstitial waters: a thermodynamic interpretation. Ph.D. Dissertation, Johns Hopkins University, MD, 114 p.

Westrich, J.T. & Berner, R.A. 1984. The role of sedimentary organic matter in bacterial sulfate reduction: the G model tested. Limnology and Oceanography, 29(2): 236-249.

Wezernak, C.T. & Gannon, J.J. 1968. Evaluation of nitrification in streams. J. of the Sanitary Engineering Division, ASCE, 94(SA5): 883-895.

Yamamoto, S., Alcauskas, J.B. & Crozler, T.E. 1976. Solubility of methane in distilled water and seawater. J. of Chemical and Engineering Data, 21(1): 78-80.

Appendix A. Program Organization for Input and Output Files

Program input and output require several data files, each of which is specified in the program by a logical unit number. Tables A-1 and A-2 list the logical unit numbers for water column and sediment models, respectively. You can run only the water column model. The sediment process model, however, should be run with the water column model since the water column model provides the depositional fluxes to the sediment process model. Hence, all input and output units for sediment process model are optional. This appendix describes input and output file organization for water column and sediment process models.

A-1. Input Data Description for Water Column Model

This section explains line-by-line the input data files for water column model. Each data group and each line are preceded by text titles for identification purpose. These text titles, which do not affect the model run, are not described, and omitted using FORMAT descriptor slash (/), in this section.

Once the model starts, it opens the unit numbers 7, 8 and 9 (Table A-1). Then, control passes to the subroutine 'RCHyd' in 'SUB-READ.FOR', where input parameters are read in from the unit number 7.

A-1-1. Logical unit 7 (GEO-HYD.IN)

The unit number 7 contains the geometric and hydrodynamic data.

VARIABLES (FORMAT)

Title(j), j=1,3 (A79)

: three-line text to identify a simulation.

NSEGm, Nbran, Tname(0) (/, 2I5, A30)

: NSEGm = number of segments in main channel.

: Nbran = number of primary branches.

: Tname(0) = main channel name.

NSEGb(m), NMT(m), Tname(m), m=1,Nbran (2I5, A30)

: NSEGb(m) = number of segments in the mth primary branch.

: $NMT(m)$ = main channel segment number to which the m^{th} branch is connected.
 : $Tname(m)$ = name of the m^{th} primary branch.
NSt (I5, /)
 : NSt = number of secondary branches (i.e., storage areas).
Title(j), $j=1,3$ (A79)
 : three-line text to identify the following data group.
Index, DIST(i), VH(i), P(i), AL(i), HA(i), i=1,NSEGm (A8, 5F8.3)
 : Input file uses **Index** for channel and segment identification only.
 : $DIST(i)$ = distance (km) from the river mouth to the i^{th} main channel transect.
 : $VH(i)$ = high tide volume (10^6 m^3) of the i^{th} main channel segment.
 : $P(i)$ = tidal prism (or intertidal volume in 10^6 m^3) upriver of the i^{th} main channel transect including those in branches.
 : $AL(i)$ = returning ratio at the i^{th} main channel transect.
 : $HA(i)$ = mean depth (m) of the i^{th} main channel segment.
(Index, DISTT(m,n), VHT(m,n), PT(m,n),
ALT(m,n), HAT(m,n), n=1,NSEGb(m)) m=1,Nbran (A8, 5F8.3)
 : The last character "T" designates the variables at the primary branches. Note that the first segment at each primary branch is in the main channel (see Section II-1). Hence, $DISTT(m,1) = 0$ and for example, $VHT(m,1) = VH(NMT(m))$.
(Index, StDIST(m,n), StVH(m,n), StP(m,n),
StAL(m,n), StHA(m,n), n=1,NSEGb(m)) m=1,Nbran (A8, 5F8.3)
 : The first two characters "St" designates the variables at the secondary branches. For those segments without storage area, $StP(m,n)$ must be set to zero.

At this point, the unit number 7 is closed and control passes to the main program and hence to the subroutine 'RWQC1'. Two subroutines 'RWQC1' and 'RWQC2' in 'SUB-READ.FOR' read in input parameters from the unit number 8.

A-1-2. Logical unit 8 (TPM-CONT.IN)

The unit number 8 contains the program control parameters and constant parameters for rate coefficients, initial conditions and boundary conditions, and files names for spatially and/or temporally varying conditions.

Title(j), j=1,3 (A79)

: three-line text to identify a simulation.

Title(1) (/ , A79)

: one blank line and one-line text to identify the following data group.

iPLT, iWQV, iTMP, iBEN, isi, iTSS, iSRP, iFCB (/ , 818)

: **iPLT** = 1 opens the unit number **80** and writes the model results for the last 20 tidal cycles, which will be used as input for Post-Processor. Otherwise no output to unit **80**.

: **iWQV** = 1 simulates all water column state variables. Otherwise only salinity is simulated.

: **iTMP** = 1 simulates water temperature. If **iTMP** = 0, spatially and temporally constant temperature is read in from the unit number **8**. If **iTMP** = 2, a sinusoidal curve is used to generate spatially constant temperature with coefficients read in from the unit **8**. If **iTMP** = 3, spatially and/or temporally varying temperatures are read in from the unit **17**.

: **iBEN** = 1 activates the sediment process model. If **iBEN** = 0, spatially and temporally constant benthic fluxes are read in from the unit number **8**. If **iBEN** = 2, spatially and/or temporally varying benthic fluxes are read in from the unit **16**.

: **isi** = 1 simulates silica state variables, available silica (AS) and particulate biogenic silica (SU). Otherwise no silica simulation.

: **iTSS** = 1 simulates suspended solid (TSS). Otherwise no TSS simulation and thus no effect of TSS on light attenuation and sorption of phosphate (PO₄) and AS.

: **iSRP** = 1 if total active metal (TAM) is simulated to account for the sorption of PO₄ and AS. If **iSRP** = 2, TSS is simulated to account for the sorption of PO₄ and AS: an error will be issued and the program be stopped if **iSRP** = 2 and **iTSS** ≠ 1. Otherwise no sorption of PO₄ and AS is simulated: TSS may be simulated but not TAM.

: **iFCB** = 1 simulates fecal coliform bacteria (FCB). Otherwise no FCB simulation. Note that if any of **iTMP**, **iBEN**, **isi**, **iTSS**, **iSRP** and **iFCB** is equal to 1, **iWQV** should be 1. Otherwise an error will be issued and the program be stopped.

iUKin, iBcs, izk, iNR, iNC (/ , 518)

: **iUKin** = number of kinetic update over half tidal cycle (Section II-4).

: **iBcs** = 1 if salinity toxicity is applied to cyanobacteria (Eq. 3-1b), i.e., freshwater

species. Otherwise no salinity toxicity to cyanobacteria, i.e., saltwater species.

: **izk** = 1 opens the unit number **22** and writes the diagnostic information for zero K° (Section III-12). Otherwise no output to unit **22**.

: **inr** = 1 opens the unit number **23** and writes the diagnostic information for negative R° (Section III-12). Otherwise no output to unit **23**.

: **inc** = 1 opens the unit number **24** and writes the diagnostic information for zero concentration. Otherwise no output to unit **24**.

Lsa1, Lbc, Lbd, Lpo4, Lnh4, Lno3, Lsa, Lo2, Ltmp (/ , 918)

: **Lsa1** = 1 opens the unit number **25** and writes the diagnostic information for salinity. Otherwise no output to unit **25**.

: **Lbc, Lbd, Lpo4, Lnh4, Lno3, Lsa, Lo2** OR **Ltmp** = 1 opens the unit number **26, 27, 28, 29, 30, 31, 32** or **33** and writes the diagnostic information for cyanobacteria, diatoms, phosphate, ammonium, nitrate, available silica, dissolve oxygen or temperature.

iICI, iAGR, iSTL, iSUN, iPSL, iNPL (/ , 618)

: **iICI** = 1 reads in spatially and/or temporally varying initial conditions for water column state variables from the unit number **11**. Otherwise constant conditions are read in from the unit **8**.

: **iAGR** = 1 reads in spatially and/or temporally varying algal growth, respiration and predation rates, and base light extinction coefficient from the unit number **12**. Otherwise constant coefficients are read in from the unit **8**.

: **iSTL** = 1 reads in spatially and/or temporally varying settling velocities for algae, refractory particulates, labile particulates, particulate metal and TSS from the unit number **13**. Otherwise constant coefficients are read in from the unit **8**.

: **iSUN** = 1 reads in temporally varying parameters for light intensity (daily light intensity and fractional daylength) and temperature (heat exchange coefficient and equilibrium temperature) from the unit number **14**. Otherwise constant coefficients are read in from the unit **8**.

: **iPSL** = 1 reads in temporally varying point source discharges and loadings from the unit number **18**. Otherwise constant inputs are read in from the unit **8**.

: `iNPL = 1` reads in spatially and/or temporally varying nonpoint source discharges and loadings from the unit number **19**. Otherwise constant inputs are read in from the unit **8**.

`iBCSal, iBCB, iBCCO, iBCPO, iBCPI, iBCNO, iBCNI, iBCSU, iBCSA (/, 9I8)`
`iBCCOD, iBCO2, iBCTSS, iBCTAM, iBCFCB, iBCT (/, 6I8)`

: control parameters for downriver boundary conditions of salinity (`iBCSal`), algae (`iBCB`), organic carbon (`iBCCO`), organic phosphorus (`iBCPO`), inorganic phosphorus (`iBCPI`), organic nitrogen (`iBCNO`), inorganic nitrogen (`iBCNI`), particulate biogenic silica (`iBCSU`), available silica (`iBCSA`), COD (`iBCCOD`), DO (`iBCO2`), TSS (`iBCTSS`), TAM (`iBCTAM`), fecal coliform bacteria (`iBCFCB`) and temperature (`iBCT`). For example, if `iBCCO = 1`, temporally varying downriver boundary conditions for three organic carbon variables (refractory particulate, labile particulate and dissolved) are read in from the unit number **15**. If `iBCCO ≠ 1`, the boundary conditions are generated using:

$$C_{DBC} = c_0 + c_1 \cdot \text{SIN} \left[\frac{2\pi t}{T_p} \right] + c_2 \cdot \text{COS} \left[\frac{2\pi t}{T_p} \right] \quad (\text{A-1})$$

where t = time (day); T_p = period (365 days). Three coefficients, c_0 , c_1 and c_2 , are obtained from multiple linear regression, and read in from the unit **8**. If c_1 and c_2 are zero, it is temporally constant boundary conditions, otherwise sinusoidally varying boundary conditions (Eq. A-1) are used.

If any of the above 15 parameters is equal to one, `iDBC` is set to one, and if all of the above 15 parameters are equal to one, `iDBC = 2`. Otherwise, `iDBC = 0`.

`Tstrt (/, F8.4)`

: `Tstrt` = Julian day to start the model run.

`iTmax, Nprn, iTimes, iSTS, iETS (/, 5I8, /)`

: `iTmax` = time duration (in tidal cycles) for model run.

: `Nprn` = number of times to write the snapshot longitudinal distribution output.

: Write time-series output starting from `iSTS` (tidal cycles) till `iETS` (tidal cycles) at `iTimes` locations. Note that the present model implementation allows the maximum of 10 locations of time-series output and that `iTimes ≤ 10`. Setting `iTimes ≤ 0` results in no time-series output.

iTSCH(j), iTSSEG(j), j=1,iTimeS (2I8)

: To the unit numbers 34 to 43 (one unit for one location), the subroutine 'TSwrite' in 'SUB-READ.FOR' writes time-series output for salinity and 23 water quality variables (Chapter III) at the channel number of **iTSCH(j)** and segment number of **iTSSEG(j)**. If **iTSCH(j) = 0**, it is main channel. If **iTSCH(j) = -m**, it is secondary branch connecting to the m^{th} primary branch.

iTout(j), j=1,Nprn (/, 15I5)

: To the unit number 21, the subroutine 'LDwrite' in 'SUB-READ.FOR' prints out the snapshot information for salinity and 23 water quality variables (Chapter III) at the time of **iTout(j)** tidal cycles from the model start. Note that the present model implementation allows the maximum of 15 times of output printing and that $0 \leq \text{iTout}(j) \leq \text{iTmax}$.

Title(1) (/, A79)

: one blank line and one-line text to identify the following data group (algae).

KHnc, KHnd, KHng, KHpc, KHpd, KHpg, KHS, STOX (/, 8F8.4)
KeTSS, KeChl, CChlc, CChld, CChlg, DOPTc, DOPTd, DOPTg (/, 8F8.4)
rIO, rIsMIN, FD, CIa, CIb, CIc (/, 6F8.4)
TMc, TMd, TMg, KTG1c, KTG2c, KTG1d, KTG2d, KTG1g, KTG2g (/, 9F8.4)
TRc, TRd, TRg, KTBc, KTBd, KTBg (/, 6F8.4)

: **KHN_x** = half-saturation constant for nitrogen uptake (g N m^{-3}) by algal group **x** (**x = c** for cyanobacteria, **x = d** for diatoms and **x = g** for green algae).

: **KHP_x** = half-saturation constant for phosphorus uptake (g P m^{-3}) by algal group **x**.

: **KHS** = half-saturation constant for silica uptake (g Si m^{-3}) by diatoms.

: **STOX** = salinity (ppt) at which Microcystis growth is halved, which is applied to cyanobacteria only when **iBcs = 1**.

: **KeTSS** = light extinction coefficient for TSS (m^{-1} per g m^{-3}).

: **Kechl** = light extinction coefficient for chlorophyll 'a' (m^{-1} per mg Chl m^{-3}).

: **CChl_x** = carbon-to-chlorophyll ratio (g C per mg Chl) in algal group **x**.

: **DOPT_x** = depth of maximum algal growth (m) for algal group **x**.

: **rIO** = initial daily light intensity at water surface (langleys day^{-1}).

: **rIsMIN** = minimum optimum light intensity (langleys day^{-1}).

: **FD** = fractional daylength, which is used only when **iSUN \neq 1**.

: **CIa, CIb** and **CIc** = weighting factors for I_0, I_1 and I_2 , respectively (**CIa + CIb +**

$c_{1c} = 1$, see Eq. 3-1j).

- : TM_x = optimal temperature for algal growth ($^{\circ}C$) for algal group x .
- : $KTG1_x$ = temperature effect below TM_x on algal growth ($^{\circ}C^{-2}$) for algal group x .
- : $KTG2_x$ = temperature effect above TM_x on algal growth ($^{\circ}C^{-2}$) for algal group x .
- : TR_x = reference temperature for basal metabolism ($^{\circ}C$) for algal group x .
- : KTB_x = effect of temperature on basal metabolism ($^{\circ}C^{-1}$) for algal group x .

Title(1) (/ , A79)

: one blank line and one-line text to identify the following data group (carbon).

FCRP, FCLP, FCDP, FCDc, FCDd, FCDg, KHRc, KHRd, KHRg (/ , 9F8.4)

KRC, KLC, KDC, KRCalg, KLCalg, KDCalg (/ , 6F8.4)

TRHDR, TRMNL, KTHDR, KTMNL, KHORDO, KHDNN, AANOX (/ , 7F8.4)

: FCRP, FCLP and FCDP = fraction of predated carbon produced as refractory particulate, labile particulate and dissolved organic carbon, respectively.

: FCD_x = fraction of basal metabolism exuded as dissolved organic carbon at infinite dissolved oxygen concentration for algal group x .

: KHR_x = half-saturation constant of dissolve oxygen ($g\ O_2\ m^{-3}$) for algal dissolved organic carbon excretion by algal group x .

: KRC and KLC = minimum dissolution rate (day^{-1}) of refractory and labile particulate organic carbon, respectively.

: KDC = minimum respiration rate (day^{-1}) of dissolved organic carbon.

: $KRCalg$ and $KLCalg$ = constants that relate dissolution of refractory and labile particulate organic carbon, respectively, to algal biomass (day^{-1} per $g\ C\ m^{-3}$).

: $KDCalg$ = constant that relates respiration to algal biomass (day^{-1} per $g\ C\ m^{-3}$).

: $TRHDR$ = reference temperature for hydrolysis of particulate organic matter ($^{\circ}C$).

: $TRMNL$ = reference temperature for mineralization of dissolved organic matter ($^{\circ}C$).

: $KTHDR$ = temperature effect on hydrolysis of particulate organic matter ($^{\circ}C^{-1}$).

: $KTMNL$ = temperature effect on mineralization of dissolved organic matter ($^{\circ}C^{-1}$).

: $KHORDO$ = oxic respiration half-saturation constant for dissolved oxygen ($g\ O_2\ m^{-3}$).

: $KHDNN$ = denitrification half-saturation constant for nitrate ($g\ N\ m^{-3}$).

: $AANOX$ = rate ratio of denitrification to oxic dissolved organic carbon respiration.

Title(1) (/ , A79)

: one blank line and one-line text to identify the following data group (phosphorus).

FPRP, FPLP, FPDp, FPIP, FPRc, FPRd, FPRg, FPLc, FPLd, FPLg (/ , 10F8.4)
FPDc, FPDd, FPDg, FPIc, FPI d, FPIg, KPO4p (/ , 7F8.4)
KRP, KLP, KDP, KRPalg, KLPalg, KDPalg, CPprm1, CPprm2, CPprm3 (/ , 9F8.4)

: FPRP, FPLP, FPDp and FPIP = fraction of predated phosphorus produced as refractory particulate organic, labile particulate organic, dissolved organic and inorganic phosphorus, respectively.

: FPRx, FPLx, FPDx and FPIx = fraction of metabolized phosphorus by algal group x produced as refractory particulate organic, labile particulate organic, dissolved organic and inorganic phosphorus, respectively.

: KPO4p = coefficient relating phosphate sorption to TSS (per g m⁻³) if iSRP = 2 or TAM (per mol m⁻³) if iSRP = 1. If iSRP ≠ 1 and iSRP ≠ 2, KPO4p is forced to be 0.

: KRP and KLP = minimum hydrolysis rate (day⁻¹) of refractory and labile particulate organic phosphorus, respectively.

: KDP = minimum mineralization rate (day⁻¹) of dissolved organic phosphorus.

: KRPalg and KLPalg = constants that relate hydrolysis of refractory and labile particulate organic phosphorus, respectively, to algal biomass (day⁻¹ per g P m⁻³).

: KDPalg = constant that relates mineralization to algal biomass (day⁻¹ per g P m⁻³).

: CPprm1 (g C per g P), CPprm2 (g C per g C) and CPprm3 (per g P m⁻³) = constants used to determine phosphorus-to-carbon ratio (Eq. 3-8e).

Title(1) (/ , A79)

: one blank line and one-line text to identify the following data group (nitrogen).

FNRp, FNLP, FNDP, FNIP, FNRc, FNRd, FNRg, FNLc, FNLd, FNLg (/ , 10F8.4)
FNDc, FNDd, FNDg, FNIC, FNID, FNIG, ANCC, ANCD, ANCG (/ , 9F8.4)
ANDC, rNitM, KHNitDO, KHNitN, TNit, KNit1, KNit2 (/ , 7F8.4)
KRN, KLN, KDN, KRNa1g, KLNa1g, KDNa1g (/ , 6F8.4)

: FNRp, FNLP, FNDP and FNIP = fraction of predated nitrogen produced as refractory particulate organic, labile particulate organic, dissolved organic and inorganic nitrogen, respectively.

: FNRx, FNLP, FNDx and FNIX = fraction of metabolized nitrogen by algal group x produced as refractory particulate organic, labile particulate organic, dissolved organic and inorganic nitrogen, respectively.

- : ANC_x = nitrogen-to-carbon ratio (g N per g C) in algal group x.
- : $ANDC$ = mass of nitrate nitrogen reduced per mass of dissolved organic carbon oxidized (0.933 g N per g C, see Eq. 3-13).
- : r_{NitM} = maximum nitrification rate ($g\ N\ m^{-3}\ day^{-1}$) at temperature T_{Nit} .
- : K_{HNitDO} = nitrification half-saturation constant for dissolved oxygen ($g\ O_2\ m^{-3}$).
- : K_{HNitN} = nitrification half-saturation constant for ammonium ($g\ N\ m^{-3}$).
- : T_{Nit} = optimum temperature ($^{\circ}C$).
- : K_{Nit1} and K_{Nit2} = temperature effect on nitrification rate ($^{\circ}C^{-2}$) below and above T_{Nit} , respectively.
- : K_{RN} and K_{LN} = minimum hydrolysis rate (day^{-1}) of refractory and labile particulate organic nitrogen, respectively.
- : K_{DN} = minimum mineralization rate (day^{-1}) of dissolved organic nitrogen.
- : K_{RNalg} and K_{LNalg} = constants that relate hydrolysis of refractory and labile particulate organic nitrogen, respectively, to algal biomass (day^{-1} per $g\ N\ m^{-3}$).
- : K_{DNalg} = constant that relates mineralization to algal biomass (day^{-1} per $g\ N\ m^{-3}$).

Title(1) (/ , A79)

- : one blank line and one-line text to identify the following data group (silica).
- FSPP, FSIP, FSPd, FSId, ASCd, KSAP, KSU, TRSUA, KTSUA (/ , 9F8.4)**
- : $FSPP$ and $FSIP$ = fraction of predated diatom silica produced as particulate biogenic and available silica, respectively.
- : $FSPd$ and $FSId$ = fraction of metabolized silica by diatoms produced as particulate biogenic and available silica, respectively.
- : $ASCd$ = silica-to-carbon ratio of diatoms (g Si per g C).
- : $KSAP$ = coefficient relating available silica sorption to TSS (per $g\ m^{-3}$) if $i_{SRP} = 2$ or TAM (per $mol\ m^{-3}$) if $i_{SRP} = 1$. If $i_{SRP} \neq 1$ and $i_{SRP} \neq 2$, $KSAP$ is forced to be 0.
- : KSU = dissolution rate of particulate biogenic silica (day^{-1}) at temperature $TRSUA$.
- : $TRSUA$ = reference temperature for dissolution of particulate biogenic silica ($^{\circ}C$).
- : $KTSUA$ = temperature effect on dissolution of particulate biogenic silica ($^{\circ}C^{-1}$).

Title(1) (/ , A79)

: one blank line and one-line text to identify the following data group (COD and DO).

AOCR, AONT, KRO, KTR, KHCOD, KCD, TRCOD, KTCOD (/ , 8F8.4)

: AOCR = dissolved oxygen-to-carbon ratio in respiration (2.67 g O₂ per g C, see Eq. 3-17).

: AONT = mass of dissolved oxygen consumed per unit mass of ammonium nitrogen nitrified (4.33 g O₂ per g N, see Eq. 3-17).

: KRO = proportionality constant in reaeration (3.933 in MKS unit, see Eq. 3-17e).

: KTR = constant for temperature adjustment of reaeration rate.

: KHCOD = half-saturation constant of dissolved oxygen required for oxidation of chemical oxygen demand (g O₂ m⁻³).

: KCD = oxidation rate of chemical oxygen demand (day⁻¹).

: TRCOD = reference temperature for oxidation of chemical oxygen demand (°C).

: KTCOD = temperature effect on oxidation of chemical oxygen demand (°C⁻¹).

Title(1) (/ , A79)

: one blank line and one-line text to identify the following data group (TSS, TAM, fecal coliform bacteria and temperature).

**RDTSS, KHbmf, BFTAM, Tmptam, Ktam, TAMdmx, Kdotam, KFCB, TmpFCB (/ , 9F8.4)
TmpMax, TmpMin, DTmax, Cp, Rho, KT, Te (/ , 7F8.4)**

: RDTSS = net rate of resuspension and deposition (g m⁻² day⁻¹).

: KHbmf = dissolved oxygen concentration at which TAM release is half anoxic release rate (g O₂ m⁻³).

: BFTAM = anoxic release rate of TAM (mol m⁻² day⁻¹).

: Tmptam = reference temperature for sediment release of TAM (°C).

: Ktam = temperature effect on sediment release of TAM (°C⁻¹).

: TAMdmx = solubility of TAM under anoxic conditions (mol m⁻³).

: Kdotam = constant that relates TAM solubility to dissolved oxygen (per g O₂ m⁻³).

: KFCB = first-order die-off rate of fecal coliform bacteria (day⁻¹).

: TmpFCB = temperature effect on die-off of fecal coliform bacteria (°C⁻¹).

: TmpMAX and TmpMIN = annual maximum and minimum water temperatures (°C), respectively (Eq. 3-21-1).

- : ΔT_{\max} = number of days since January 1 to reach T_{mpMAX} (Eq. 3-21-1).
- : c_p = specific heat of water (4186 watt sec $\text{kg}^{-1} \text{ }^\circ\text{C}^{-1}$, see Eq. 3-21).
- : ρ = density of water (1000 kg m^{-3} , see Eq. 3-21).
- : κ_T and T_e = heat exchange coefficient (watt $\text{m}^{-2} \text{ }^\circ\text{C}^{-1}$) and equilibrium temperature ($^\circ\text{C}$), respectively, which are used only when $i_{\text{SUN}} \neq 1$.

At this point, control passes to the main program and hence to the subroutine 'RWQC2' in subroutine 'SUB-READ.FOR'.

Title (/ , A79)

: one blank line and one-line text to identify the following data group.

S(2), Bc(2), Bd(2), Bg(2), C1(2), C2(2), C3(2), APCi (/ , 8F8.4)
P1(2), P2(2), P3(2), PO4t(2), N1(2), N2(2), N3(2), NH4(2), NO3(2), (/ , 9F8.4)
SU(2), SA(2), COD(2), O2(2), TSS(2), TAM(2), FCB(2), T(2) (/ , 8F8.4)

: spatially constant initial conditions (g m^{-3})

: s = salinity in ppt, B_c = cyanobacteria, B_d = diatoms, B_g = green algae, c_1 = refractory POC (particulate organic carbon), c_2 = labile POC, c_3 = DOC (dissolved organic carbon), p_1 = refractory POP (particulate organic phosphorus), p_2 = labile POP, p_3 = DOP (dissolved organic phosphorus), PO_4t = total phosphate, N_1 = refractory PON (particulate organic nitrogen), N_2 = labile PON, N_3 = DON (dissolved organic nitrogen), NH_4 = ammonium nitrogen, NO_3 = nitrate nitrogen, SU = particulate biogenic silica, SA = available silica, COD = COD (chemical oxygen demand), O_2 = DO (dissolved oxygen), TSS = total suspended solid, TAM = TAM (total active metal in mol m^{-3}), FCB = fecal coliform bacteria (MPN per 100 mL) and T = water temperature ($^\circ\text{C}$). APC_i is the mean phosphorus-to-carbon ratio (g P per g C) in all algal groups for the initial condition, which is used to estimate phosphorus content in algal biomass. These values are used only when $i_{ICI} \neq 1$.

Title (/ , A79)

: one blank line and one-line text to identify the following data group.

PMc(2), PMd(2), PMg(2),
BMRc(2), BMRd(2), BMRg(2), PRRc(2), PRRd(2), PRRg(2), Keb(2) (/ , 10F8.4)

: spatially and temporally constant growth rate (PM_x in day^{-1}), basal metabolism rate

(BMR_x in day^{-1}) and predation rate (PRR_x in day^{-1}) for algal group x , and base light extinction coefficient (κ_{eb} in m^{-1}). These values are used only when $iAGR \neq 1$.

Title (/ , A79)

: one blank line and one-line text to identify the following data group.

WSc(2), Wsd(2), Wsg(2), Wsrp(2), Wslp(2), Wss(2), Wstss(2) (/ , 7F8.4)

: spatially and temporally constant settling velocities ($m\ day^{-1}$) for cyanobacteria (wsc), diatoms (wsd), green algae (wsg), refractory particulate ($wsrp$), labile particulate ($wslp$), particulate metal (wss) and TSS ($wstss$). These values are used only when $istl \neq 1$.

Title (/ , A79)

: one blank line and one-line text to identify the following data group.

c0S, c1S, c2S, c0T, c1T, c2T, APCd (/ , 7F8.4)
c0Bc, c1Bc, c2Bc, c0Bd, c1Bd, c2Bd, c0Bg, c1Bg, c2Bg (/ , 9F8.4)
c0C1, c1C1, c2C1, c0C2, c1C2, c2C2, c0C3, c1C3, c2C3 (/ , 9F8.4)
c0P1, c1P1, c2P1, c0P2, c1P2, c2P2, c0P3, c1P3, c2P3 (/ , 9F8.4)
c0PO4t, c1PO4t, c2PO4t (/ , 3F8.4)
c0N1, c1N1, c2N1, c0N2, c1N2, c2N2, c0N3, c1N3, c2N3 (/ , 9F8.4)
c0NH4, c1NH4, c2NH4, c0NO3, c1NO3, c2NO3 (/ , 6F8.4)
c0SU, c1SU, c2SU, c0SA, c1SA, c2SA (/ , 6F8.4)
c0COD, c1COD, c2COD, c0O2, c1O2, c2O2 (/ , 6F8.4)
c0TSS, c1TSS, c2TSS, c0TAM, c1TAM, c2TAM, c0FCB, c1FCB, c2FCB (/ , 9F8.4)

: temporally constant or sinusoidally varying boundary conditions are generated with Eq. A-1 using the above coefficients, obtained from multiple linear regression. These values are used only when the corresponding control parameters (iBC^*) $\neq 1$. The units are $g\ m^{-3}$ except $s(1)$ in ppt, $TAM(1)$ in $mol\ m^{-3}$, $FCB(1)$ in MPN per 100 mL and $T(1)$ in $^{\circ}C$. $APCd$ is the mean phosphorus-to-carbon ratio ($g\ P$ per $g\ C$) in all algal groups at the downriver boundary, which is used to estimate phosphorus content in algal biomass.

Title (/ , A79)

: one blank line and one-line text to identify the following data group.

BFPO4d(2), BFNH4(2), BFNO3(2), BFSAd(2), BFCOD(2), BFO2(2) (/ , 6F8.4)

: spatially and temporally constant benthic fluxes ($g\ m^{-2}\ day^{-1}$) of dissolved phosphate ($BFPO4d$), ammonium ($BFNH4$), nitrate ($BFNO3$), dissolved silica ($BFSAd$), COD ($BFCOD$) and DO ($BFO2$). These values are used only when $iBEN = 0$.

Title (/ , A79)

: one blank line and one-line text to identify the following data group (spatially and temporally constant point source discharge and loadings). All values under this title are used only when $iPSL \neq 1$.

iMCPS (8X, I5)

iBRPS (8X, I5)

iSTPS (8X, I5)

: number of segments into which point source input discharges for main channel (iMCPS), primary branch (iBRPS) and secondary branch (iSTPS).

Title (A79)

: one-line text to identify the following data.

ID2, i, xPSQ, xPS,

xPBc, xPBd, xPBg, xPC1, xPC2, xPC3, j=1, iMCPS (A2, 3X, I3, 8F8.3)

: Input file uses ID2 for channel identification only.

: $xPSQ$ = point source discharge ($m^3 \text{ sec}^{-1}$) into the i^{th} main channel segment.

: xPS = salinity in point source discharge (ppt).

: point source loadings (in $kg \text{ TC}^{-1}$, where TC is tidal cycle) into the i^{th} main channel segment for cyanobacteria ($xPBc$), diatoms ($xPBd$), green algae ($xPBg$), refractory POC ($xPC1$), labile POC ($xPC2$) and DOC ($xPC3$).

ID2, m, n, xPSQT, xTPS,

xTPBc, xTPBd, xTPBg, xTPC1, xTPC2, xTPC3, j=1, iBRPS (A2, 2I3, 8F8.3)

: The character "T" designates the variables at the primary branches.

: Point source input enters the n^{th} segment in the m^{th} primary branch.

ID2, m, n, xStPSQ, xStPS,

xStPBc, xStPBd, xStPBg, xStPC1, xStPC2, xStPC3, j=1, iSTPS (A2, 2I3, 8F8.3)

: The character "St" designates the variables at the secondary branches.

: Point source input enters the n^{th} segment in the m^{th} secondary branch (storage area).

Title (A79)

: one-line text to identify the following data.

ID2, i, xPP1, xPP2, xPP3,

xPPO4t, xPN1, xPN2, xPN3, xPNH4, xPNO3, j=1, iMCPS (A2, 3X, I3, 9F8.3)

: point source loadings (in $kg \text{ TC}^{-1}$) into the i^{th} main channel segment for refractory POP ($xPP1$), labile POP ($xPP2$), DOP ($xPP3$), total phosphate ($xPPO4t$), refractory PON ($xPN1$), labile PON ($xPN2$), DON ($xPN3$), ammonium ($xPNH4$) and nitrate ($xPNO3$).

ID2, m, n, xTPP1, xTPP2, xTPP3,

xTPPO4t, xTPN1, xTPN2, xTPN3, xTPNH4, xTPNO3, j=1, iMCPS (A2, 3X, I3, 9F8.3)

: The character "T" designates the variables at the primary branches.

: Point source input enters the n^{th} segment in the m^{th} primary branch.

**ID2, m, n, xStPP1, xStPP2, xStPP3, xStPPO4t,
xStPN1, xStPN2, xStPN3, xStPNH4, xStPNO3, j=1, iMCPS (A2, 3X, I3, 9F8.3)**

: The character "St" designates the variables at the secondary branches.

: Point source input enters the n^{th} segment in the m^{th} secondary branch (storage area).

Title (A79)

: one-line text to identify the following data.

**ID2, i, xPSU, xPSA, xPCOD,
xPO2, xPTSS, xPTAM, xPFCB, xPT, j=1, iMCPS (A2, 3X, I3, 8F8.3)**

: point source loadings (in kg TC^{-1}) into the i^{th} main channel segment for particulate biogenic silica (xPSU), available silica (xPSA), COD (xPCOD), TSS (xPTSS) and TAM (xPTAM in kmol TC^{-1}).

: xPO2 = DO in point source discharge (g m^{-3}).

: xPFCB = fecal coliform bacteria in point source discharge (MPN per 100 mL).

: xPT = temperature in point source discharge ($^{\circ}\text{C}$).

**ID2, m, n, xTPSU, xTPSA, xTPCOD,
xTPO2, xTPTSS, xTPTAM, xTPFCB, xTPT, j=1, iMCPS (A2, 3X, I3, 8F8.3)**

: The character "T" designates the variables at the primary branches.

: Point source input enters the n^{th} segment in the m^{th} primary branch.

**ID2, m, n, xStPSU, xStPSA, xStPCOD,
xStPO2, xStPTSS, xStPTAM, xStPFCB, xStPT, j=1, iMCPS (A2, 3X, I3, 8F8.3)**

: The character "St" designates the variables at the secondary branches.

: Point source input enters the n^{th} segment in the m^{th} secondary branch (storage area).

Title (/, A79)

: one blank line and one-line text to identify the following data group.

**xDSQ, xNS, xNBc, xNBd, xNBg, xNC1, xNC2, xNC3 (/, 8F8.4)
xNP1, xNP2, xNP3, xNPO4t, xNN1, xNN2, xNN3, xNNH4, xNNO3, (/, 9F8.4)
xNSU, xNSA, xNCOD, xNO2, xNTSS, xNTAM, xNFCB, xNT (/, 8F8.4)**

: spatially and temporally constant nonpoint source discharge and loadings into all segments including branches.

: xDSQ = nonpoint source discharge (m sec^{-1}).

: The first two characters "xN" designates nonpoint source input, and the definition and unit of variables are the same as point source input except xNFCB in 10^9 MPN TC^{-1} .

: These values are used only when $\text{iNPL} \neq 1$.

Title (/, A79)

: one blank line and one-line text to identify the following data group.

ICIFN (44X, A50)

: input file name for spatially and/or temporally varying initial conditions for water column state variables. If $iICI = 1$, ICIFN is opened with the unit number 11. If $iICI \neq 1$, then ICIFN must be 'none', otherwise an error will be issued and the program be stopped.

AGRFN (44X, A50)

: input file name for spatially and/or temporally varying algal growth, respiration and predation rates, and base light extinction coefficient. If $iAGR = 1$, AGRFN is opened with the unit number 12. If $iAGR \neq 1$, then AGRFN must be 'none', otherwise an error will be issued and the program be stopped.

STLFN (44X, A50)

: input file name for spatially and/or temporally varying settling velocities. If $iSTL = 1$, STLFN is opened with the unit number 13. If $iSTL \neq 1$, then STLFN must be 'none', otherwise an error will be issued and the program be stopped.

SUNFN (44X, A50)

: input file name for temporally varying parameters for light intensity and temperature. If $iSUN = 1$, SUNFN is opened with the unit number 14. If $iSUN \neq 1$, then SUNFN must be 'none', otherwise an error will be issued and the program be stopped.

DBC FN (44X, A50)

: input file name for temporally varying downriver boundary conditions for water column state variables. If $iDBC = 1$, DBCFN is opened with the unit number 15. If $iDBC \neq 1$, then DBCFN must be 'none', otherwise an error will be issued and the program be stopped.

BENFN (44X, A50)

: input file name for spatially and/or temporally varying benthic fluxes. If $iBEN = 2$, BENFN is opened with the unit number 16. If $iBEN \neq 2$, then BENFN must be 'none', otherwise an error will be issued and the program be stopped.

TMPFN (44X, A50)

: input file name for spatially and/or temporally varying water temperatures. If $iTMP = 3$, TMPFN is opened with the unit number 17. If $iTMP \neq 3$, then TMPFN must be 'none', otherwise an error will be issued and the program be stopped.

PSLFN (44X, A50)

: input file name for temporally varying point source discharges and loadings. If $i_{PSL} = 1$, PSLFN is opened with the unit number 18. If $i_{PSL} \neq 1$, then PSLFN must be 'none', otherwise an error will be issued and the program be stopped.

NPLFN (44X, A50)

: input file name for spatially and/or temporally varying nonpoint source discharges and loadings. If $i_{NPL} = 1$, NPLFN is opened with the unit number 19. If $i_{NPL} \neq 1$, then NPLFN must be 'none', otherwise an error will be issued and the program be stopped.

SMIFN (44X, A50)

: input file name for sediment process model. If $i_{BEN} = 1$, SMIFN is opened with the unit number 20. If $i_{BEN} \neq 1$, then SMIFN must be 'none', otherwise an error will be issued and the program be stopped.

ZKOFN (44X, A50)

: output file name for diagnostic information for zero K^0 (Section III-12). If $i_{ZK} = 1$, ZKOFN is opened with the unit number 22. If $i_{ZK} \neq 1$, then ZKOFN must be 'none', otherwise an error will be issued and the program be stopped.

NROFN (44X, A50)

: output file name for diagnostic information for negative R^0 (Section III-12). If $i_{NR} = 1$, NROFN is opened with the unit number 23. If $i_{NR} \neq 1$, then NROFN must be 'none', otherwise an error will be issued and the program be stopped.

NCOFN (44X, A50)

: output file name for diagnostic information for negative concentration. If $i_{NC} = 1$, NCOFN is opened with the unit number 24. If $i_{NC} \neq 1$, then NCOFN must be 'none', otherwise an error will be issued and the program be stopped.

DSOFN (44X, A50)

: output file name for diagnostic information for salinity. If $L_{Sal} = 1$, DSOFN is opened with the unit number 25. If $L_{Sal} \neq 1$, then DSOFN must be 'none', otherwise an error will be issued and the program be stopped.

DBCOFN (44X, A50)

: output file name for diagnostic information for cyanobacteria. If $L_{Bc} = 1$, DBCOFN is opened with the unit number 26. If $L_{Bc} \neq 1$, then DBCOFN must be 'none', otherwise an error will be issued and the program be stopped.

DBdOFN (44X, A50)

: output file name for diagnostic information for diatoms. If $L_{Bd} = 1$, DBdOFN is opened with the unit number 27. If $L_{Bd} \neq 1$, then DBdOFN must be 'none', otherwise an error will be issued and the program be stopped.

DPOFN (44X, A50)

: output file name for diagnostic information for phosphate. If $L_{Po4} = 1$, DPOFN is opened with the unit number 28. If $L_{Po4} \neq 1$, then DPOFN must be 'none', otherwise an error will be issued and the program be stopped.

DNOFNH4 (44X, A50)

: output file name for diagnostic information for ammonium. If $L_{Nh4} = 1$, DNOFNH4 is opened with the unit number 29. If $L_{Nh4} \neq 1$, then DNOFNH4 must be 'none', otherwise an error will be issued and the program be stopped.

DNOFN (44X, A50)

: output file name for diagnostic information for nitrate. If $L_{No3} = 1$, DNOFN is opened with the unit number 30. If $L_{No3} \neq 1$, then DNOFN must be 'none', otherwise an error will be issued and the program be stopped.

DSiOFN (44X, A50)

: output file name for diagnostic information for available silica. If $L_{Ssa} = 1$, DSiOFN is opened with the unit number 31. If $L_{Ssa} \neq 1$, then DSiOFN must be 'none', otherwise an error will be issued and the program be stopped.

DO2OFN (44X, A50)

: output file name for diagnostic information for dissolved oxygen. If $L_{O2} = 1$, DO2OFN is opened with the unit number 32. If $L_{O2} \neq 1$, then DO2OFN must be 'none', otherwise an error will be issued and the program be stopped.

DTOFN (44X, A50)

: output file name for diagnostic information for temperature. If $L_{tmp} = 1$, DTOFN is opened with the unit number 33. If $L_{tmp} \neq 1$, then DTOFN must be 'none', otherwise an error will be issued and the program be stopped.

LDOFN (44X, A50)

: output file name for snapshot longitudinal distribution of water column state variables. If $N_{prn} \geq 1$, LDOFN is opened with the unit number 21. If $N_{prn} \leq 0$, then LDOFN must be 'none', otherwise an error will be issued and the program be stopped.

TSOFN(j), j=1,iTimes (44X, A50)

: output file name for time-series output of water column state variables. If *iTimes* \geq 1, *TSOFN(j)*'s are opened with the unit numbers 34 to 44 (one unit for one location). If *iTimes* \leq 0, this line will not be executed.

At this point, the unit number 8 is closed and control passes to the main program. If *iBEN* = 1, control passes to the subroutine 'RSEDIn' and then to 'RSEDVIn'. These two subroutines in 'SUB-SM.FOR' read in input parameters for sediment process model from the unit number 20 (see Appendix A-2). After this point, depending on the values of control parameters, various subroutines read in spatially and/or temporally varying input parameters, which are described in the remaining of this section.

A-1-3. Logical unit 11 (if *iICI* = 1)

If *iICI* = 1, the subroutine 'RICAL' in 'SUB-READ.FOR' reads in spatially and/or temporally varying initial conditions from the unit number 11.

Title(j), j=1,3 (A79)

: three-line text to identify the input file. These lines are read in only once at the first reading, i.e., they are needed only when *iTICI* = 0.

Title(1) (/ , A79)

: one blank line and one-line text to identify the following data group.

Index, S(i), Bc(i), Bd(i), Bg(i), C1(i), C2(i), C3(i), APCi, i=2, NSEGM (A8, 8F8.3)
(**Index, TS(m,n), TBc(m,n), TBd(m,n), TBg(m,n),**
TC1(m,n), TC2(m,n), TC3(m,n), n=2, NSEGB(m)) m=1, Nbran (A8, 7F8.3)
ID2, m, n, StS(m,n), StBc(m,n), StBd(m,n),
StBg(m,n), StC1(m,n), StC2(m,n), StC3(m,n), j=1, Nst (A2, 2I3, 7F8.3)

: Input file uses the first 8 columns (*Index* and *ID2*) to identify channel and segment.

: spatially varying initial conditions (see Appendix A-1-2 for definition of variables).

: *APCi* = mean phosphorus-to-carbon ratio (g P per g C) in all algal groups for the initial condition, which is used to estimate phosphorus content in algal biomass.

Title(1) (A79)

: one-line text to identify the following data group.

Index, P1(i), P2(i), P3(i),
PO4t(i), N1(i), N2(i), N3(i), NH4(i), NO3(i), i=2, NSEGM (A8, 9F8.3)
(**Index, TP1(m,n), TP2(m,n), TP3(m,n), TPO4t(m,n), TN1(m,n), TN2(m,n),**
TN3(m,n), TNH4(m,n), TNO3(m,n), n=2, NSEGB(m)) m=1, Nbran (A8, 9F8.3)

ID2, m, n, StP1(m, n), StP2(m, n), StP3(m, n), StPO4t(m, n), StN1(m, n),
StN2(m, n), StN3(m, n), StNH4(m, n), StNO3(m, n), j=1, NSt (A2, 2I3, 9F8.3)

: Input file uses the first 8 columns (Index and ID2) to identify channel and segment.

: spatially varying initial conditions (see Appendix A-1-2 for definition of variables).

Title(1) (A79)

: one-line text to identify the following data group.

Index, SU(i), SA(i),
COD(i), O2(i), TSS(i), TAM(i), FCB(i), T(i), i=2, NSEGM (A8, 8F8.3)
(Index, TSU(m, n), TSA(m, n), TCOD(m, n), TO2(m, n), TTSS(m, n),
TTAM(m, n), TFCB(m, n), TT(m, n), n=2, NSEGB(m)) m=1, Nbran (A8, 8F8.3)
ID2, m, n, StSU(m, n), StSA(m, n), StCOD(m, n), StO2(m, n),
StTSS(m, n), StTAM(m, n), StFCB(m, n), StT(m, n), j=1, NSt (A2, 2I3, 8F8.3)

: Input file uses the first 8 columns (Index and ID2) to identify channel and segment.

: spatially varying initial conditions (see Appendix A-1-2 for definition of variables).

iTICI, ICICont (I7, 1X, A3)

: ICICont = 'END' indicates no more reading from the unit number 11. Otherwise,
the subroutine 'RICI' will read temporally varying initial conditions at iTICI tidal cycles.

A-1-4. Logical unit 12 (if IAGR = 1)

If IAGR = 1, the subroutine 'RAGR' in 'SUB-READ.FOR' reads in spatially and/or
temporally varying parameters for algal growth, base metabolism and predation rates, and
base light extinction coefficient from the unit number 12.

Title(j), j=1,3 (A79)

: three-line text to identify the input file. These lines are read in only once at the first
reading, i.e., they are needed only when iTAGR = 0.

Title(1) (/ , A79)

: one blank line and one-line text to identify the following data group.

Index, PMc(i), PMd(i), PMg(i), BMRc(i),
BMRd(i), BMRg(i), PRRc(i), PRRd(i), PRRg(i), Keb(i), i=2, NSEGM (A8, 10F8.3)
(Index, TPMc(m, n), TPMd(m, n), TPMg(m, n),
TBMRc(m, n), TBMRd(m, n), TBMRg(m, n), TPRRc(m, n),
TPRRd(m, n), TPRRg(m, n), TKeb(m, n), n=2, NSEGB(m)) m=1, Nbran (A8, 10F8.3)
ID2, m, n, StPMc(m, n), StPMd(m, n), StPMg(m, n),
StBMRc(m, n), StBMRd(m, n), StBMRg(m, n),
StPRRc(m, n), StPRRd(m, n), StPRRg(m, n), j=1, NSt (A2, 2I3, 10F8.3)

: Input file uses the first 8 columns (Index and ID2) to identify channel and segment.

: spatially varying parameters for algal dynamics (see Appendix A-1-2 for definition of
variables).

iTAGR, AGRCont (I7, 1X, A3)

: AGRCont = 'END' indicates no more reading from the unit number 12. Otherwise, the subroutine 'RAGR' will read temporally varying parameters at iTAGR tidal cycles.

A-1-5. Logical unit 13 (if iSTL = 1)

If iSTL = 1, the subroutine 'RSTL' in 'SUB-READ.FOR' reads in spatially and/or temporally varying settling velocities for algae, refractory particulates, labile particulates, particulate metal and TSS from the unit number 13.

Title(j), j=1,3 (A79)

: three-line text to identify the input file. These lines are read in only once at the first reading, i.e., they are needed only when iTSTL = 0.

Title(1) (/ , A79)

: one blank line and one-line text to identify the following data group.

**Index, WSc(i), WSBd(i), WSSd(i),
WSg(i), WSRp(i), WSlp(i), WSS(i), WStss(i), i=2, NSEGm (A8, 8F8.3)
(Index, TWSc(m,n), TWBd(m,n), TWSSd(m,n), TWG(m,n), TWRp(m,n),
TWLp(m,n), TWSS(m,n), TWStss(m,n), n=2, NSEGb(m)) m=1, Nbran (A8, 8F8.3)
ID2, m,n, StWSc(m,n), StWSBd(m,n), StWSSd(m,n), StWSG(m,n), StWSRp(m,n),
StWSLp(m,n), StWSS(m,n), StWStss(m,n), j=1, NSt (A2, 2I3, 8F8.3)**

: Input file uses the first 8 columns (Index and ID2) to identify channel and segment.

: spatially varying settling velocities (see Appendix A-1-2 for definition of variables).

iTSTL, STLCont (I7, 1X, A3)

: STLCont = 'END' indicates no more reading from the unit number 13. Otherwise, the subroutine 'RSTL' will read temporally varying parameters at iTSTL tidal cycles.

A-1-6. Logical unit 14 (if iSUN = 1)

If iSUN = 1, the subroutine 'RSUN' in 'SUB-READ.FOR' reads in temporally varying parameters for light intensity (daily light intensity, rI0, and fractional daylength, FD) and temperature (heat exchange coefficient, κT, and equilibrium temperature, Te) from the unit number 14.

Title(j), j=1,3 (A79)

: three-line text to identify the input file. These lines are read in only once at the first reading, i.e., they are needed only when iTSUN = 0.

Title(1) (/ , A79)

: one blank line and one-line text to identify the following data group.

rIO,FD,KT,Te (4F8.3)

: temporally varying parameters (see Appendix A-1-2 for definition of variables).

iTSUN, SUNCont (I7, 1X, A3)

: SUNCont = 'END' indicates no more reading from the unit number 14. Otherwise, the subroutine 'RSUN' will read temporally varying parameters at iTSUN tidal cycles.

A-1-7. Logical unit 15 (if iDBC = 1)

If iDBC = 1, the subroutine 'RDBC' in 'SUB-READ.FOR' reads in temporally varying downriver boundary conditions from the unit number 15.

Title(j), j=1,3 (A79)

: three-line text to identify the input file. These lines are read in only once at the first reading, i.e., they are needed only when iTDBC = 0.

Title(1) (/ , A79)

: one blank line and one-line text to identify the following data group.

S(1),Bc(1),Bd(1),Bg(1),C1(1),C2(1),C3(1),APCd (8F8.3)

: temporally varying downriver boundary conditions (see Appendix A-1-2 for definition of variables), and APca is the mean phosphorus-to-carbon ratio (g P per g C) at the downriver boundary.

Title(1) (A79)

: one-line text to identify the following data group.

P1(1),P2(1),P3(1),PO4t(1),N1(1),N2(1),N3(1),NH4(1),NO3(1) (9F8.3)

: temporally varying downriver boundary conditions (see Appendix A-1-2 for definition of variables).

Title(1) (A79)

: one-line text to identify the following data group.

SU(1),SA(1),COD(1),O2(1),TSS(1),TAM(1),FCB(1),T(1) (8F8.3)

: temporally varying downriver boundary conditions (see Appendix A-1-2 for definition of variables).

iTDBC, DBCCont (I7, 1X, A3)

: DBCCont = 'END' indicates no more reading from the unit number 15. Otherwise, the subroutine 'RDBC' will read temporally varying parameters at iTDBC tidal cycles.

Note that the 25 values are read in each time. However only those, for which the corresponding control parameters ($i_{BC*} = 1$) (see Appendix A-1-2), are used. Those for which $i_{BC*} \neq 1$, the boundary conditions are generated using Eq. A-1 in the subroutine 'RDBCsin'.

A-1-8. Logical unit 16 (if $i_{BEN} = 2$)

If $i_{BEN} = 2$, the subroutine 'RBEN' in 'SUB-READ.FOR' reads in spatially and/or temporally varying benthic fluxes from the unit number 16.

Title(j), j=1,3 (A79)

: three-line text to identify the input file. These lines are read in only once at the first reading, i.e., they are needed only when $i_{TBEN} = 0$.

Title(1) (/ , A79)

: one blank line and one-line text to identify the following data group.

**Index, BFPO4d(i),
BFNH4(i), BFNO3(i), BFSAd(i), BFCOD(i), BFO2(i) i=2, NSEgm (A8, 6F8.3)
(Index, TBFPO4d(m,n), TBFNH4(m,n), TBFNO3(m,n),
TBFSAd(m,n), TBFCOD(m,n), TBFO2(m,n) n=2, NSEGb(m)) m=1, Nbran (A8, 6F8.3)
ID2, m, n, StBFPO4d(m,n), StBFNH4(m,n), StBFNO3(m,n),
StBFSAd(m,n), StBFCOD(m,n), StBFO2(m,n) j=1, NSt (A2, 2I3, 6F8.3)**

: Input file uses the first 8 columns (Index and ID2) to identify channel and segment.

: spatially varying benthic fluxes (see Appendix A-1-2 for definition of variables).

iTBEN, BENCont (I7, 1X, A3)

: BENCont = 'END' indicates no more reading from the unit number 16. Otherwise, the subroutine 'RBEN' will read temporally varying parameters at i_{TBEN} tidal cycles.

A-1-9. Logical unit 17 (if $i_{TMP} = 3$)

If $i_{TMP} = 3$, the subroutine 'RTMP' in 'SUB-READ.FOR' reads in spatially and/or temporally varying temperatures from the unit number 17.

Title(j), j=1,3 (A79)

: three-line text to identify the input file. These lines are read in only once at the first reading, i.e., they are needed only when $i_{TTMP} = 0$.

Title(1) (/ , A79)

: one blank line and one-line text to identify the following data group.

Index,T(i), i=2,NSEGM (A8, F8.3)
(Index,TT(m,n), n=2,NSEGB(m)) m=1,Nbran (A8, F8.3)
ID2,m,n,StT(m,n), j=1,NSt (A2, 2I3, F8.3)

: Input file uses the first 8 columns (Index and ID2) to identify channel and segment.
: spatially varying temperatures (°C).

iTTMP, TMPCont (I7, 1X, A3)

: TMPCont = 'END' indicates no more reading from the unit number 17. Otherwise, the subroutine 'RTMP' will read temporally varying parameters at iTTMP tidal cycles.

A-1-10. Logical unit 18 (if iPSL = 1)

If iPSL = 1, the subroutine 'RPSL' in 'SUB-READ.FOR' reads in temporally varying point source discharges and loadings from the unit number 18.

Title(j), j=1,3 (A79)

: three-line text to identify the input file.

iMCPS (8X, I5)
iBRPS (8X, I5)
iSTPS (8X, I5)

: number of segments into which point source input discharges for main channel (iMCPS), primary branch (iBRPS) and secondary branch (iSTPS).

The above three-line text and three integer variables are read in only once at the first reading, i.e., they are needed only when iTPSL = 0.

Title(1) (/ , A79)

: one blank line and one-line text to identify the following data group.

ID2,i,xPSQ,xPS,
xPBc,xPBd,xPBg,xPC1,xPC2,xPC3, j=1,iMCPS (A2, 3X, I3, 8F8.3)

: Input file uses ID2 for channel identification only.

: temporally varying point source discharge and loadings for algae and carbon (see Appendix A-1-2 for definition of variables).

ID2,m,n,xPSQT,xTPS,
xTPBc,xTPBd,xTPBg,xTPC1,xTPC2,xTPC3, j=1,iBRPS (A2, 2I3, 8F8.3)

: The character "T" designates the variables at the primary branches.

: Point source input enters the nth segment in the mth primary branch.

ID2,m,n,xStPSQ,xStPS,
xStPBc,xStPBd,xStPBg,xStPC1,xStPC2,xStPC3, j=1,iSTPS (A2, 2I3, 8F8.3)

: The character "St" designates the variables at the secondary branches.

: Point source input enters the n^{th} segment in the m^{th} secondary branch (storage area).

Title (A79)

: one-line text to identify the following data.

```
ID2,i,xPP1,xPP2,xPP3,  
  xPPO4t,xPN1,xPN2,xPN3,xPNH4,xPNO3, j=1,iMCPS (A2, 3X, I3, 9F8.3)  
ID2,m,n,xTPP1,xTPP2,xTPP3,  
  xTPPO4t,xTPN1,xTPN2,xTPN3,xTPNH4,xTPNO3, j=1,iMCPS (A2, 3X, I3, 9F8.3)  
ID2,m,n,xStPP1,xStPP2,xStPP3,xStPPO4t,  
  xStPN1,xStPN2,xStPN3,xStPNH4,xStPNO3, j=1,iMCPS (A2, 3X, I3, 9F8.3)
```

: point source input for phosphorus and nitrogen (see Appendix A-1-2 for definition of variables).

Title (A79)

: one-line text to identify the following data.

```
ID2,i,xPSU,xPSA,xPCOD,  
  xPO2,xPTSS,xPTAM,xPFCB,xPT, j=1,iMCPS (A2, 3X, I3, 8F8.3)  
ID2,m,n,xTPSU,xTPSA,xTPCOD,  
  xTPO2,xTPTSS,xTPTAM,xTPFCB,xTPT, j=1,iMCPS (A2, 3X, I3, 8F8.3)  
ID2,m,n,xStPSU,xStPSA,xStPCOD,  
  xStPO2,xStPTSS,xStPTAM,xStPFCB,xStPT, j=1,iMCPS (A2, 3X, I3, 8F8.3)
```

: point source input (see Appendix A-1-2 for definition of variables).

iTPSL, PSLCont (I7, 1X, A3)

: PSLCont = 'END' indicates no more reading from the unit number 18. Otherwise, the subroutine 'RPSL' will read temporally varying parameters at iTPSL tidal cycles.

A-1-11. Logical unit 19 (if iNPL = 1)

If iNPL = 1, the subroutine 'RNPL' in 'SUB-READ.FOR' reads in spatially and/or temporally varying nonpoint source discharges and loadings from the unit number 19.

Title(j), j=1,3 (A79)

: three-line text to identify the input file. These lines are read in only once at the first reading, i.e., they are needed only when iTNPL = 0.

Title (/ , A79)

: one blank line and one-line text to identify the following data group.

```
Index,xDSQ,xNS,xNBc,xNBd,xNBg,xNC1,xNC2,xNC3, j=2,NSEGM (A8, 8F8.4)  
(Index,xDSQT,xTNS,xTNBc,  
  xTNBd,xTNBg,xTNC1,xTNC2,xTNC3, n=2,NSEGB(j)) j=1,Nbran (A8, 8F8.4)  
ID2,m,n,xStDSQ,xStNS,  
  xStNBc,xStNBd,xStNBg,xStNC1,xStNC2,xStNC3, j=1,Nst (A2, 2I3, 8F8.4)
```

: spatially varying nonpoint source discharge and loadings for algae and carbon (see Appendix A-1-2 for definition of variables).

Title (A79)

: one blank line and one-line text to identify the following data group.

Index, xNP1,
xNP2, xNP3, xNPO4t, xNN1, xNN2, xNN3, xNNH4, xNNO3, j=2, NSEGM (A8, 9F8.4)
(Index, xTNP1, xTNP2, xTNP3, xTNPO4t,
xTNN1, xTNN2, xTNN3, xTNNH4, xTNNO3, n=2, nsegB(J)) j=1, NBRAN (A8, 9F8.4)
ID2, m, n, xStNP1, xStNP2, xStNP3,
xStNPO4t, xStNN1, xStNN2, xStNN3, xStNNH4, xStNNO3, j=1, Nst (A2, 2I3, 9F8.4)

: nonpoint source loadings for phosphorus and nitrogen (see Appendix A-1-2 for definition of variables).

Title (A79)

: one blank line and one-line text to identify the following data group.

Index, xNSU, xNSA, xNCOD, xNO2, xNTSS, xNTAM, xNFCB, xNT, j=2, NSEGM (A8, 8F8.4)
(Index, xTNSU, xTNSA, xTNCOD,
xTNO2, xTNTSS, xTNTAM, xTNFCB, xTNT, n=2, NSEGB(j)) j=1, Nbran (A8, 8F8.4)
ID2, m, n, xStNSU, xStNSA,
xStNCOD, xStNO2, xStNTSS, xStNTAM, xStNFCB, xStNT, j=1, Nst (A2, 2I3, 8F8.4)

: nonpoint source loadings (see Appendix A-1-2 for definition of variables).

iTNPL, NPLCont (I7, 1X, A3)

: NPLCont = 'END' indicates no more reading from the unit number 19. Otherwise, the subroutine 'RNPL' will read temporally varying parameters at iTNPL tidal cycles.

A-2. Input Data Description for Sediment Process Model

As explained at the end of Appendix A-1-2, if iBEN = 1, two subroutines 'RSEDIn' and 'RSEDVIn' in 'SUB-SM.FOR' read in input parameters for sediment process model from the unit number 20 (Table A-2). This section explains line-by-line the input data files for sediment process model. Each data group and each line are preceded by text titles for identification purpose. These text titles, which do not affect the model run, are not described, and omitted using FORMAT descriptor slash (/), in this section.

Title(j), j=1,3 (A79)

: three-line text to identify a simulation of sediment process model.

Title(1) (/, A79)

: one blank line and one-line text to identify the following data group.

iHyst, LBcom, LBnh4, LBno3, LBpo4, LBsod, LBsi, LBfB (/, 8I8)

: iHyst = 1 activates the hysteresis in benthic mixing described in Section IV-3-1B. Otherwise, no hysteresis in benthic mixing due to low oxygen conditions.

: **LBnh4**, **LBno3**, **LBpo4**, **LBsod**, **LBsi** OR **LBfB** = 1 opens the unit number **47**, **48**, **49**, **50**, **51**, **52** or **53** and writes the diagnostic information for common sediment parameters, sediment ammonium, sediment nitrate, sediment phosphate, sediment oxygen demand, sediment silica or settling and diagenetic fluxes, respectively. If water column silica is not simulated (i.e., $i_{si} \neq 1$), **LBsi** must be $\neq 1$.

iBTimeS, **iBSTS**, **iBETS**, **iBTScha**, **iBTSseg** (/ , 518)

: If **iBTimeS** = 0, no time-series output for sediment process model. If **iBTimeS** = 1, 2 or 3, writes time-series output for sediment process model at one location. Otherwise, an error will be issued and the program be terminated.

: Write time-series output starting from **iBSTS** (tidal cycles) till **iBETS** (tidal cycles) at the channel number of **iBTScha** and segment number of **iBTSseg**. If **iBTScha** = 1, it is main channel. If **iBTScha** = 2, it is primary branch and if **iBTScha** = 3, it is secondary branch.

DifT (/ , F8.3)

: heat diffusion coefficient ($m^2 \text{ sec}^{-1}$) between the water column and sediment.

Title(1) (/ , A79)

: one blank line and one-line text to identify the following data group.

FNBc(1), **FNBc(2)**, **FNBc(3)**,
FNBd(1), **FNBd(2)**, **FNBd(3)**, **FNBg(1)**, **FNBg(2)**, **FNBg(3)** (/ , 9F8.3)
FPBc(1), **FPBc(2)**, **FPBc(3)**,
FPBd(1), **FPBd(2)**, **FPBd(3)**, **FPBg(1)**, **FPBg(2)**, **FPBg(3)** (/ , 9F8.3)
FCBc(1), **FCBc(2)**, **FCBc(3)**,
FCBd(1), **FCBd(2)**, **FCBd(3)**, **FCBg(1)**, **FCBg(2)**, **FCBg(3)** (/ , 9F8.3)

: **FMBx(i)** = fraction of POM (M = N, P or C) in algal group x routed into the i^{th} G class in sediment. Note that $FMBx(1) + FMBx(2) + FMBx(3) = 1$ for $x = c, d$ or g .

Title(1) (/ , A79)

: one blank line and one-line text to identify the following data group.

KPON(1), **KPON(2)**, **KPON(3)**,
KPOP(1), **KPOP(2)**, **KPOP(3)**, **KPOC(1)**, **KPOC(2)**, **KPOC(3)** (/ , 9F8.3)
ThKN(1), **ThKN(2)**, **ThKN(3)**,
ThKP(1), **ThKP(2)**, **ThKP(3)**, **ThKC(1)**, **ThKC(2)**, **ThKC(3)** (/ , 9F8.3)

: **KPOM(i)** = decay rate (day^{-1}) of the i^{th} G class POM (M = N, P or C) at 20°C in anoxic layer (Layer 2).

: **ThKM(i)** = constant for temperature adjustment for **KPOM(i)**.

Title(1) (/ , A79)

: one blank line and one-line text to identify the following data group.

rM1, rM2, ThDd, ThDp, GPOCr, KMDp, KBST, DpMIN, RBIBT (/ , 9F8.3)
O2BSc, TDMBS, TCMBS (/ , 3F8.3)

: rM1, rM2 = solid concentrations (kg L^{-1}) in Layers 1 and 2, respectively.

: ThDd, ThDp = constants for temperature adjustment for D_d and D_p , respectively.

: GPOCr = reference concentration (g C m^{-3}) for G_{POC1} (see Eq. 4-13).

: KMDp = particle mixing half-saturation constant for oxygen ($\text{g O}_2 \text{ m}^{-3}$).

: KBST = first-order decay rate for stress (day^{-1}).

: DpMIN = minimum diffusion coefficient for particle mixing ($\text{m}^2 \text{ day}^{-1}$).

: RBIBT = Ratio of bio-irrigation to bioturbation, i.e., dissolved phase mixing to particle mixing.

: O2BSc = critical oxygen concentration (g m^{-3}) for retaining maximum benthic stress (Section IV-3-1B).

: TDMBS = time lag (days) for the maximum stress to be kept.

: TCMBS = critical hypoxic days (days). If the overlying oxygen is lower than O2BSc for longer than TCMBS days, then the maximum benthic stress is retained for TDMBS days.

Title(1) (/ , A79)

: one blank line and one-line text to identify the following data group.

P1NH4, P2NH4, KMNH4, KMNH4O2, ThNH4, ThNO3, P2PO4, DOcPO4 (/ , 8F8.3)

: P1NH4 = partition coefficient (per kg L^{-1}) for sediment ammonium in Layer 1.

: P2NH4 = partition coefficient (per kg L^{-1}) for sediment ammonium in Layer 2.

: KMNH4 = nitrification half-saturation constant for ammonium (g N m^{-3}).

: KMNH4O2 = nitrification half-saturation constant for dissolved oxygen ($\text{g O}_2 \text{ m}^{-3}$).

: ThNH4 = constant for temperature adjustment for nitrification reaction velocity.

: ThNO3 = constant for temperature adjustment for denitrification reaction velocities.

: P2PO4 = partition coefficient (per kg L^{-1}) for sediment phosphate in Layer 2.

: DOcPO4 = critical oxygen concentration (g m^{-3}) for phosphate sorption in Layer 1.

Title(1) (/ , A79)

: one blank line and one-line text to identify the following data group.

P1H2S, P2H2S, KH2Sd1, KH2Sp1, ThH2S, KMH2S, KCH4, ThCH4, cSHSCH (/ , 9F8.3)

aO2C, aO2NO3, aO2NH4 (/ , 3F8.3)

- : P1H2S = partition coefficient (per kg L⁻¹) for sediment sulfide in Layer 1.
- : P2H2S = partition coefficient (per kg L⁻¹) for sediment sulfide in Layer 2.
- : KH2sd1, KH2sp1 = reaction velocities (m day⁻¹) at 20°C in Layer 1 for dissolved and particulate, respectively, sulfide oxidation.
- : ThH2S = constant for temperature adjustment for KH2sd1 and KH2sp1.
- : KMH2S = constant to normalize the sulfide oxidation rate for oxygen (g O₂ m⁻³).
- : KCH4 = reaction velocity (m day⁻¹) for dissolved methane oxidation in Layer 1 at 20°C.
- : ThCH4 = constant for temperature adjustment for KCH4.
- : cSHSCH = critical salinity (ppt) to divide sulfide and methane oxidation.
- : aO2C = stoichiometric coefficient for carbon diagenesis consumed by sulfide oxidation (2.6667 g O₂-equivalents per g C).
- : aO2NO3 = stoichiometric coefficient for carbon diagenesis consumed by denitrification (2.8571 g O₂-equivalents per g N).
- : aO2NH4 = stoichiometric coefficient for oxygen consumed by nitrification (4.33 g O₂ per g N: see Section III-7-2).

Title(1) (/ , A79)

- : one blank line and one-line text to identify the following data group.

KSi, ThSi, KMPSi, SiSat, P2Si, DP1Si, DOcSi, DetFPSi (/ , 8F8.3)

- : KSi = dissolution rate (day⁻¹) for particulate biogenic silica in Layer 2 at 20°C.
- : ThSi = constant for temperature adjustment for KSi.
- : KMPSi = silica dissolution half-saturation constant for particulate silica (g Si m⁻³).
- : SiSat = saturation concentration of silica in the pore water (g Si m⁻³).
- : P2Si = partition coefficient (per kg L⁻¹) for sediment silica in Layer 2.
- : DP1Si = increment in partition coefficient for silica in Layer 1 as a function of dissolved oxygen.
- : DOcSi = critical oxygen concentration (g m⁻³) for silica sorption in Layer 1.
- : DetFPSi = detrital flux of particulate biogenic silica (g Si m⁻² day⁻¹).

Title (/, A79)
Title (A79)

: one blank line and two-line text to identify the following data group.

**Index, Hsed(i), W2(i),
Dd(i), Dp(i), KNH4(i), K1NO3(i), K2NO3(i), DP1PO4(i), i=2, NSEGM (A8, 8F8.4)**

: Input file uses **Index** for channel and segment identification only.

: (i) = ith main channel segment.

: **Hsed(i)** = sediment depth (m) including Layers 1 and 2.

: **W2(i)** = burial rate (m day⁻¹).

: **Dd(i)** = dissolved phase diffusion coefficient in pore water (m² day⁻¹).

: **Dp(i)** = apparent diffusion coefficient for particle mixing (m² day⁻¹).

: **KNH4(i)** = optimal reaction velocity (m day⁻¹) for nitrification at 20°C.

: **K1NO3(i)** = reaction velocity (m day⁻¹) for denitrification in Layer 1 at 20°C.

: **K2NO3(i)** = reaction velocity (m day⁻¹) for denitrification in Layer 2 at 20°C.

: **DP1PO4(i)** = increment in partition coefficient for phosphate in Layer 1 as a function of dissolved oxygen.

**(Index, THsed(m, n), TW2(m, n), TDd(m, n), TDp(m, n), TKNH4(m, n), TK1NO3(m, n),
TK2NO3(m, n), TDP1PO4(m, n), n=2, NSEGB(m)) m=1, Nbran (A8, 8F8.4)**

: Input file uses **Index** for channel and segment identification only.

: The first character "T" designates the variables at the primary branches, i.e., variables at the nth segment of the mth primary branch.

**ID2, m, n, SHsed(m, n), SW2(m, n), SDd(m, n), SDp(m, n), SKNH4(m, n),
SK1NO3(m, n), SK2NO3(m, n), SDP1PO4(m, n), j=1, NST (A2, 2I3, 8F8.4)**

: Input file uses **ID2** for channel and segment identification only.

: The first character "S" designates the variables at the secondary branches, i.e., variables at the nth segment of the mth primary branch.

Title (/, A79)
Title (A79)

: one blank line and two-line text to identify the following data group.

**Index, FMRP2(i), FMRP3(i),
FPRP2(i), FPRP3(i), FCRP2(i), FCRP3(i), i=2, NSEGM (A8, 6F8.4)**

: Input file uses **Index** for channel and segment identification only.

: **FMRP2(i)** = fraction of water column refractory POM (M = N, P or C) routed into the 2nd G class in sediment at the ith main channel segment.

: $FMRP3(i)$ = fraction of water column refractory POM ($M = N, P$ or C) routed into the 3rd G class in sediment at the i^{th} main channel segment.

Note that 100% of water column labile POM is routed to the 1st G class in sediment, and that $FMRP2(i) + FMRP3(i) = 1$.

(**Index**, **TFNRP2(m,n)**, **TFNRP3(m,n)**, **TFPRP2(m,n)**, **TFPRP3(m,n)**,
TFCRP2(m,n), **TFCRP3(m,n)**, **n=2,NSEGb(m)**) **m=1,Nbran** (A8, 6F8.4)

: Input file uses **Index** for channel and segment identification only.

: The first character "T" designates the variables at the primary branches, i.e., variables at the n^{th} segment of the m^{th} primary branch.

ID2,m,n,SFNRP2(m,n), **SFNRP3(m,n)**, **SFPRP2(m,n)**,
SFPRP3(m,n), **SFCRP2(m,n)**, **SFCRP3(m,n)**, **j=1,NSt** (A2, 2I3, 6F8.4)

: Input file uses **ID2** for channel and segment identification only.

: The first character "S" designates the variables at the secondary branches, i.e., variables at the n^{th} segment of the m^{th} primary branch.

Title (/ , A79)

Title (A79)

: one blank line and two-line text to identify the following data group (initial conditions in $g\ m^{-3}$).

Index, **GPON1(i)**, **GPON2(i)**, **GPON3(i)**, **GPOP1(i)**,
GPOP2(i), **GPOP3(i)**, **GPOC1(i)**, **GPOC2(i)**, **GPOC3(i)** **i=2,NSEGm** (A8, 9F8.4)

: Input file uses **Index** for channel and segment identification only.

: $GPOM1(i)$, $GPOM2(i)$, $GPOM3(i)$ = 1st, 2nd and 3rd, respectively, G class particulate organic matter ($M = N, P$ or C) at the i^{th} main channel segment.

(**Index**, **TGPON1(m,n)**, **TGPON2(m,n)**, **TGPON3(m,n)**,
TGPOP1(m,n), **TGPOP2(m,n)**, **TGPOP3(m,n)**,
TGPOC1(m,n), **TGPOC2(m,n)**, **TGPOC3(m,n)** **n=2,NSEGb(m)**) **m=1,Nbran** (A8, 9F8.4)

: Input file uses **Index** for channel and segment identification only.

: The first character "T" designates the variables at the primary branches, i.e., variables at the n^{th} segment of the m^{th} primary branch.

ID2,m,n,SGPON1(m,n), **SGPON2(m,n)**, **SGPON3(m,n)**,
SGPOP1(m,n), **SGPOP2(m,n)**, **SGPOP3(m,n)**,
SGPOC1(m,n), **SGPOC2(m,n)**, **SGPOP3(m,n)** **j=1,NSt** (A2, 2I3, 9F8.4)

: Input file uses **ID2** for channel and segment identification only.

: The first character "S" designates the variables at the secondary branches, i.e., variables at the n^{th} segment of the m^{th} primary branch.

Title (/ , A79)

: one blank line and one-line text to identify the following data group (initial conditions in $g\ m^{-3}$ continued).

**Index, G1NH4(i), G2NH4(i), G2NO3(i),
G2PO4(i), G2H2S(i), GPSi(i), G2Si(i), BST(i), GT(i) i=2, NSEGm (A8, 9F8.4)**

: Input file uses **Index** for channel and segment identification only.

: **G1NH4(i), G2NH4(i)** = ammonium concentrations in sediment Layers 1 and 2, respectively.

: **G2NO3(i), G2PO4(i), G2H2S(i), G2Si(i)** = nitrate, phosphate, hydrogen sulfide (methane in freshwater, see Section IV-3-5) and available silica concentrations, respectively, in sediment Layer 2.

: **GPSi(i)** = particulate biogenic silica concentration in sediment Layer 2.

: **BST(i)** = accumulated benthic stress (day), see Eq. 4-14.

: **GT(i)** = sediment temperature ($^{\circ}C$).

Note that the solution of the mass-balance equation for Layer 1, because of the steady-state assumption made for this layer, does not require the Layer 1 variables at an old time step, and thus the initial conditions for Layer 1. The only exception is **G1NH4(i)**, which is used to calculate nitrification in Layer 1.

**(Index, TG1NH4(m, n), TG2NH4(m, n), TG2NO3(m, n),
TG2PO4(m, n), TG2H2S(m, n), TGPSi(m, n),
TG2Si(m, n), TBST(m, n), TGT(m, n) n=2, NSEGb(m)) m=1, Nbran (A8, 9F8.4)**

: Input file uses **Index** for channel and segment identification only.

: The first character "T" designates the variables at the primary branches, i.e., variables at the n^{th} segment of the m^{th} primary branch.

**ID2, m, n, SG1NH4(m, n), SG2NH4(m, n), SG2NO3(m, n), SG2PO4(m, n), SG2H2S(m, n),
SGPSi(m, n), SG2Si(m, n), SBST(m, n), SGT(m, n) j=1, NSt (A2, 2I3, 9F8.4)**

: Input file uses **ID2** for channel and segment identification only.

: The first character "S" designates the variables at the secondary branches, i.e., variables at the n^{th} segment of the m^{th} primary branch.

Table A-1. Data file organization for water column model.

UNIT NO	READ or WRITE	EXAMPLE	DESCRIPTION
7	read	GEO-HYD.IN ^a	constant input for geometric and hydrodynamic data
8	read	TPM-CONT.IN	program control parameters, constant coefficients, and time-varying input and output file names
9	read	TPM.OUT ^a	general model output listing read-in parameters
11	read	TPM-ICI.IN ^b	spatially and/or temporally varying initial conditions for water column model
12	read	TPM-AGR.IN ^b	spatially and/or temporally varying coefficients for algal dynamics
13	read	TPM-STL.IN ^b	spatially and/or temporally varying settling velocities
14	read	TPM-SUN.IN ^b	temporally varying coefficients for light intensity and temperature
15	read	TPM-DBC.IN ^b	temporally varying downriver boundary conditions
16	read	TPM-BEN.IN ^b	spatially and/or temporally varying benthic fluxes
17	read	TPM-TEMP.IN ^b	spatially and/or temporally varying temperature
18	read	TPM-PSL.IN ^b	temporally varying point source inputs
19	read	TPM-NPL.IN ^b	spatially and/or temporally varying nonpoint source inputs
21	write	TPM-LDO.DAT ^b	output file for longitudinal distributions
34	write	TPM-TSO*.DAT ^b	10 time-series output files: one unit for one segment

^a These file names are fixed in the source code.

^b Optional units depending on control parameters.

Table A-1. (continued).

UNIT NO	READ or WRITE	EXAMPLE	DESCRIPTION
22	write	DIA-ZK.LOG ^b	diagnostic output for zero K ^o (see Section III-12)
23	write	DIA-NR.LOG ^b	diagnostic output for negative R ^o (see Section III-12)
24	write	DIA-NC.LOG ^b	diagnostic output for negative concentrations
25	write	DIA-S.LOG ^b	diagnostic output for salinity
26	write	DIA-BC.LOG ^b	diagnostic output for cyanobacteria
27	write	DIA-BD.LOG ^b	diagnostic output for diatoms
28	write	DIA-PO4.LOG ^b	diagnostic output for phosphate
29	write	DIA-NH4.LOG ^b	diagnostic output for ammonium
30	write	DIA-NO3.LOG ^b	diagnostic output for nitrate
31	write	DIA-Si.LOG ^b	diagnostic output for available silica
32	write	DIA-O2.LOG ^b	diagnostic output for dissolved oxygen
33	write	DIA-BG.LOG ^b	diagnostic output for temperature
80	write	TPM-PLT.DAT ^{a,b}	output data file for Post-Processor

Table A-2. Data file organization for sediment process model^a.

UNIT NO	READ or WRITE	EXAMPLE	DESCRIPTION
20	read	TPM-SM.IN ^b	input coefficients for sediment process model
46	write	TPM-SM.TS.DAT ^c	time-series output file for sediment process model
45	write	ZBRENT.LOG ^{b,c}	diagnostic output for FUNCTION ZBRENT
47	write	DIAB-COM.LOG ^c	diagnostic output for common sediment parameters
48	write	DIAB-NH4.LOG ^c	diagnostic output for ammonium in sediment
49	write	DIAB-NO3.LOG ^c	diagnostic output for nitrate in sediment
50	write	DIAB-PO4.LOG ^c	diagnostic output for phosphate in sediment
51	write	DIAB-SOD.LOG ^c	diagnostic output for sediment oxygen demand
52	write	DIAB-Si.LOG ^c	diagnostic output for dissolved silica
53	write	DIAB-fB.LOG ^c	diagnostic output for settling and diagenetic fluxes

^a All input and output units for sediment process model are optional.

^b These files are not optional once the sediment process model is activated.

^c These file names are fixed in the source code.

Appendix B. Graphic Interface

To facilitate its use, the present model package includes a graphic interface. The model package consists of three parts: tidal prism model, Pre-Processor and Post-Processor. The enclosed 3½" disk (high density) contains the following 8 files:

- 1) Tidal prism model (TPM-VIMS.EXE), which calculates 23 water quality and 16 sediment state variables, and show the model calculation on the screen as the model computation progresses.
- 2) Pre-Processor (TPM-PRE.EXE), which allows limited editing of the control input data file, TPM-CONT.IN, for point source loadings, i.e., for wasteload allocation.
- 3) Post-Processor (TPM-POST.EXE), which shows on the screen, and produces a hardcopy of, the selected model outputs saved from the model runs, in either longitudinal or time-series plot.
- 4) TPM-CONT.IN, which is the control input data file for program control parameters, constant conditions, coefficients, point source loadings, and time-varying input and output file names.
- 5) TPM-SM.IN, which is an input data file for sediment process model.
- 6) GEO-HYD.IN, which is an input file for geometric and hydrodynamic data used by TPM-VIMS.EXE and TPM-PRE.EXE.
- 7) DRAW.IN, which is an input data file for graphic interface used by TPM-VIMS.EXE.
- 8) DRAW-PST.IN, which is an input data file for graphic interface used by TPM-POST.EXE.

Following the hardware/software description, each of these files are explained in the remaining of this chapter, using the application of the model package to the Lynnhaven River system as an example.

B-1. Hardware/Software Description

The model package is coded in FORTRAN 77, and compiled using Lahey F77L-EM/32. The following FORTRAN libraries are used for the user interface; HALO Professional Library, Lahey Spindrift Utility Library and Lahey Spindrift Windows

Library.

The model package runs on IBM compatible personal computers with 80386 (with math-coprocessor) or higher CPUs, though 486 machine is highly recommended for speed consideration. You must have VGA monitor, at least 4 MB of memory, a hard disk with about 1 MB for execution file and input data files. You must have a HP Laser printer to produce hardcopies using Post-Processor. The hard disk space required for output files depends on the number of segments and the output files you select to generate.

Because of disk space requirement, you cannot run the model package from floppy drives. You should run the model before Post-Processor because the enclosed disk does not contain the model output file that Post-Processor requires as input.

B-2. Tidal Prism Model (TPM-VIMS.EXE)

Tidal prism model run requires several input data files. You need at least 3 files, TPM-CONT.IN, GEO-HYD.IN and DRAW.IN, for any model run. For time varying conditions, you need additional input data files, which are described in Appendix A. You also need TPM-SM.IN if you activate the sediment process model. The graphic interface of TPM-VIMS.EXE is self-explanatory, and a brief description is given in this section.

The graphic interface divides the screen into four parts: upper left (Plot A), upper right (Plot B), lower left (Plot C) and lower right (Plot D). Each plot shows the model results for the selected state variable at the selected channel. The present model implementation handles 39 state variables (23 water quality and 16 sediment variables), and 12 channels. When you execute TPM-VIMS.EXE, you will be first asked to specify the control input data file for tidal prism model: press ENTER key to use the default input file (TPM-CONT.IN) or type another file name. The file, TPM-CONT.IN, that is included in the disk, is for timewise constant conditions. If you like to simulate the time varying conditions, additional input files for time varying input conditions (Table A-1) should be in the same directory. Note that once you specify the control input data file, the existing output files from previous model run in the same directory will be lost. This is so whether you complete the new model run or not. If you want to save the existing output files, you should move these files to another directory or rename them.

After you specify the control input file, you will see the default selections of variables and channels for four plots: salinity at main channel (Eastern Branch) for Plot A, salinity at Western Branch for Plot B, chlorophyll 'a' at main channel for Plot C and dissolved oxygen at main channel for Plot D. You may change variables and channels for any plot by following the on-screen instructions. To distinguish sediment variables from those in water column, sediment variable names are preceded by "s". Also note that positive sediment oxygen demand (sSOD) indicates the oxygen flux into the sediment, while other fluxes are positive to the overlying water column.

Upon pressing ENTER key, the next screen shows four plots that you choose. In addition to these, the graphic screen has a clock showing the progress of model run. It also has a line for time in Julian days and a line of menu at the bottom, which is

```
(P)ause (R)esume re(S)tart (O)ther-plots (Y)scale-change ESC-to-exit
```

Pressing P will pause the model run until you press R or any other key. Pressing S restarts the model run from the beginning. Pressing O brings you to the previous menu to let you change variable and channel selection for the plots. The model continues its run after new selection. Pressing Y allows you to change the y-axis scale for four plots at any time. You can abort the model run by pressing ESCAPE key. Note that the current output files will be deleted if you abort the model run before its normal termination. The marks, ▲, at the top of each plot indicate the transect locations, and all state variables are defined at the center of each segment. Since the 1st segments for both main channel and branches are outside of the mouth (Section II-1), an arbitrary distance of -0.5 km is assigned to designate the center of the 1st segments.

B-3. Pre-Processor (TPM-PRE.EXE)

The Pre-Processor allows limited editing of the control input data file, TPM-CONT.IN, for point source loadings, i.e., for wasteload allocation. When running TPM-PRE.EXE, you need one more input file, GEO-HYD.IN, in the current directory. When you execute TPM-PRE.EXE, you will be first asked to specify the control input data file that you like to edit. You can press ENTER key to use the default data file (TPM-CONT.IN) or type another file name.

Upon specifying the input data file, you will see the next screen displaying a menu.

You can choose each item either by moving cursor key followed by ENTER or by pressing the first character. The one-line help for each item at the bottom of the screen explains the meaning of above 16 items. For example, if you choose item D (Default), it will read and display the values for each of the first 11 items from the default input data file (TPM-CONT.IN), which should be in the current directory with TPM-PRE.EXE. Choosing item P (Previous) will bring you back to the previous menu for input file specification. Choosing item N (Next) will bring you to the next screen. Branch number of zero indicate the point source loading entering the main channel, while positive branch number indicates the point source loading into the primary branches. Negative branch number indicates the point source loading into the secondary branch (storage area) connected to the primary branch denoted by the branch number. For example, branch number of -3 indicates the point source loading into the storage area connected to the 3rd primary branch.

It should be noted that the Pre-Processor allows limited editing of the control input data file: only the locations and loadings of no more than 4 point sources, which discharge timewise constant waste water, are allowed. The model, however, can handle time-varying point source discharges. You can edit the input parameters that the Pre-Processor cannot modify using any ASCII editor: the input data file organization is described in detail in Appendix A.

Upon choosing item N), you will see the next screen displaying another menu, which allows you to edit the following parameters:

- : discharge rate ($\text{m}^3 \text{sec}^{-1}$),
- : loadings (kg per tidal cycle) for RPOC, LPOC, DOC, RPOP, LPOP, DOP, PO_{4t}, RPON, LPON, DON, NH₄, NO₃, SU, SA, TSS and TAM (kmol per tidal cycle),
- : concentration for DO (g m^{-3}), FCB (MPN per 100 mL) and T ($^{\circ}\text{C}$).

You can choose each item either by moving cursor key followed by ENTER or by pressing the first character. The one-line help for each item at the bottom of the screen explains the meaning of the item. Again, it should be noted that the above parameters are timewise constant point source discharges, although the model can handle time-varying ones.

B-4. Post-Processor (TPM-POST.EXE)

The tidal prism model generates, if `IPLT = 1`, a file (TPM-PLT.DAT) containing the model results for all state variables over the last 20 tidal cycles. The Post-Processor lets you examine, and produce hardcopy of, the model output in this file, in either longitudinal or time-series plot. In addition to TPM-PLT.DAT, you need another input file, DRAW-PST.IN, in the current directory. When you execute TPM-POST.EXE, you will be first asked to specify the input data file. You can press ENTER key to use the default data file (TPM-PLT.DAT) or type another file name.

The Post-Processor divides the screen into four parts: three parts for plots, upper left (Plot A), upper right (Plot B) and lower left (Plot C), and lower right part for model values. The three plots show the model results in either longitudinal or time-series plot. The longitudinal plot shows the snapshot information at the last tidal cycle for the selected state variable at the selected channel. The time-series plot shows the time-series information over the last 20 tidal cycles for the selected variable at all segments in selected channel.

After you specify the input file, you will see the default selections of variables and channels for three plots: longitudinal plot of salinity at main channel (Eastern Branch) for Plot A, time-series plot of salinity at main channel for Plot B, and longitudinal plot of dissolved oxygen at main channel for Plot C. You may change variables and channels for any plot by following the on-screen instructions. As in TPM-VIMS.EXE, to distinguish sediment variables from those in water column, sediment variable names are preceded by "s". Also note that positive sediment oxygen demand (sSOD) indicates the oxygen flux into the sediment, while other fluxes are positive to the overlying water column.

Upon pressing ENTER key, the next screen shows three plots that you choose with a line of menu at the bottom, which is

```
(O)ther-plots  (Y)scale-change  (P)rint  (R)eset-view  ESC-to-exit
```

Pressing O brings you to the previous menu to let you change variable and channel selection. Pressing Y allows you to change the y-axis scale for three plots at any time. Pressing P produces a hardcopy of current screen image. Pressing R redraws the current screen. You can exit the Post-Processor by pressing ESCAPE key. The lower right part

of the screen shows the model values for the longitudinal plots only, i.e., the model results for the selected variable at the last tidal cycle for all segments at the selected channel.